Review Article

Mohammad Azad Alam*, Hamdan B. Ya*, Mohammad Azeem, Mazli Mustapha, Mohammad Yusuf, Faisal Masood, Roshan Vijay Marode, Salit Mohd Sapuan, and Akhter Husain Ansari

Advancements in aluminum matrix composites reinforced with carbides and graphene: A comprehensive review

https://doi.org/10.1515/ntrev-2023-0111 received February 27, 2023; accepted August 3, 2023

Abstract: Automotive and aircraft industries are advancing swiftly, creating a constant need for innovative and trustworthy materials. Aluminum composites (aluminum matrix composites [AMCs]) exhibit enhanced mechanical and tribological behaviors when contrasted to their conventional equivalents and as a result have superior potential to be widely accepted for automotive and aircraft engineering and other component applications. This study aims to provide a thorough and critical analysis of the most recent research initiatives concerning the processing, characteristics, and applications of AMCs. It covers the recent advancements in the aluminum-based composites reinforced with SiC, TiC, and graphene, fabrication methods, and mechanical properties of AMCs. Graphene nanoplatelets are many times stronger and yet lighter than steel and other metals, and thus a good contender for reinforcing them. However, the homogeneous

distribution of graphene into the metal or aluminum is a challenging aspect for material researchers. The fabrication techniques for AMCs for achieving homogeneous distribution of graphene are critically reviewed. The mechanical properties, specifically microhardness, wear behavior, and tensile strength of aluminum-based composites, are reviewed and analyzed. Finally, a way forward for fostering further development in this area has been discussed.

Keywords: aluminum matrix composites, ceramics particles, graphene nanoplatelets, mechanical characteristics, wear behavior

1 Introduction

Competition to boost fuel efficiency and reduce CO2 emissions has intensified in the automotive and aerospace sectors as a result of new fuel economy requirements being adopted by governments throughout the world and increasing consumer demand for more fuel-efficient cars. As an illustration, according to a report from the Environmental Protection Agency (EPA) in April 2020, the transportation industry in the United States (US) generated around 28% of all US GHG emissions in 2018. To increase the fuel efficiency of vehicles (passenger cars and light trucks) and reduce CO₂ emissions, CAFE (Corporate Average Fuel Economy) requirements have been devised in the United States. The CAFE criterion for passenger cars has increased from 18 mpg (miles per gallon) in 1978 to 42 mpg currently, and it is expected to increase to 54.5 mpg by 2025. For the model years 2021–2026, the National Highway Traffic Safety Administration and the EPA amended the CAFE criteria and proposed a new value of 43.7 mpg. Every nation has its fuel economy regulations, and many of them are stricter than American regulations. The combined objectives of lowering CO₂ emissions and enhancing fuel efficiency, however, are shared by all countries. For most nations and regions, achieving the average fuel efficiency target for passenger vehicles is difficult in terms of CO₂ emissions per kilometer of driving (g/km) as depicted in Figure 1(a) [1]. In particular, the United States set the 2025 target for average CO₂ emissions to be 89 g/km, down nearly 40% from the 2015

Mohammad Azeem, Mazli Mustapha, Roshan Vijay Marode: Mechanical Engineering Department, Universiti Teknologi PETRONAS, Seri Iskandar 32610, Malaysia

Mohammad Yusuf: Clean Energy Technologies Research Institute (CETRI), Process Systems Engineering, Faculty of Engineering & Applied Science, University of Regina, 3737 Wascana Parkway, SK, S4S 0A2, Canada Faisal Masood: Department of Electrical Engineering, University of Engineering and Technology Taxila, 47080, Rawalpindi, Pakistan Salit Mohd Sapuan: Department of Mechanical and Manufacturing Engineering, Universiti Putra Malaysia, 43400 Serdang, Selangor, Malaysia; Advanced Engineering Materials and Composite Research Centre (AEMC), Department of Mechanical and Manufacturing Engineering, Faculty of Engineering, Universiti Putra Malaysia, 43400, UPM Serdang, Selangor Darul Ehsan, Malaysia

Akhter Husain Ansari: Mechanical Engineering Department, Aligarh Muslim University, Aligarh 202002, U.P, India

^{*} Corresponding author: Mohammad Azad Alam, Mechanical Engineering Department, Universiti Teknologi PETRONAS, Seri Iskandar 32610, Malaysia; Interdisciplinary Research Centre for Renewable Energy and Power System (IRC-REPS), Research Institute, King Fahd University of Petroleum and Minerals (KFUPM), Dhahran 31261, Saudi Arabia, e-mail: azad.alam@utp.du.my

^{*} Corresponding author: Hamdan B. Ya, Mechanical Engineering Department, Universiti Teknologi PETRONAS, Seri Iskandar 32610, Malaysia, e-mail: hamdan.ya@utp.edu.my

level. Beyond increased fuel efficiency and emission reduction, higher performance and simpler recycling also help to advance the development of lighter, stronger, and more environmentally friendly cars.

Vehicle weight reduction is one of the many strategies that manufacturers have tried to meet fuel efficiency criteria and satisfy customer demands. Either the vehicle's size can be reduced, or lightweight materials can be used [2]. The safety and comfort of the passengers may be jeopardized if the size of the vehicle is reduced. As a result, it is common to try to reduce vehicle weight by using lighter materials while maintaining performance. Light vehicle production has increased steadily during the past few years in all the major markets (Figure 1(b)) [1]. According to reports, a 10% weight reduction in a car can increase fuel efficiency by 8–10%, and a 100 kg weight reduction can reduce CO₂ emissions by 12.5 g/km [3,4]. Additionally, the lighter vehicle offers better performance without compromising occupant safety.

1.1 Demand for aluminum in engineering sectors

There is an urgent need to produce high-performance, lightweight materials for the following generation of transportation sectors given the increasing demand for CO_2 control, fuel economy, and lightweight in other industries (such as maritime transportation). Low-carbon steel and cast iron were the two materials that the automotive industry used the most until the 1970s. A passenger car's engine block and cylinder head are among its two most important parts. Cast iron has traditionally been used for both parts due to its superior wear resistance, high-temperature strength, and castability. However, because cast

iron has a very high specific gravity (7.87 g/cm³), the engine block is the heaviest part of the car, comprising up to 3-4% of its overall weight [4]. The materials landscape for engine blocks is shifting toward adopting alternative, lightweight materials with a focus on lowering vehicle weight and CO₂ emissions. Aluminum and its alloys have increasingly risen to the top of the list of lightweight materials used in automobiles in recent years from the perspective of automotive engineering (Figure 2(a)). Additionally, the market is aiming for light vehicle aluminum content to reach 570 net pounds per vehicle by 2030, with cast aluminum alloy potentially making up more than 50% of that total (Figure 2(b)). Mercedes Benz used a sophisticated material composition with a high aluminum content to create the bodyshell architecture of the new AMG SL in order to guarantee low weight while maximizing stiffness (Figure 2(c)).

Due to their lightweight (2.7 g/cm³), which is around 65% lower than that of cast iron, aluminum alloys were thought to be an immediate replacement for cast irons and steels. Engine blocks with Al alloys instead of cast iron had a fair chance of losing up to 45% of their weight. Al alloy engine blocks have been produced since the late 1970s, and over the past 10 years, Al alloy cylinder heads have completely replaced cast iron ones [4]. Figure 3 depicts the trend in the weight percentages of aluminum, steel, and cast iron in light-duty American automobiles. As a result of the enormous demand from the automotive and aerospace industries, market observers anticipate a significant increase in Al production over the next years.

1.2 Need of aluminum alloys and composites

Lightweight materials for automobiles can be broadly categorized into four groups as potential replacements for

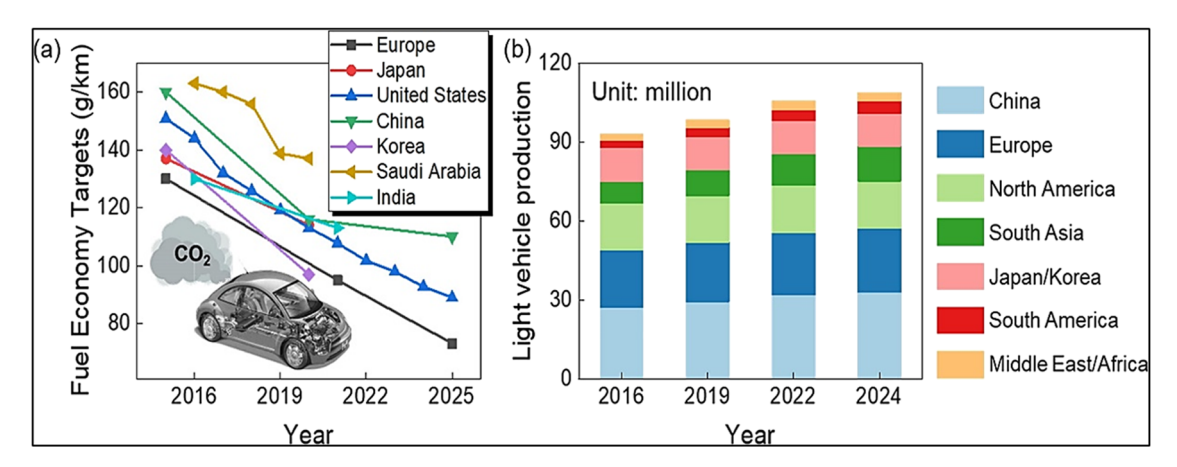


Figure 1: Pushing demand for lighter materials of automotives. (a) Various countries have different fuel economy goals (passenger vehicles). (b) Production of light vehicles in the main market, in million units [1].

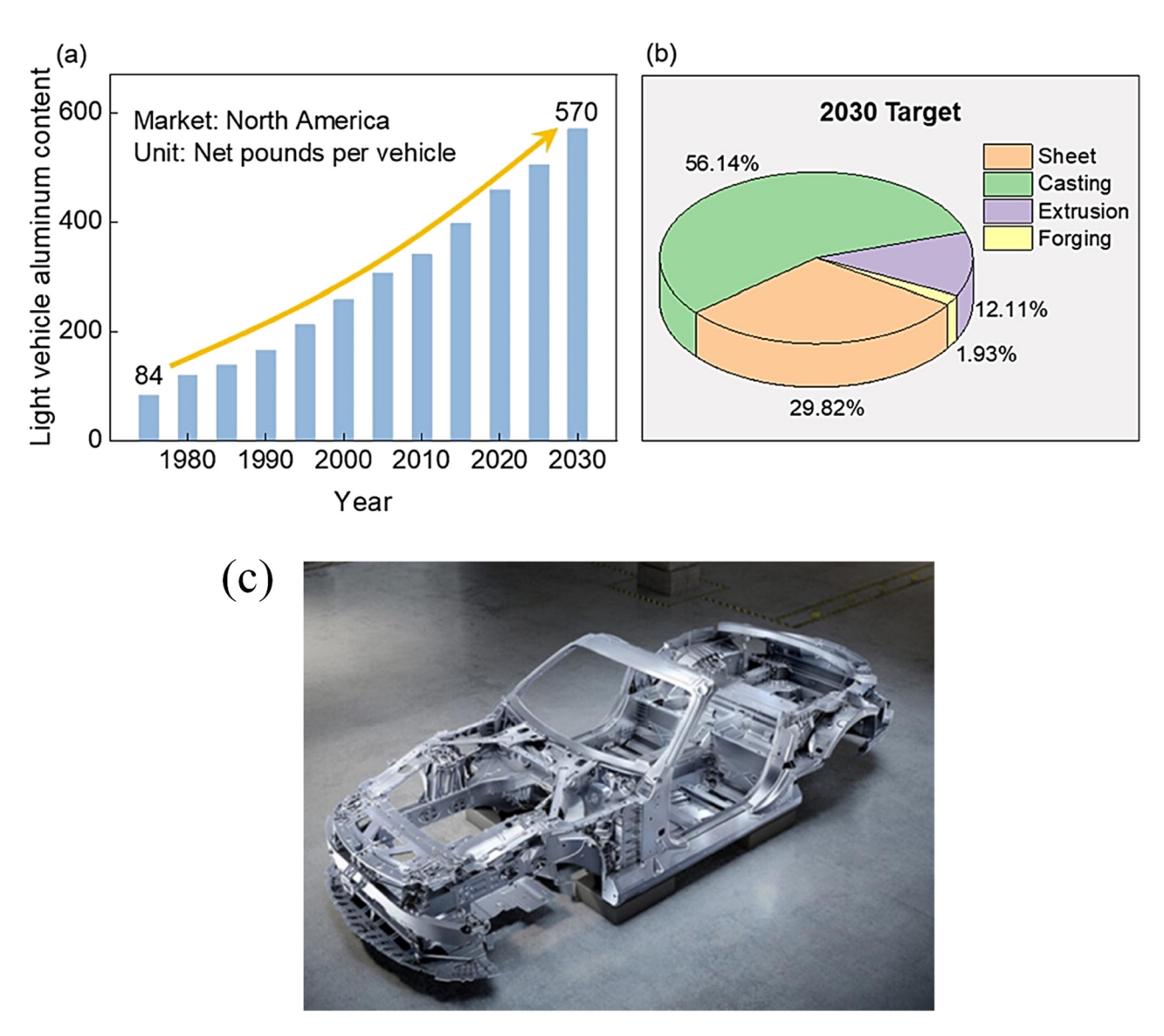


Figure 2: (a) Yearly change of aluminum content in the light vehicle from 1975 to 2030 (North American market. (b) Predicted proportion of different types of aluminum alloy in 2030. (c) New Mercedes AMG SL with high aluminum content in the bodyshell architecture to lower weight while achieving maximum rigidity (from Mercedes Benz [1]).

traditional engineering materials (such as steel and cast iron), including light alloys (such as aluminum, magnesium, and titanium alloys), the high-speed steel (HSS) family (such as conventional HSSs and advanced high-strength steels), composites (such as Al-based composites or carbon-fiber-reinforced plastics), and advanced materials (e.g., mechanical metamaterials). These lightweight materials have been used extensively in the automotive industry since the turn of the century for a variety of parts including the dashboard, bumper, engine, body shell, wheel, suspension system, brake, steering system, battery, seat, and gearbox (Figure 4).

1.3 Composites

Composites can save weight by 15–40% depending on the type of reinforcement used, and they also have other desirable qualities for the automotive sector, including high specific strength, strong corrosion resistance, design flexibility, and low thermal conductivity [5]. Hard ceramic materials are utilized as reinforcement particles, while ductile metal alloys are the preferred matrix materials. In metal matrix composites (MMCs), a second phase serves as reinforcement for the metal matrix. Ceramic particles and fibers made of different materials, such as other

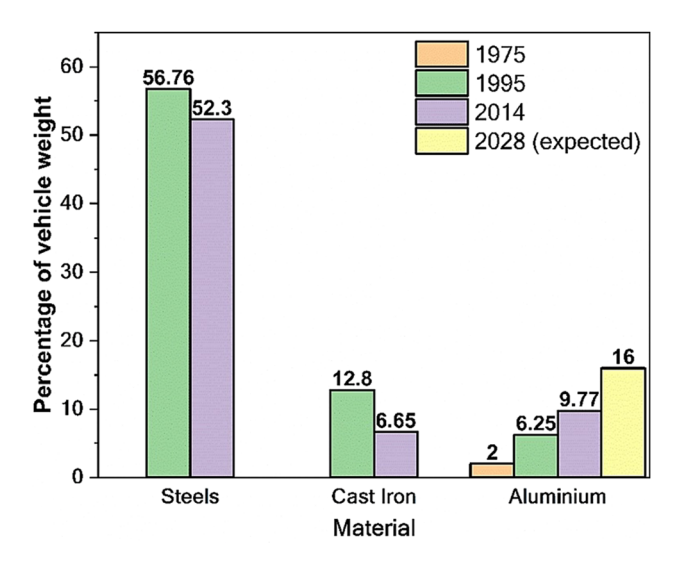


Figure 3: A trend in the proportion of steel, cast iron, and aluminum in the weight of automobiles [3].

metals, ceramics, and carbon, are two common types of reinforcing phases. There are various matrix materials available, including copper, magnesium, titanium, and aluminum (Al, Mg) (Cu). Al is the most favored matrix material accessible due to its remarkable qualities, including high strength-to-weight ratio, good corrosion resistance, better toughness, lower melting point, and affordability [6].

Aluminum matrix composites (AMCs) have drawn the attention of numerous researchers for the past 30 years to investigate their physical, tribological, mechanical, thermal, and electrical properties. When utilized in the production of composite materials, aluminum is preferred over other matrices due to its advantageous qualities, which can be adjusted by paying attention to the matrix, reinforcements, and processing techniques [7–16]. AMCs are a type of lightweight material that are frequently used in the automotive, aerospace, and defense industries [17,18] due to their wide range of characteristics, including low density, high strength, large elastic modulus, and excellent corrosion resistance [19,20]. Today's applications for aluminum alloys also include novel ones, such as 3D printing, the composite material industry, and aircraft. Because of aluminum's superior qualities, low cost, high scrap value, and

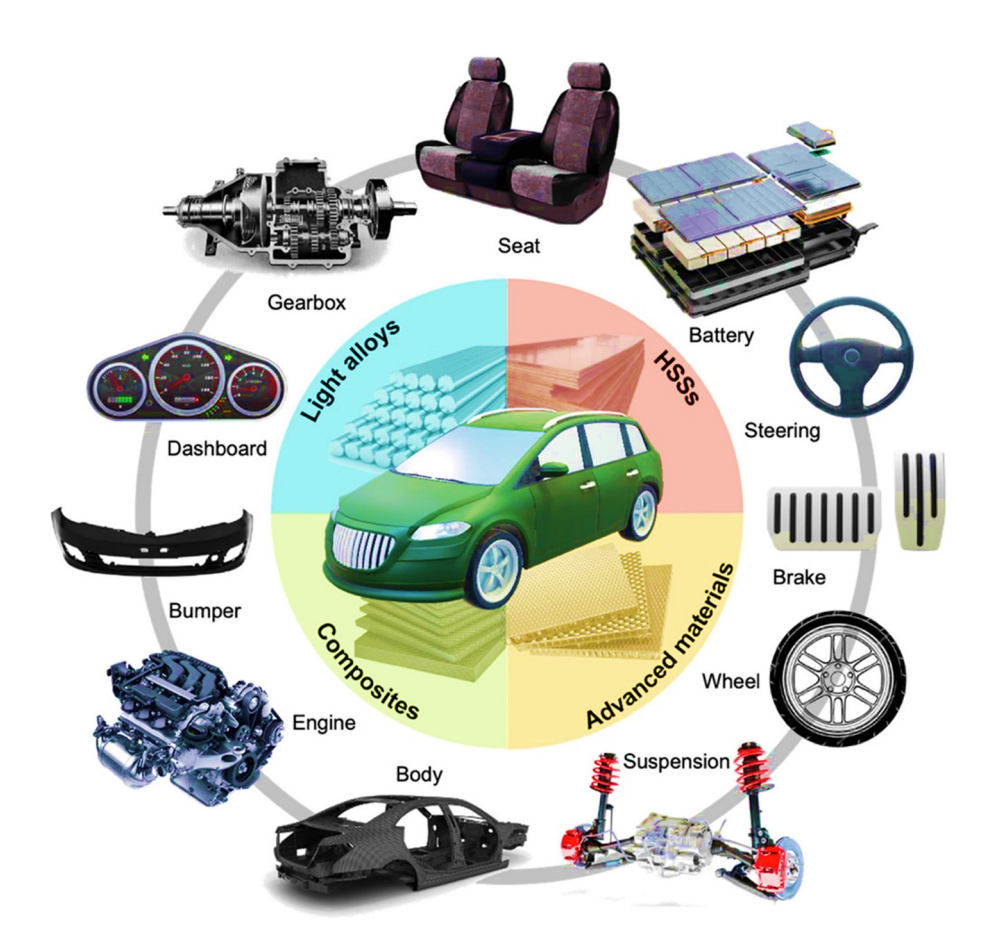


Figure 4: Typical lightweight materials for use in vehicle components include light alloys (such as aluminum, magnesium, and titanium alloys), HSSs, composites, and innovative materials.

Table 1: Frequently utilized Al alloy as a matrix material

Matrix material	Main alloying element	Characteristics	Applications	Ref.
Pure Al AA 2024	Aluminum 98.8–99.99 wt% Copper	Recyclability, ductility, and workability High machinability, surface finish, and fatigue strength	Automobiles, aerospace, and structural applications Wheels for cars, sheets for labs, biomedical applications, and aircraft parts	[22] [23]
AA 3003 AA 4043	Manganese Silicon	Good machinability, formability, and weldability Excellent resistance against corrosion	Heat exchangers, pressure vessels, and storage tanks Filler material	[24] [25]
AA 5083	Magnesium	Excellent corrosion resistance, medium-to-high wear resistance, good weldability	Appropriate for marine applications, hydraulic tubes for aviation, and various sheet metal operations	[56]
AA 6061	Magnesium and silicon (heat-treatable)	Enhanced strength, strong heat-treatment-induced corrosion resistance, excellent machinability, and weldability	Pipelines, storage tanks, truck parts, multipurpose alloy, and [27] railroad cars	[27]
AA 7075	Zinc (heat-treatable)	Good machinability and fatigue strength, medium-to-high corrosion resistance, low toughness, excellent strength for structural applications	Aircraft wings, airframes, gears and shafts for cars, and bicycle components	[28]
A356 (cast alloy) Silicon	Silicon	Superior machinability, resistance to wear, and exceptional fatigue strength	Pistons, castings for aircraft, and car chassis, pump impeller [29]	[59]

expanding recycling market, the aluminum industries are predicted to expand throughout the twenty-first century, and metal will likely continue to play a key role in our culture and daily lives [21]. To get even more desirable results, researchers need to have a better understanding of the many series of aluminum alloys when creating composite materials. Table 1 provides details about the matrix elements, along with their key characteristics and areas of use.

1.4 Necessity of reinforcements

The mechanical and tribological behavior of AMCs has recently been improved, thanks to the ongoing efforts of material scientists and engineers to develop novel and cutting-edge techniques. The performance of composites as a whole is determined by the reinforcement materials, hence efforts were made to choose the best ones. The most popular technique for enhancing mechanical and tribological behavior involves embedding hard ceramic particles. In a metal matrix, a wide range of ceramic particles are reinforced. However, TiC, SiC, and B₄C are the most popular ceramics in usage. The mechanical characteristics of MMCs are noticeably improved by their inclusion. Additionally, their inclusion improves the composites' wear resistance and frictional coefficient [30-32]. The key reinforcementrelated variables influencing the tribological performance of AMCs are as follows: volume/weight ratio, reinforcement size, and reinforcement shape, in that order. The right choice of reinforcement and its quantity enhances the physical, thermal, and mechanical properties of AMCs in addition to their tribological features. Since these materials determine the overall performance of the composites, studies were carried out to select the best-suited reinforcement materials. Particulate reinforcements were heavily utilized among the various types since they are readily available and have greater dispersive qualities. Additionally, the distribution of reinforcement is a significant factor when analyzing the mechanical and wear characteristics of aluminum composites [33-40].

If adequate reinforcements are not chosen and combined with aluminum alloy with care, it might be challenging to obtain the necessary qualities of the composite. Therefore, learning about different reinforcements and how they are used is crucial. Table 2 lists the characteristics of various types of reinforcements utilized in the creation of aluminum composites. Many researchers have studied the microstructural characterization of aluminum composites with improvements to their structural characteristics.

Table 3 highlights the results of MMCs after taking into account various types and forms of reinforcements.

To further improve the microstructure and mechanical properties of AMCs, several reinforcements are being developed [5,6]. When selecting reinforcements, three common issues are encountered: low density, high strength, and strong contact bonding with the matrix [7]. Currently, particle reinforcements (such as SiC, TiC, and GNP) clearly outperform fiber reinforcements in terms of pricing [8–10]. Additionally, it has been demonstrated that mixing the particle reinforcements with the matrix is simpler [11]. Ceramics are frequently chosen as the primary raw material for particle reinforcements [12]. Ceramic particles, however, frequently render poor microstructure in AMCs (such as aggregation and voids) [13). Because the thermal expansion coefficients of ceramic particles and the matrix are different, the agglomeration of ceramic particles frequently results in the early failure of AMCs [14]. Researchers have been searching for novel particle reinforcements to help solve this issue. Due to the extensive use of ceramic-reinforced composites with magnesium matrix for orthopedic implants. an emphasis on fabrication techniques, in vitro corrosion, and in vitro biocompatibility have been studied recently by Khorashadizade et al. [54].

1.4.1 Silicon carbide (SiC)-reinforced Al composites

SiC is one of the most often utilized ceramic particles that belong to the carbide nature category. It has exceptional resilience to wear and thermal shock. It behaves mechanically well at high temperatures. Mechanical seals frequently use SiC due to their chemical and wear resistance [55]. SiC is a synthetic (man-made) mineral distinguished by extremely high hardness and resistance to abrasion. Pump seals, valve parts, and wear-intensive applications like rollers and retainers for the paper industry are examples of common applications. Numerous scholars have studied how the homogeneous distribution of SiC microns or nanoparticles in the matrix of aluminum improves the interfacial, physical, and mechanical properties [5,56–59].

The fabrication process used as well as the quantity, size, and distribution of ceramic inclusions all affect the mechanical properties of Al/SiC composites. Al-based composite materials have a limited range of applications due to rapid strain softening at high temperatures [60].

Due to their unusual combination of low density and high strength, aluminum-SiC (Al-SiC) composites have been regarded as promising materials for lightweight structural applications. Several SiC-reinforced aluminum composites have been reported to improve the mechanical properties of the aluminum matrix by adding SiC [61-65]. SiC is a well-known reinforcing element and a classic essential component in the creation of composite materials based on aluminum [66-69]. Roy et al. [70] reported that the grain refinement effect greatly lowers the wear rate when SiC and CB are added to AA 7075 alloys. Bathula et al. [71] produced Al 5083/SiC nanocomposite powders via high-energy ball milling and by spark plasma sintering (SPS) at 500°C at a heating rate of 300°C/min and a cycle of 8 min. The mechanical properties were found to substantially increase after sintering employing SPS. By combining AA 6061 powders with varied SiC volume fractions in a WC vial using a planetary mill, Li et al. [72] produced the combinations. Then, using the SPS method, the composites were produced using a compaction pressure of 50 MPa and a heating rate of 50°C/ min. The sintering temperature and duration were maintained at 560°C for 3 min. As the proportion of SiC particles increased, the AA 6061-SiC composites became stronger. When the volume percentage of SiC was 20%, the composites' yield strength, ultimate tensile strength (UTS), and elasticity modulus were 373, 414 MPa, and 95 GPa, respectively. Dislocation, grain boundary, and secondary phase strengthening were all present in the composites. The effect of sintering temperature on the microstructure and selected properties of spark plasma sintered Al-SiC composites were investigated by Leszczyńska-madej et al. [73]. It was established that composites sintered at 600°C have higher bending strengths. The best degree of mechanical qualities was discovered to be present in composites sintered at 600°C with a 20 wt% SiC strengthening phase. These composites have a hardness of 55 HB and a transverse

Table 2: Physical properties of some reinforcements [41–43]

Characteristics	SiC	TiC	TiB ₂	Al ₂ O ₃	GNP
Density (g/cm³)	3.16	4.93	4.52	3.99	1.8-2.2
Melting point (°C)	1,955	3,067	3,225	2,043	3,600
Thermal conductivity (W/m/K)	16-120	17-32	60-120	30	4,840-5,300
Modulus of elasticity (GPa)	448	400	560	400	1,000
Hardness, Vickers (GPa)	35–45	24–32	25-35	18-21	_

Table 3: Frequently used reinforcements in AMCs and the study's findings

Reinforcement	Relevant properties	Applications	Ref.
TiC	High wear resistance and good strength	Automotive applications, brake disc, rotor, and cutting tools	[44-46]
SiC	High thermal conductivity, stiffness, hardness, and refractoriness	Rotors, braking discs, shafts, connecting rods, rubber tires, <i>etc</i> .	[47,48]
GNP	High strength-to-weight ratio	Tribological applications, nanofluids, memory devices, and energy storage	[49–51]
CNT	Ductility, corrosion resistance, excellent strength-to-weight ratio, and low density	Cylinder liners, sports utilities, and gears	[52]
TiB ₂	High strength and resistance to abrasion	Aerospace and automotive structural applications	[53]

rupture strength of 331 MPa for flexural strength. The effect of SiC wt% and sintering duration on the microstructural and mechanical behavior of Al 6061/SiC composites manufactured by powder metallurgy (PM) route were investigated by Surva [74]. The key factor for increasing the physical and mechanical properties of the composites was discovered to be a high interfacial bonding between Al and SiC in 15 wt% SiC. The finer microstructure is produced by reinforcing at its ideal proportion. The grain growth is slowed down by the hard ceramic particles, which function as a barrier to the grain boundaries. When the sintering time is increased from 1 to 3 h, Al 6061/SiC contacts are improved; however, when the sintering time was prolonged from 1 to 3 h, the hardness value of the 15 wt% SiC composite increased from 70 to 81 HRB. Reddy et al. [75] studied the performance of nanosized SiC-reinforced (0, 0.3, 0.5, 1.0, and 1.5 vol%) Al metal matrix nanocomposites that were created using hot extrusion and microwave sintering processes. With the addition of SiC, a discernible improvement in the strength (compressive and tensile) of the Al-SiC nanocomposites was observed. However, it has been found that as the volume proportion of SiC is increased, the ductility of Al-SiC nanocomposites diminishes. According to the thermal analysis, the coefficient of thermal expansion (CTE) of Al-SiC nanocomposites reduces as harder SiC nanoparticles are gradually added. In comparison to other produced Al-SiC nanocomposites, hot extruded Al 1.5 vol% SiC nanocomposites showed the best mechanical and thermal performance. Rahman and Al Rashed [76] studied the wear characteristics, microstructure, and mechanical properties of SiC-reinforced AMCs. An AMC reinforced with 7 wt% SiC showed maximum wear resistance, tensile strength, and compressive strength. The addition of SiC significantly improves the mechanical and wear characteristics of the base metal. Devaganesh et al. [77] examined the mechanical and tribological characteristics of hybrid SiC-Al 7075 MMCs. The results show that Al 7075 with 5%

SiC and 5% graphite composite outperforms all other hybrid composites by demonstrating superior mechanical and tribological properties; this may be because graphite and Al 7075-SiC work synergistically.

1.4.2 Titanium carbide (TiC)-reinforced Al composites

TiC is incredibly interesting due to its exceptional physical and mechanical qualities and, most importantly, its adequate wettability with aluminum [7]. It is also a very fascinating material due to its low density (4.93 g/cm³), high Young's modulus (400 GPa), and high hardness. As a result, it is possible to considerably improve the mechanical behavior of aluminum alloys, particularly by adding micronsized reinforcement to the TiC hard particles. To improve the desired mechanical properties of the produced composites, many researchers reinforced TiC in the Al matrix [59-63]. By using the hot consolidation approach, Mohapatra et al. [45] examined the microstructure and mechanical characteristics of Al-TiC composites. The composites showed improved Young's modulus and mechanical characteristics with notable ductility, demonstrating the importance of using TiC reinforcement. The scientists concluded that, like other aluminum-based MMCs, Al-TiC aluminum composites made using this approach are appropriate for structural and industrial usage. Ramkumar et al. [78] prepared AA 7075/(0, 2.5, 5, and 7.5 wt%) TiC MMCs via the stircasting route. They concluded that, compared to monolithic AA 7075 alloy, the bending strength of AA 7075-7.5 wt% TiC composites had significantly increased by 5.8 times with the addition of ceramic, which was attributed to the matrix's embedding of reinforcement particles and improved grain refinement. The increasing reinforcement in the matrix exhibited improved wear resistance due to an increase in the strength in the matrix, dispersion strengthening, and effective bonding. Saravanan et al. [79] synthesized aluminum 7075 matrix composites reinforced with TiC at

different weight percentages (0, 8, and 16 wt%) through PM. A significant improvement in wear loss was observed. Baskaran et al. [80] investigated the dry sliding wear behavior of high-strength 7075 AMCs with 4 and 8 wt% of TiC particulate reinforcement, synthesized using the reactive in situ casting technique. The optimal level combination for minimum wear rate was identified as 4 wt% TiC reinforcement, 9.81 N load, 3 m/s sliding velocity, and 1,500 m sliding distance. The microhardness and wear behavior of Al-4.5 wt% Cu-TiC nanocomposites produced by the PM route were investigated by Nemati et al. [81]. A planetary ball mill was used to combine the particles. The process of consolidation involved uniaxial pressing at 650 MPa. The sintering process was conducted for 90 min at 400°C. The findings showed that while relative density, grain size, and distribution uniformity drop as the TiC particle size is decreased to the nanoscale range and the TiC concentration is increased to optimal levels, the composite gains much more hardness and wear resistance. Composites reinforced with nanoparticles had a harder surface than those with TiC reinforcement in the micron range. The hardness of the composites increased steadily as the volume fraction of nano-size TiC was increased up to 5 wt%; however, after that point, particle agglomeration decreased the amount of useful particulate that was available, and the particle strengthening effect decreased.

The mechanical characteristics and microstructure of Al-15 wt% TiC composite synthesized using spark plasma, microwave, and traditional sintering were examined by Ghasali et al. [82]. The SPS, microwave, and conventional furnaces were used to sinter the material at temperatures of 400, 600, and 700°C, respectively. The findings revealed that the maximum relative density (99% of theoretical density), bending strength (291 \pm 12 MPa), and hardness (253 \pm 23 HV) were all found in sintered samples produced using SPS. An investigation on the Al 7075–TiC nanocomposite synthesized by mechanical alloying (MA) followed by hot pressing was performed by Azimi et al. [83]. In contrast, increasing the temperature over 400°C resulted in lower hardness due to significant grain development during hot pressing. Increasing hot pressing temperature and pressure improved sintering and mechanical properties. More intriguingly, the hot-pressing pressure value had a significant impact on how the milling time affected the mechanical properties. Furthermore, consolidation under ideal conditions produced a tensile strength of 725 MPa. The nano-sized TiC (5 wt%) particle-reinforced AA 7075 Al alloy composites made by ball milling and hot pressing were the subject of research by Salur et al. [84]. In terms of grain formation behavior, hardness, tensile strength, and relative density findings, the impact of milling duration on the microstructural and mechanical characteristics of the bulk TiCn/AA

7075 composites was assessed. The findings showed that a sample of AA 7075 alloy that had been hot-pressed and milled for 10 h had a hardness value that was three times higher than the initial value (94.43 HB). This was due to the homogeneous distribution of hardened nanoparticles within the matrix and the longer milling time. Tensile tests revealed that the UTS (284.46 MPa) of the 1 h-milled TiCn/AA 7075 composite was 40% higher than that of the original AA 7075 alloy (210.24 MPa). According to the findings, TiCn gradually dissolved into the matrix as ball-milling time increased and scattered evenly after 2h of milling. The milled powders were heat-pressed for 30 min at 400 MPa and 430°C to consolidate them. Kar et al. [85] used TiC as the reinforcement for Al 7075 in their study. They found that the coefficient of friction is lowered by 20% due to the improved strength and hardness with the optimal amount of TiC. Using an electric stir-casting process, Rao et al. [86] fabricated AMMCs using TiC (2–10%) as a reinforcing material and the Al 7075 alloy as the metal matrix. A pin-on-disc device was utilized as a wear mechanism. Weight loss, friction coefficient, and wear rates for both reinforced and non-reinforced composites were measured. The findings show superior wear resistance to basic metal. The most important factor affecting the hardness of composites created by stir-casting treatment was the weight percentage of ceramic particles. As a result, Al 7075, which contains 8% TiC pieces, demonstrated the best hardness. The wear resistance increases as the weight percent of TiC increases. The wear resistance does not greatly improve with the addition of 10% TiC. As the weight proportion of TiC particles increased in comparison to the base alloy, the wear cost of the composites decreased. According to a research study, Al 7075/TiC exhibits superior mechanical and tribological capabilities. Devaneyan et al. [87] studied the mechanical behavior of aluminum 7075 reinforced with SiC (SiC) and TiC via the PM route. They found the highest value of microhardness (52.12 HV) with 90% of Al 7075, 4% of SiC, and 8% of TiC.

The experimental studies for the enhanced dry sliding properties of the AA 6063/TiC composite were carried out by Moorthy *et al.* [46]. According to the study, composite materials with higher fractions of TiC particles have much greater wear resistance, which is further improved by heat treatment. The effect of reinforcement on composite wear resistance is greatest when 9 wt% of TiC reinforcement is used for solutionized and aged conditions. Different volume fractions, ranging from 1.5, 3, and 6 vol%, of 20–30 nm diameter nano-sized TiC particles were used to strengthen the AA 6005 by Cabeza *et al.* [88]. By lengthening the milling duration, the microhardness of the unreinforced and reinforced matrix powder continuously increases. After 10 h of milling, the nanocomposite with 1.5 vol% of n-TiC particles

has a hardness that is almost 1.3 times that of the Al alloy matrix, and it has a hardness that is nearly 1.55 times that of the nanocomposite with 3 and 6 vol% of n-TiC particles. Sujith et al. [44] investigated the abrasive wear behavior of Al 7079/TiC in situ MMCs produced by the in situ melt reaction method. It explored how in situ Al-7079 would be affected by the sliding distance applied force and the weight percent (5, 7, and 9) of TiC. According to experimental findings, the weight percent of TiC and the sliding distance had a greater impact on the coefficient of friction, and the applied force had a significant impact on the weight loss. There was a reduction of almost 40% loss in the weight at 9 wt% of TiC reinforcement addition as compared to that of the base Al-7079 matrix. Ravi Kumar et al. [20] studied the TiC particles (2,4,6, 8, and 10 wt%) reinforced in aluminum alloy (AA 6063) composites fabricated by the stir-casting method. The density, hardness, and tensile strength of composites increased to a maximum of 7.8, 20, and 19.55%, respectively, while adding TiC particles. Gopalakrishnan and Murugan [89] produced and investigated specific strength and wear resistance. They concluded that the specific strength of the material improved appreciably with the increased addition of TiC. Percentage elongation was also maintained at an appreciable level even though the specific strength was increased. Hence, this method is the most economical and effective way of producing the Al-TiC composite. The wear rate increased marginally with increased TiC addition.

1.4.3 Graphene nanoplatelet (GNP)-reinforced aluminum composites

Graphene has attracted considerable attention in the last several years because of superior properties such as high mechanical strength and modulus, electrical and thermal conductivity, and optical transmittance [90-92]. A twodimensional hexagonal lattice of carbon atoms, graphene serves as the fundamental building block of other allotropic forms of carbon, such as fullerenes, diamonds, carbon nanotubes, and graphite [93]. Graphene is the thinnest material made of just a single layer of carbon atoms bound together by a backbone of overlapping sp² hybrid bonds. The unusual characteristics of graphene originate from the 2p orbitals, which form the p-state bands that delocalize over the sheet of carbons that create graphene. Table 4 summarizes the unique properties of graphene with exceptional mechanical strength, high Young's modulus, low density, excellent electrical and thermal conductivity, as well as large theoretical specific surface area with unique geometry, making them perfect reinforcement for the composites [94,95]. In comparison to diamond (1.2 TPa),

Table 4: Physical and mechanical properties of graphene [101]

Characteristics	Values
Density	1.06-2.2
Tensile strength (GPa)	130
Young's modulus (TPa)	1.02
Thermal conductivity (W/mK)	5,300
СТЕ	$(-8 \pm 0.7) \times 10^{-4}$

steel (200 GPa), and copper, Young's modulus measured by various simulations in the graphene plane can be as high as 1-1.8 TPa (100 GPa). Both have tensile strengths that are equal to annealed steel (700 MPa) and annealed copper (800 MPa), are half as dense as aluminum, and range from 100 to 200 GPa (20 times that of high-strength alloys) (200 MPa) [96,97]. Graphene's exceptional electrical characteristics, which include outstanding carrier mobility and capacity, are also well recognized and make it a desirable material for use in future high-speed electronics [98]. Exfoliated semiconducting graphene demonstrated carrier mobility ranging from 230,000 cm²/V/s in suspended structures to 100,000 cm²/V/s on insulating surfaces. Additionally, both have current carrying capacities that are 1,000 times greater than those of the copper wire (109 A/cm²) and above [99]. In a similar vein, graphene's in-plane thermal conductivity can range from 3,000 to 7,000 W/mK, which is far higher than that of copper (400 W/mK), carbon fiber (1,950 W/mK), diamond (2,000 W/mK), and carbon fiber [100]. Due to these properties, graphene has found a wide range of potential applications in medicine, paper, electronics, and composite materials.

The physical, mechanical, and wear behavior of the matrix material is improved by the addition of hard ceramic particles. Ductility and fracture toughness are sacrificed in order to obtain this gain in characteristics. Additionally, the use of hard ceramic reinforcement increases the hardness, making machining challenging and expensive. Balancing hardness, wear resistance, and machining of the ceramicreinforced composites is challenging. One of the most popular combinations is an aluminum metal matrix supplemented with GNP because GNP improves the composites' wear resistance and machinability. A thin coating of graphite is formed under sliding conditions to prevent direct metal-to-metal contact, hence minimizing wear loss [102,103].

In comparison to aluminum composites reinforced with other ceramic particles like Al₂O₃ and SiC, adding GNP particles to an aluminum matrix improves tribological characteristics. Due to the addition of GNP particles, self-lubricating composites exhibit significantly lower friction and wear rates than unreinforced matrix metals [101,104]. In addition, the intrinsic lubricating action of the GNP particles reduces the frictional heat produced at the interface. As a result of the decreased friction force, wear resistance will consequently increase [105,106]. Due to the exceptional capabilities of GNPs, aluminum MMCs with GNP reinforcement have been researched recently [107-111]. Wang et al. [112] produced graphene-reinforced aluminum composites by the PM technique. Aluminum composites with only 0.3 wt% GNPs inclusion have tensile characteristics that are 62% higher than pure aluminum. According to Rashad et al. [113], graphene has an impact on the hardness, tensile strength, and compressive strength of aluminum composites. The tensile strength (+11.1%) and Vickers hardness (+11.8%) for 0.3 wt% of pure aluminum are both higher. The compressive strength decreased by 7.8%, but the addition of GNPs increased it. Bastwros et al. [114] published a study on the flexural strength of PM-produced graphene-reinforced aluminum nanocomposites. When compared to the Al 6061 alloy, a strength improvement of 47% was found. Gürbüz et al. investigated the impact of process variables on the hardness and microstructure of aluminum composites, including sintering time, temperature, and graphene content. According to their findings, the ideal sintering conditions were 180 min, 630°C, and 0.1 wt% of graphene. Graphene-reinforced aluminum composites' hardness increased from 28 2 to 57 2.5 HV [115]. Table 5 illustrates a summary of the reported studies along with key observations for the fabrication of Gr-AMMCs by MA. A summarized overview of the studies utilizing the solution mixing technique with major observations and key findings is presented in Table 6. Recent investigations on Mg-based matrix composites incorporating GNPs have been summarized by Abazari et al. with regard to their mechanical, corrosion, and biological properties. Their findings indicate the advantages of GNPs over other reinforcing phases like ceramic particles, such as their synergistic ability to increase ductility while strengthening and decreasing weight, are quite compelling [116].

1.4.3.1 Fabrication methods for GNP-reinforced AMCs

Over the past 10 years, researchers have produced AGNPs using a variety of processing methods, including PM, friction stir processing (FSP), casting, selective laser melting (SLM), mechanical impregnation, *etc.* Casting and FSP are the next most popular techniques after PM (Figure 5). In addition to these methods, researchers have also experimented with 3D printing, high-pressure torsion, mechanical impregnation, and other methods to manufacture AGNPs.

Soon after the graphene discovery, many research investigations started using graphene as reinforcement. The interest in using graphene as reinforcement in metallic

Table 5: Reported Al/GNPs synthesized by MA

Matrix	Matrix Composition	Dispersion strategy	Consolidation treatment	Key observations	Ref.
₹	0.25-1.0 wt% GNP	Ball milling	Compaction and sintering	Longer milling times may promote graphene distribution in the matrix and lead to smaller particle sizes. However, it can also cause the structure of GNPs to amorphized	[111]
A	0.5–1.0 wt% GNF	Cryomilling	Extrusion and annealing	Low milling temperatures make it possible to prevent the formation of intermetallic compounds. However, 1.0 wt% of GNPs were observed to aggregate. A maximum of 4.0 wt% graphene concentration was suggested	[134]
I	0.3–0.7 vol% few-layer graphene (FLG)	Planetary ball milling, high- energy ball milling	Compaction and hot rolling	Graphene sheets that are rolled along the rolling axis may become partially aligned and wrinkled. FLG has a substantially wider contact area with the matrix than multiwalled carbon nanotubes (MWCNTs), which have a 2.6 times smaller surface area. When compared to MWCNTs, graphene has a higher strengthening efficiency	[135]
ΙΑ	1.0 wt% reduced graphene oxide (RGO)	Mechanical mixing and ball milling	Hot extrusion, annealing, and shot peening treatment	Shot peening can significantly improve dislocation pile-up by reducing the domain size, boosting dislocation density, and even causing the creation of nanocrystalline layers	[136]

Table 6: Reported AI/GNPs synthesized by solution-assisted mixing (semi-PM)

Matrix	Reinforcement	Dispersion strategy	Consolidation treatment	Key observations	Ref.
I	0.3 wt% Gr	Ball milling, ultrasonication, mixing, and dispersing agent	Compaction, sintering, and hot extrusion	Due to shape compatibility, the flake-like morphology of the Al powder improves interaction with graphene oxide (GO) sheets. PVA can also improve the wettability of GO and Al powder. The qualities of the composite can be compromised by incomplete GO reduction	[137]
¥	0.3 wt% RGO	Ball milling, ultrasonication, and mixing Compaction and hot pressing	Compaction and hot pressing	Milled Al powder with a flaky shape improves interaction with graphene by electrostatic interaction, which can be passivated by the formation of oxide film on the flake surface	[138]
Ι	0.75-1.50 vol% RGO	Ultrasonication, ball milling and stir mixing	Uniaxial compaction, hot pressing, and hot rolling	Dispersion is aided by the electrostatic contact between GO and Al. Because of the composite's nanolaminated structure, graphene sheet may prevent dislocations and produce high strength. Microcracks appeared when the content was more than 2.5 vol%. During processing, a layer of amorphous alumina was also formed	[139]
₹	0.1–0.5 wt% Gr	Ultrasonication, stirring, and surfactant	Press sintering	Due to the electrostatic interaction facilitated by the surfactant, the oppositely charged surfaces of GO and Al powder can bind and disperse well. However, agalomeration accelerates as loading content exceeds 0.3 wt%	[140]
₹	0.07-0.3 wt% RGO	Ultrasonication and mixing	Cold compaction and sintering	When consolidating the composite powder, a higher compaction pressure, particularly in the core, can generate parts with a high density and therefore improved mechanical performance	[141]
Ā	0.5-1.0 wt% GNP	Ultrasonication and mixing	Cold compaction and sintering	Al and graphene did not interface well. Carbide production and GNP aggregation can successfully improve characteristics up to 0.5 wt%	[142]
Α	0.5-5.0 wt%	Ultrasonication	SPS	Poor mechanical performance was the outcome of GNP aggregation above 1.0 wt%	[143]
Ι	0.1 wt% FLG, and few- layer graphene oxide	Ball milling, ultrasonication, and mixing Compaction and sintering	Compaction and sintering	Al and GO powders interacted more readily with one another when functional groups were present on the GO surface, improving the mechanical performance. However, FLG had a poor interaction with the Al matrix, and the composite's underlying strength was caused by inhomogeneous dispersion	[144]
₹	0–1.5 wt% GNP	Solution ball milling, ultrasonication, and surfactant	Cold compaction, and sintering	Density is affected by increased pressure and the presence of graphene. All matrix and graphene's interfacial interaction are not investigated	[145]

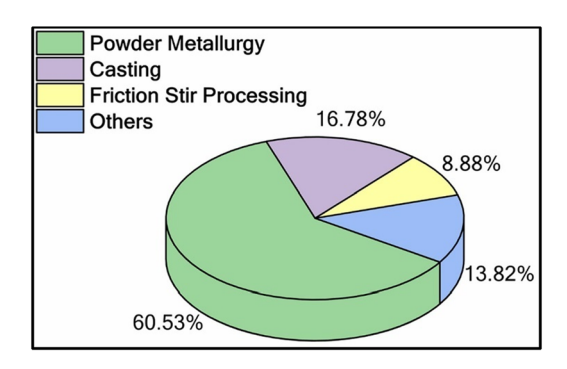


Figure 5: The percentage contribution of different processing techniques employed by researchers to produce AGNPs [3].

matrices is spurred by the successful incorporation of graphene into polymers to fabricate high-performance polymer composites with tremendous increment in the mechanical and thermal properties [117]. In comparison to polymers, metal matrix graphene is clearly superior due to its stability at higher temperatures, increased strength, rigidity, and greater electrical and thermal conductivity. However, it is quite challenging to introduce graphene into the metals successfully due to some critical issues such as difficulty in obtaining a uniform dispersion and structural retention during processing. These challenges are caused by graphene's larger surface area, which results in agglomeration clusters and twists as a result of strong van der Waal forces (surface tension) between carbon atoms in the graphitic structure [118]. This tension produces enormous surface energy that makes it difficult to wet metal and makes separation easier [119]. Thus, with such concerns, it is very important to embrace processing techniques that would ensure the successful incorporation of graphene in metal matrices by addressing these issues simultaneously. The proper processing technique plays a vital role in the final properties of composites. As per published reports, a variety of processing techniques have been followed to develop graphene-reinforced aluminum matrix nanocomposites (AMNCs). However, the most adopted methods for CNT and graphene-AMNC fabrication are PM [120-127], melting and solidification, and electrochemical deposition [128,129]. Recently, some novel processing techniques such as molecular level mixing, thermal spray, melt integration, and FSP [130-132] were also introduced to address the main challenges of graphene AMNCs. Graphene dispersion (porosity formed by agglomeration) is the core problem encountered during processing; therefore, for high-quality development of graphene-reinforced AMNCs, achievement of the uniform dispersion is a critical concern. Among the above technigues, PM is the most common and widely accepted applied technique to fabricate graphene-reinforced AMNCs. Most of

the studies carried out on carbon nanofiller (carbon nanotube and graphene) incorporation into various metallic matrices mainly with Al, Cu, and Mg using PM techniques. In the last decades, PM emerged as the most efficient method and has great potential to address issues connected with carbon nanofiller specifically graphene materials, i.e., successful uniform distribution through processing parameter optimization. Due to its widespread industrial-scale adoption, PM is regarded as the superior processing method for graphene-AMNCs. Due to several reasons such as simplicity, flexibility, and near net shape capability, any composition can be formed due to less involvement of thermodynamics and the phase diagram as in the case of ingot metallurgy. Finally, parts produced from the PM process were far better in mechanical properties due to the better capability to generate uniformly distributed particles. As in ingot metallurgy, low-density graphene gets separated due to buoyancy forces and is not fully integrated. The incorporation of graphene as reinforcement in light metals like Al matrices is majorly dependent on the PM processing steps and their parameters as they dictate the final microstructure and ultimately final properties of the AMNCs.

Developing AMNCs with the PM technique starts with the process of mixing and blending with the initial raw metal like Al metal and nanofiller (graphene) powders using high-energy ball milling (planetary ball mill) or low-energy ball milling (horizontal tumbling milling). This kind of PM processing is also termed MA, which is then followed by consolidation of the mixed nanocomposite powder [133]. The most widely adopted consolidation techniques are cold compaction and pressure sintering, cold isostatic pressing, deformation-assisted sintering, hot isostatic pressing (HIP), and SPS.

1.4.3.2 Influence of aluminum carbide (Al₄C₃) formed at the Al-GNP interface

The interaction between graphene and aluminum leads to the formation of aluminum carbide (Al_4C_3) due to its low Gibbs free energy of $-196\,\mathrm{kJ/mol}$ at 298 K. The reaction between carbon and aluminum is thermodynamically favorable, making it challenging to control the interface reaction in graphene-reinforced MMCs. It is worth noting that the effects of the Al_4C_3 phase on the mechanical properties of AMCs reinforced with graphene are currently a topic of ongoing discussion. It has been explained by numerous recent studies with microstructural observations of graphene-reinforced Al composites.

Recently, Yu *et al.* [146] investigated the microstructural evolution of graphene-reinforced aluminum composites. Figure 6 presents transmission electron microscopy

(TEM) images illustrating the microstructure of an extruded composite consisting of aluminum (Al) and 0.5 wt% GNPs. As shown in Figure 6(a), the Al matrix exhibits equiaxed grains with a relatively uniform grain size of approximately 450 nm, which aligns closely with the calculated value obtained from X-ray diffraction (XRD) results. Figure 6(b) displays the SAED pattern for the region highlighted by a white ellipse in Figure 6(a). This SAED pattern confirms the presence of both Al and GNPs, with the GNPs specifically marked by blue dotted lines in Figure 6(a). Furthermore, the two-dimensional TEM images in Figure 6(c) and (d) demonstrate that the GNPs are linearly distributed, indicating successful dispersion within the Al matrix. The high-resolution TEM (HRTEM) micrograph in Figure 6(d) reveals the interface between the Al matrix and GNPs. The blue box highlights a well-defined GNPs/Al interface, suggesting the absence of any interfacial reaction. Conversely, the green box indicates the presence of an Al₄C₃/Al interface, where layers with a d-spacing of approximately 0.2897 nm,

corresponding to the (101) orientation of the Al_4C_3 phase, are identified in the inset of Figure 6(d). Additionally, an orientation relationship of $(200)_{GNPs}//(101)_{Al4C_3}$ is observed, indicating that Al_4C_3 nucleated at the GNPs/Al interface and grew toward the GNPs. Consequently, it is confirmed that some of the GNPs reacted with the Al matrix, which could explain the absence of GNP peaks in the XRD patterns obtained after the extrusion process.

In another investigation, Zhou *et al.* [147] demonstrated the improvement in the interfacial load transfer and strength of FLG/Al composites through interfacial reaction. By manipulating the sintering temperature, monocrystalline Al_4C_3 nanorods were formed, tightly connecting the FLG platelets with the Al matrix. By TEM analysis and a shear lag model, it was observed that the Al_4C_3 nanorods effectively facilitated load transfer at the FLG–Al interface, resulting in a significant enhancement of composite strength. It was observed that upon increasing the sintering temperature to 883 K, it was confirmed through X-ray photoelectron

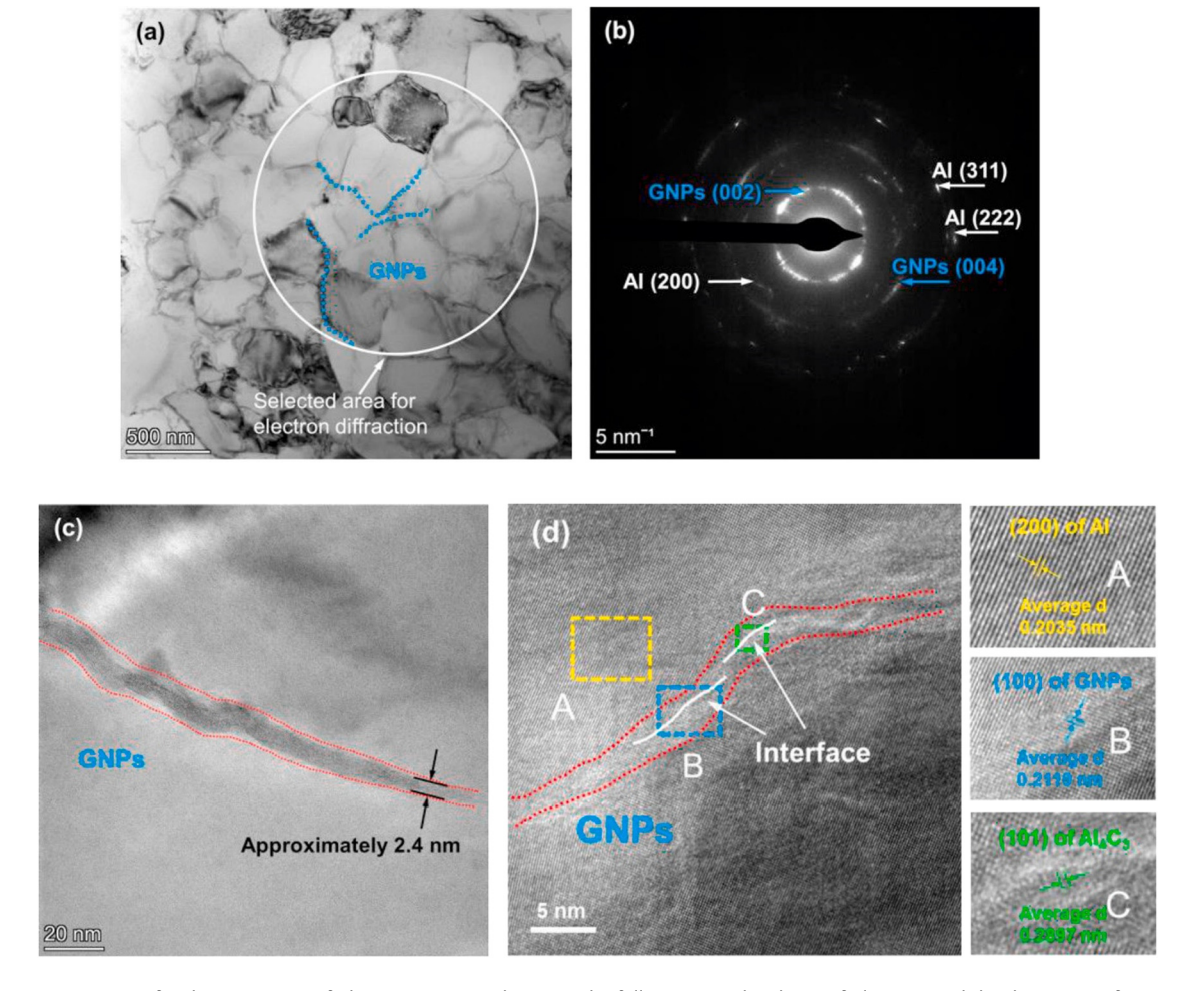


Figure 6: TEM images for the composite of Al–0.5 wt% GNPs, depicting the following: (a) the shape of Al grains and the dispersion of GNPs, (b) the SAED pattern illustrating the presence of Al and GNPs, (c) the characteristic morphology of GNPs, and (d) the condition of the interface [146].

spectroscopy (XPS) analysis that an interfacial reaction occurred at the interfaces between FLG and Al. The presence of the Al_4C_3 phase with a rhombohedral crystal structure, characterized by lattice parameters a=0.334 nm and c=2.50 nm, was identified by the SAED patterns (insets in Figure 7(a) and (c)) and lattice images (Figure 7(d)). The Al_4C_3 phase

exhibited a rod-like morphology, distinct from the initial sheet-like GO. Based on statistical analysis of 50 TEM images, the Al_4C_3 rods were found to have an average length of approximately 90 nm and a diameter of approximately 25 nm. Notably, one end of the Al_4C_3 rod was tightly bonded to the FLG platelet, while the other end was embedded in the

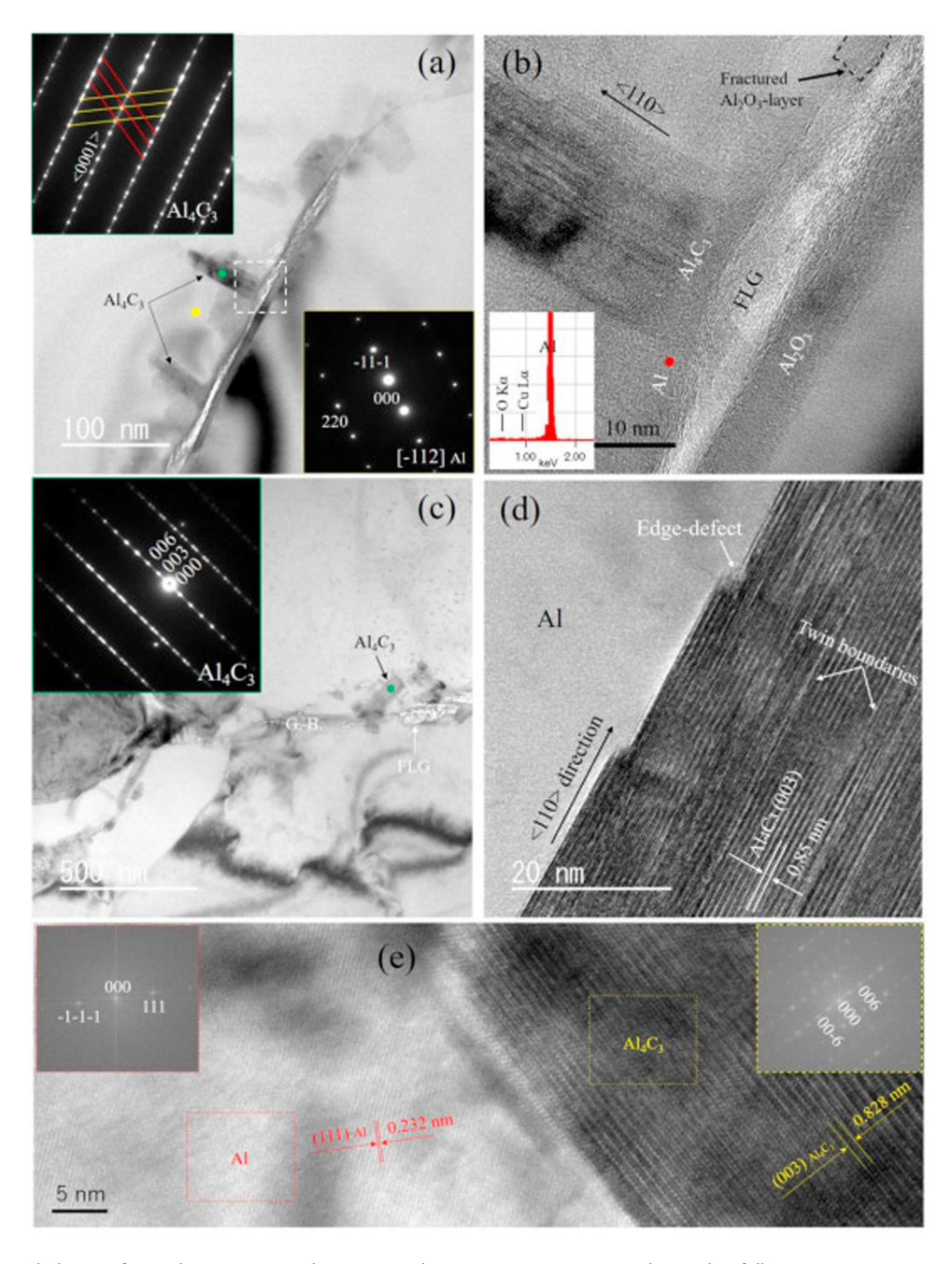


Figure 7: The morphologies of FLG/Al composites in the transversal cross-section at 883 K are depicted as follows: (a–c) a TEM image illustrating the formation of Al_4C_3 at the FLG–Al interface, and (d–e) high-resolution TEM (HRTEM) images displaying the Al_4C_3 –Al interface. In (b), the white square area in (a) is magnified. The insets in (a) showcase the diffraction patterns of Al_4C_3 obtained from the green spot and Al obtained from the yellow spot. The inset in (b) exhibits the energy-dispersive spectroscopy analysis taken from the red spot. The inset in (c) reveals the diffraction pattern of Al_4C_3 acquired from the green spot. Lastly, the insets in (e) display the fast Fourier transform patterns of Al from the red square and Al_4C_3 from the yellow square [147].

Al matrix (Figure 7(a)–(c)). The formation of this unique structure can be explained as follows: during the high-temperature SPS, the liquid Al momentarily infiltrated the boundaries of Al particles through the partially fractured side of the Al₂O₃ layer (Figure 7(b)) at the sandwiched Al₂O₃-FLG-Al₂O₃ interface, facilitated by the surface-cleaning effect of the SPS process. This infiltrated liquid Al directly contacted the FLG platelets, allowing for a possible reaction of carbon with aluminum, leading to the formation of Al₄C₃ $(C + Al \rightarrow Al_4C_3)$. While pristine graphene surfaces are chemically stable and do not react with molten Al, reduced graphene oxide (r-GO) contains intrinsic defects such as vacancies or topological defects that can serve as preferred reaction sites for aluminum atoms. Due to the higher free energy of the graphitic prism planes compared to the basal planes, Al₄C₃ preferentially grew along the (110) direction (Figure 7(b) and (d)). Some edge defects were observed in the Al₄C₃ crystals (Figure 7(d)), attributed to their rapid growth rate. Assuming a lateral size of approximately 700 nm and a thickness of approximately 2 nm for FLG, it can be concluded that certain graphene sheets within the FLG acted as carbon sources, contributing to the formation of Al₄C₃ rods. In this scenario, the Al₄C₃ phase strongly connected the Al matrix and the unreacted FLG sheets through a locking effect (Figure 7(b)). The interface linking Al₄C₃ and Al exhibits a highly clean and tightly bound structure (Figure 7(d)–(e)). Within the Al₄C₃ phase, a twinned structure was observed (Figure 7(d)), with a mirror plane of (001) and a twinning direction of [110] (Figure 7(a), inset). This twinning phenomenon is attributed to the compressive stress generated by the disparate CTEs between Al (2.5 \times 10^{-5} /K) and Al₄C₃ (3.6 × 10^{-6} /K) [30]. The formation of twins signifies a robust Al₄C₃/Al interface capable of transferring loads. This suggests that a small amount of Al₄C₃ was formed, enhancing the strength of the FLG-Al interface through covalent bonding, while simultaneously maintaining the inherent strength of FLG for reinforcing the composite.

Additional reports have supported that Al₄C₃ formation could reduce mechanical characteristics due to the induction of microcracks, leading to the early failure of Al/graphene composites [120,148,149].

In conclusion, it is still debatable whether the presence of Al₄C₃ strengthens the interfacial interaction between aluminum and graphene. According to some reports, Al₄C₃ increased graphene's ability to transfer loads and offered a strengthening impact that helped the material's strength. The integrity of graphene also influences the creation of Al₄C₃, with the possibility of Al₄C₃ formation increasing with decreasing graphene integrity. According to some reports, Al₄C₃ serves as a harmful interfacial phase and causes early failure as a result of the formation of microcracks. Nevertheless, the parameter affecting Al₄C₃ formation is well worth addressing and optimizing in future studies to attain enhanced properties because they may have positive or negative consequences on the strength.

2 Processing techniques of aluminum-based composites

Composites for the aluminum matrix can be produced using a variety of techniques. Mechanical performance, including tensile strength, impact strength, hardness, fatigue, and cost-effectiveness, is significantly impacted by the fabrication procedures. The fabrication procedures are divided into different categories, as shown in Figure 8, based on how the matrix is handled, whether it is in a solid, liquid, or other form (such as semi-liquid, compo-casting, etc.). An overview of the processes available for producing aluminum MMCs is given in this section.

2.1 Solid-state processing

Metal is processed in a solid or semi-solid state using the solid-state method. The issue of metal and reinforcement materials oxidizing is solved by processing at a lower temperature. High pressure is used in solid state operations at temperatures above ambient but below the melting point of the metal in order to produce a bonding or interacting interaction. Al-MMCs were produced using a variety of solid-state methods, including PM and diffusion bonding.

2.1.1 Powder metallurgy

The mass manufacturing of porous bronze bushes for bearings and the production of tungsten carbides in the 1920s marked the beginning of modern PM technology. The production of a wide range of ferrous and nonferrous materials, including various composites, advanced throughout the Second World War, and from the years following the war until the early 1960s, there was a sustained growth period. Since then, the increase in PM has accelerated due to three possible causes: cost-effective processing, distinctive features, and captive processes. The PM process is primarily a quick, affordable, and high-volume manufacturing technique for producing precise components from powders. It is possible to roll powders into sheets, extrude them into bars, etc., or condense them isostatically into

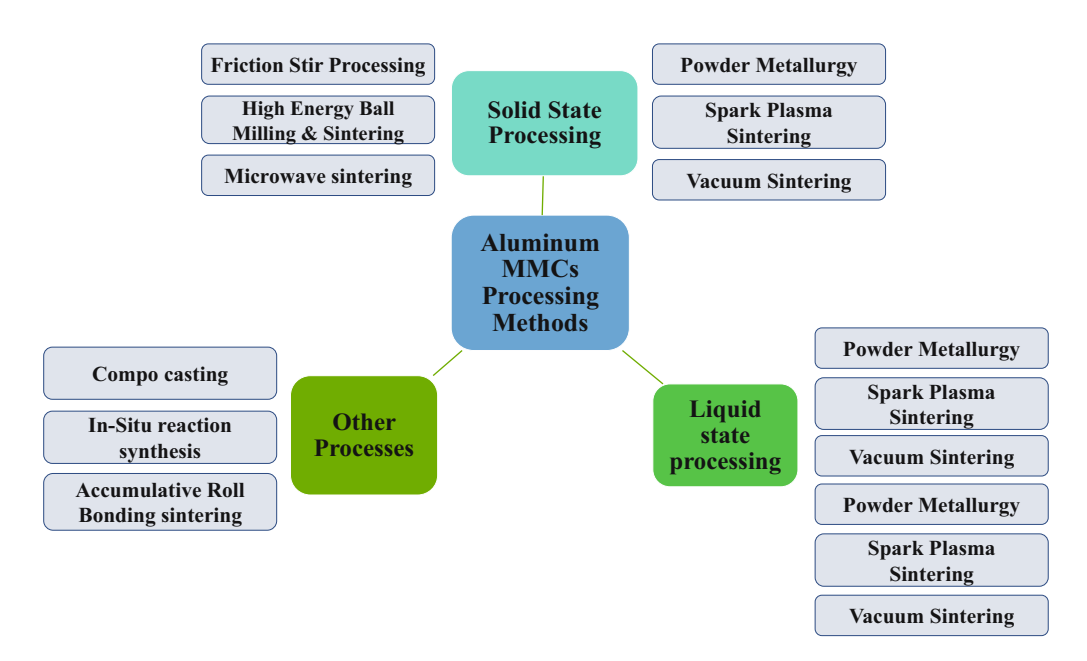


Figure 8: Process classification for manufacturing aluminum MMCs.

components with more complex geometries using a variety of related consolidation techniques. The technology of powder forging has become well-established over the past 10 years for creating precision engineering parts with qualities similar to those of traditional forgings from powders. The general flow diagram for processing PM is shown in Figure 9.

PM is a method of processing metals in which metallic powders are used to create parts. The powders are compressed into the proper shape as part of the standard PM production process, and then they are heated to cause the bonding of the particles into a hard, rigid mass. The process of pressing, also known as compression, is carried out in a press-type machine with tools made, especially for the component being produced. PM and tooling are therefore best suited for medium and high production levels. Tooling typically comprises a die and one or more punches. Sintering, a type of heating procedure, is carried out below the metal's melting point. Mass production of PM parts in net or nearly net shape can eliminate or minimize the requirement for

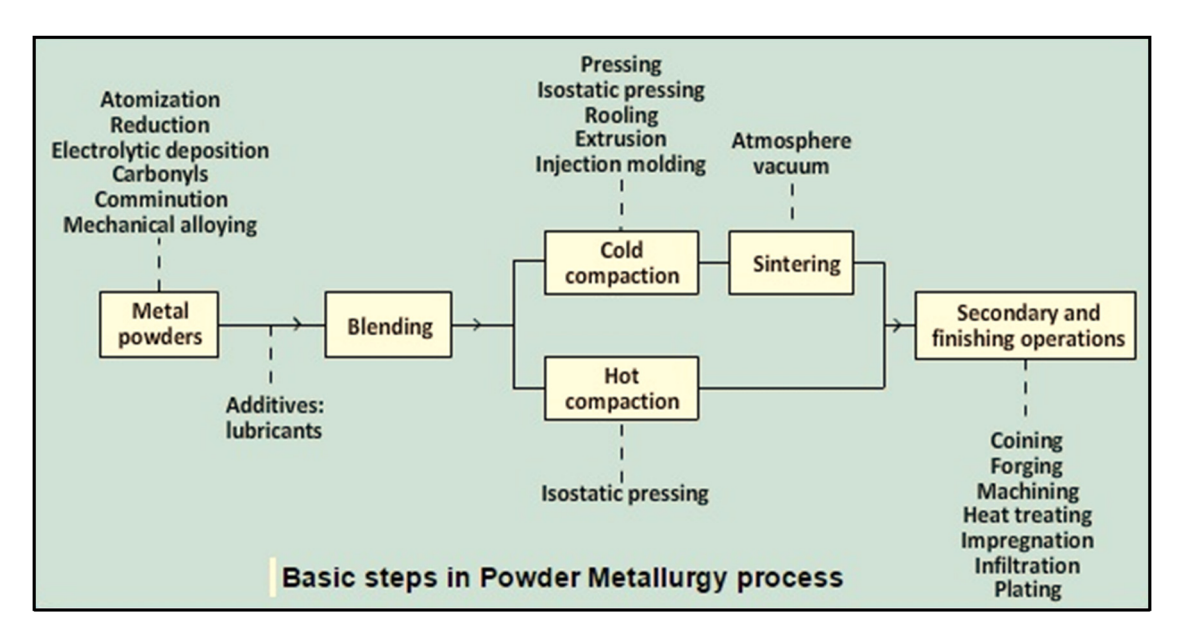


Figure 9: Processing steps for PM.

further processing. Only a small amount of raw materials is wasted during the PM process itself; roughly 97% of the initial powders are transformed into finished goods. This contrasts positively with casting procedures where the production cycle wastes material in the form of sprues, runners, and risers. Three steps make up the traditional PM process: blending and mixing the powders; compaction, which involves pressing the powders into the desired part shape; and sintering, which entails heating to a temperature below the melting point in order to strengthen the part and causing the particles to form solid-state bonds. Figure 10 depicts the three phases, which are also known as primary operations in PM.

2.1.1.1 Blending and mixing of powders

When using materials processing techniques with powders as the initial material, powder mixing is a crucial procedure. No matter if these metals are to form an alloy with certain desired attributes or to remain in the compact as independent constituents while preserving their unique properties, thorough and consistent mixing is always necessary. The metallic powders must first be completely homogenized in order to obtain good compaction and sintering results. Both the words "blending" and "mixing" are appropriate here. When powders with the same chemical makeup but potentially varying particle sizes are mixed, the process is known as blending. To lessen porosity, different

particle sizes are frequently combined. Powders of various chemistries are blended when something is mixed. The ability to combine different metals into alloys that would be challenging or impossible to create through conventional methods is one benefit of PM technology. In industrial practice, the line between blending and mixing is not always clear. Convection, diffusion, and shear are the three mechanisms that influence powder mixing. Usually, when blending and/ or combining metallic powders, other substances are used. These additives consist of (1) lubricants, such as zinc and aluminum stearates, which are used sparingly to lessen friction between particles and at the die wall during compaction; (2) binders, which are occasionally needed to achieve adequate strength in the pressed but unsintered parts; and (3) deflocculants, which prevent powder agglomeration for better flow characteristics during subsequent processing.

2.1.1.1.1 Turbula mixing and MA

Mixing of the nanoparticles and micron particles is also done by Turbula mixing. A laboratory-scale mixer called the Turbula is frequently used in the process of making or test powder formulations [151]. The rotation, translation, and inversion actions that are applied to the powders in this mixer are intense and pulsating on a regular basis [152,153]. MA is a dry powder processing method that has been utilized to create equilibrium and metastable phases of useful and intriguing materials for both business and

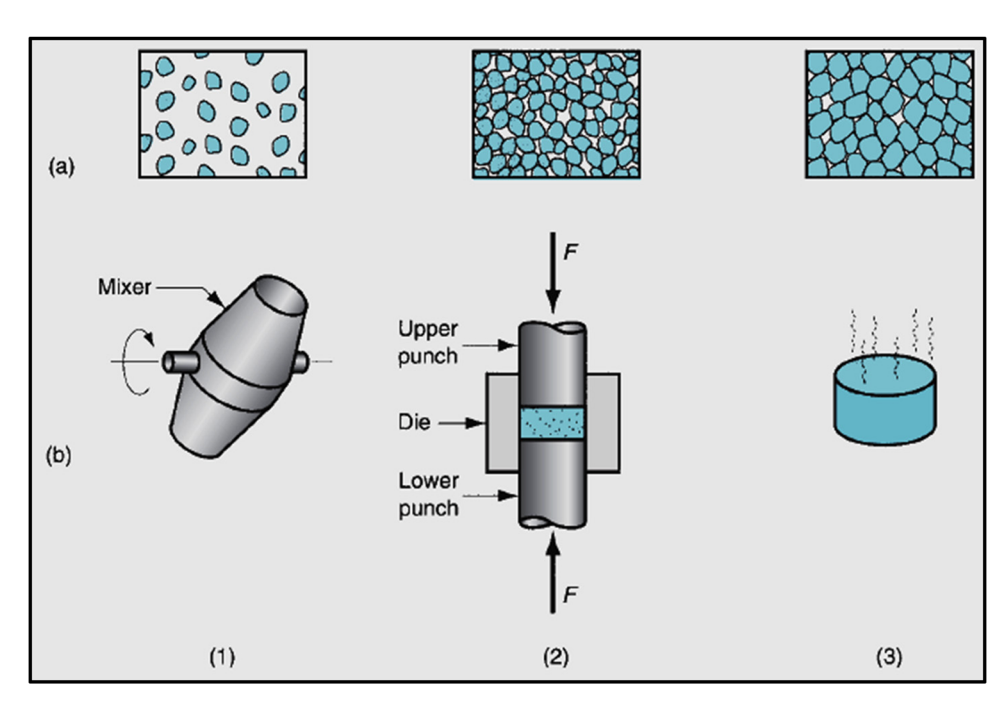
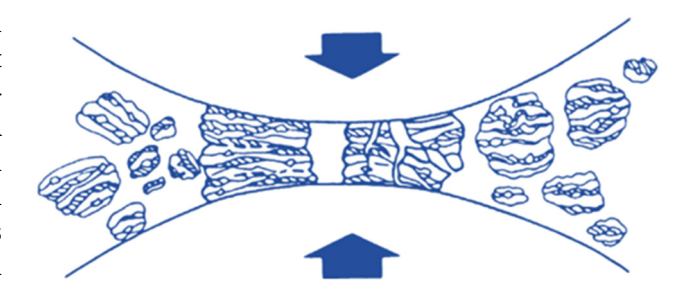


Figure 10: The conventional PM production sequence: (1) blending, (2) compacting, and (3) sintering; (a) the condition of the particles; (b) the operation and/or work part during the sequence [150].

science. The method was first developed by Benjamin [11,12] in 1966 to create a superalloy based on nickel that combines oxide dispersion strengthening with precipitation hardening for use in gas turbine applications. A method of processing in the solid state was required because the oxides cannot be disseminated in a liquid form. Thus, an industrial necessity is responsible for MA's inception. MA is a straightforward and adaptable method that is also economically viable and has significant technical advantages. One of MA's major benefits is the ability to synthesize unique alloys that are impossible to make using any other method, such as alloying of ordinarily immiscible elements. This is because MA is an entirely solid-state processing method, hence any restrictions imposed by phase diagrams do not apply. Dry, elemental, or simple alloy powders are attired at high speeds in modified, high-energy ball mills as part of the process. Figure 11 depicts a typical flow diagram for the high-energy ball milling and sintering process. Ball-powder-ball and ball-powder-container collisions that take place during milling cause the powder particles to repeatedly deform, cold weld, and shatter (Figure 12). The interplay between welding and particle breakage, along with strain-enhanced diffusion, gradually homogenizes the powders, leading to alloy formation in the end. About 1 µm or smaller particle sizes are possible, and solid solubilities can be increased past their equilibrium ranges.

In MA, the individual elemental powders or prealloyed powders are loaded into a high-energy ball mill together with the grinding medium (usually hardened steel or tungsten carbide balls), typically maintaining a ball-to-powder



DE GRUYTER

Figure 12: Ball-powder-ball collision of powder mixture in MA [133].

weight ratio of 10:1 or greater. The MA procedure is carried out in a stainless-steel container sealed under a protective argon environment for the required amount of time to avoid/minimize oxidation and nitridation during milling. Powder particles are repeatedly cold-welded, fractured, and re-welded in this process. By balancing the fracturing and welding events during the process, the size of the resultant powder can be managed. When milling powders of ductile metals, in particular, a process control agent (often stearic acid) is typically added in amounts of around 1–2 wt% to prevent excessive cold welding among the powder particles. Figure 13 summarizes the many sectors in which the MA products are used.

2.1.1.2 Powder compaction

The compaction of the metal powders is done to consolidate the powder into the desired shape, to impart the desired final dimensions with due consideration to any

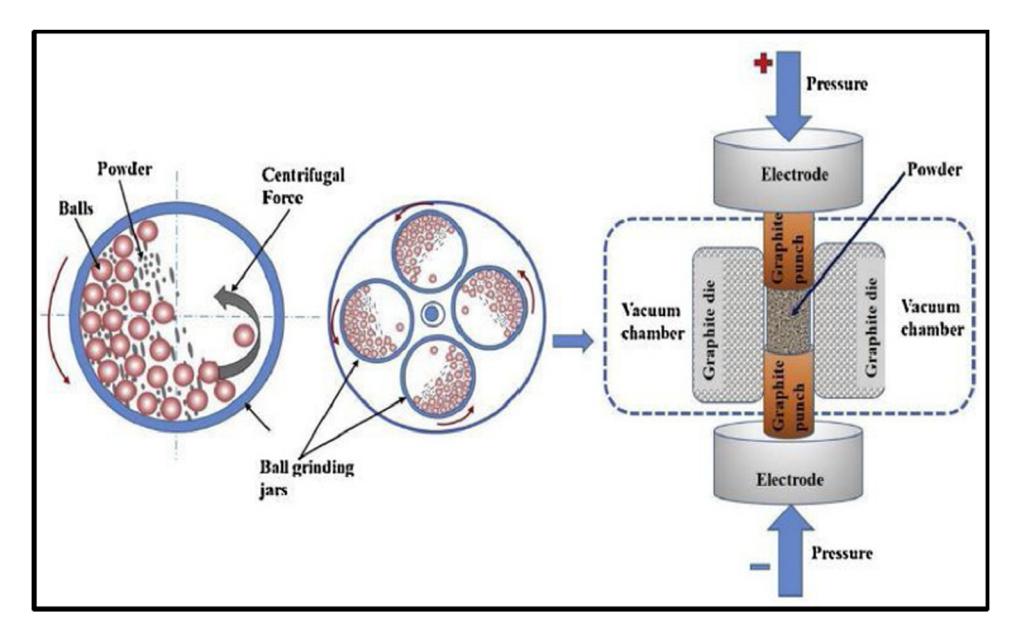


Figure 11: High-energy ball milling and sintering [154].

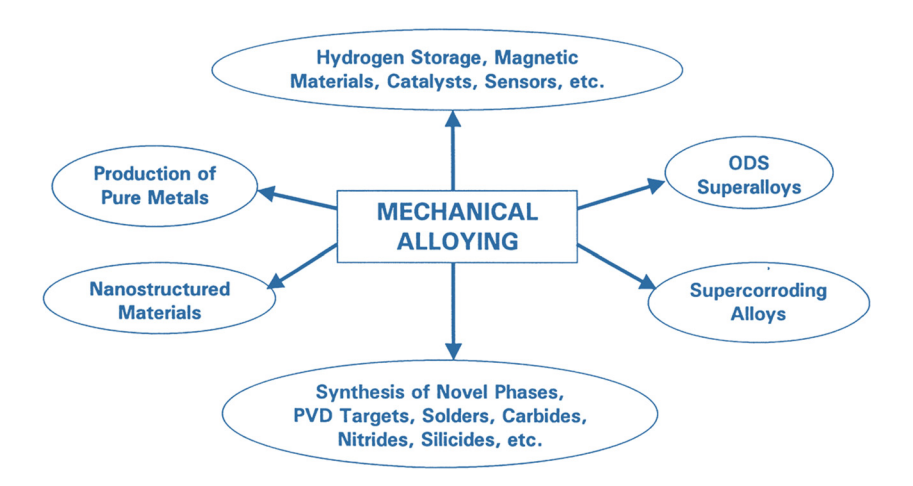


Figure 13: An overview of applications of the mechanically alloying process [133].

dimensional changes resulting from sintering, to impart the desired level of porosity, and to impart adequate strength for subsequent handling. When powders are compacted, enough pressure is applied to give them the desired shape. The pressing method, in which powders contained in a die are squeezed by opposing punches, is the traditional method of compaction. Figure 14 depicts the pressing cycle's steps. After pressing, the work component is referred to as a "green compact," with "green" denoting incomplete processing. The part's density after pressing, known as the green density, is significantly higher than the initial bulk density. When pressed, the part's green strength is sufficient for handling but significantly less than that attained

following sintering. The powders are initially repacked into a more effective configuration as a result of the applied pressure during compaction, which also reduces pore space and increases the number of contacting points between particles while removing "bridges" created during filling. The particles are plastically deformed as pressure increases, expanding the interparticle contact area and bringing more particles into contact. Additionally, the pore volume is reduced as a result. Figure 15(a) shows the evolution of starting particles with a spherical shape in three different perspectives. Three perspectives as a function of applied pressure are frequently used to depict the associated density.

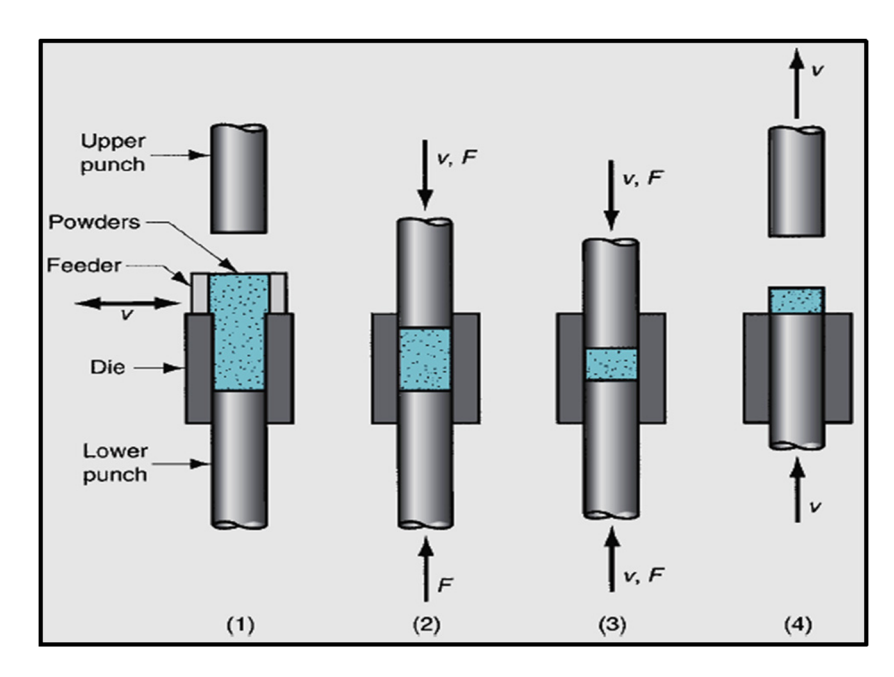


Figure 14: Pressing the common method of compacting powders in PM: (1) filling the die with the powder, (2) initial, and (3) final positions of upper and lower punches during compaction, and (4) ejection of the part [150].

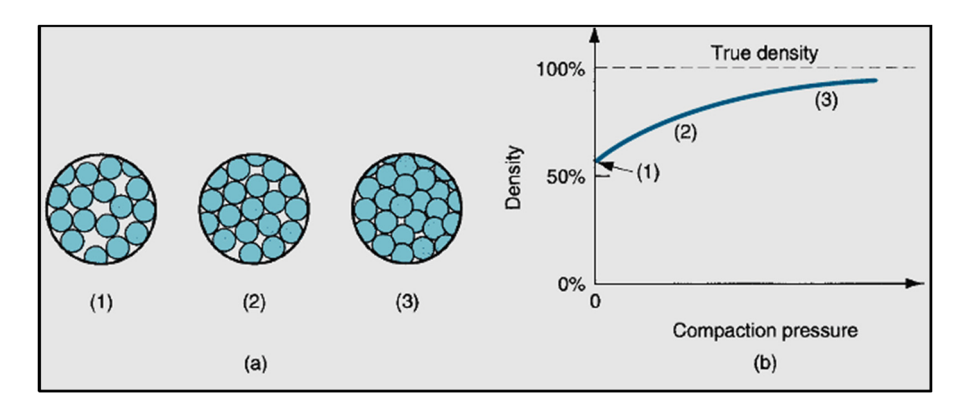


Figure 15: Influence of pressure during compaction: (1) loose particles at first after filling, (2) refilling, and (3) particle deformation; and (b) particles' density in relation to pressure. Here, the order is step-based 1, 2, and 3 in Figure 2.8 [150].

The presses used in conventional PM compaction are hydraulic, mechanical, or a combination of the two. For producing PM, a press's capacity is typically expressed in tons, kN, or MN. The predicted size of the PM component (area in the horizontal plane for a vertical press) multiplied by the pressure necessary to compact the supplied metal powders determines the required force for pressing. Expressing it in an equation form,

$$F = A^*P, (2.1)$$

where *F* is the force, N; *A* is the area of the part, mm²; and *P* is the compaction pressure required to give up powder material. Compaction pressure typically ranges from 70 to 500 MPa. The effect of applied pressure during compaction is shown in Figure 15(b).

2.1.1.3 Sintering of compacts

The green compact is weak and brittle after pressing, thus it crumbles rapidly under light strains. The compact is put through a heat-treatment process called sintering to bind the metallic particles, which boosts the strength and hardness. Usually, the treatment is performed between 0.7 and 0.9 of the metal's melting point (absolute scale). Because the metal does not melt at these treatment temperatures, the names solid-state sintering or solid-phase sintering are occasionally used to describe this traditional sintering. Researchers generally concur that the fundamental driving mechanism for sintering is a decrease in surface energy [155,156]. The green compact has a relatively large total surface area since it is made up of numerous unique particles, each with its unique surface. The development and growth of bonds between the particles causes the surface area to decrease under the impact of heat, which also results in a decrease in surface energy. The overall surface area is higher and the pushing force behind the process is greater the finer the initial powder size.

The illustrations in Figure 16 depict the changes that take place during the sintering of metallic particles on a microscopic level. To produce the necks and transform

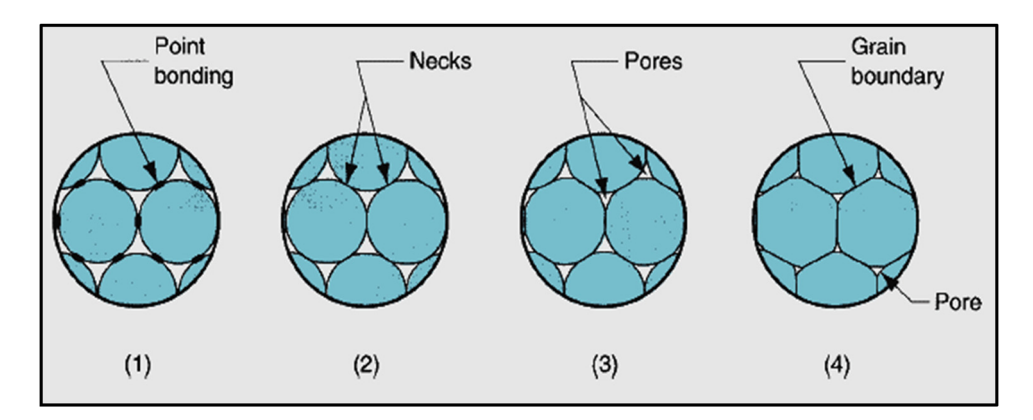


Figure 16: Sintering on a microscopic scale: (1) particle bonding is initiated at contact points; (2) contact points grow into "necks"; (3) the pores between particles are reduced in size; and (4) grain boundaries develop between particles in place of the necked regions [150].

them into grain boundaries during sintering, mass transfer is required. Diffusion is the main process that takes place here; however, plastic flow is another potential one. Pore size reduction during sintering causes shrinkage. This heavily depends on the density of the green compact, which is dependent on the compaction pressure. In general, shrinkage may be predicted when processing conditions are strictly monitored.

Even at room temperature, almost all technical metals react with the gas in their surrounding atmosphere, but this reaction is amplified when the metal is heated. The primary goal of employing special sintering atmospheres is to protect sintered metal powders against oxidation and re-oxidation. The fundamental sintering process can be affected by a sintering environment in various ways. The environment may produce highly mobile metal atoms by lowering the oxides. The environment in the furnace is regulated by current sintering procedures. A regulated environment serves four functions: (1) protecting against oxidation, (2) providing a reducing atmosphere to eliminate any existing oxides, (3) supplying a carburizing atmosphere, and (4) helping to remove any lubricants and binders used during pressing. An inert gas, nitrogen-based, dissociated ammonia, hydrogen, and natural gas are common sintering furnace atmospheres [156,157]. For some metals, such as stainless steel and tungsten, vacuum environments are employed. The majority of common metals and alloys are inert to nitrogen. It is also utilized as a safety purge for flammable atmospheres because it is nonflammable. Molecular nitrogen is the primary component of the nitrogen-based system. Air, which contains about 78% N₂, 21% O₂, 0.93% argon, 0.03% carbon dioxide, and a minor quantity of rare gases like neon and helium, is the source of molecular

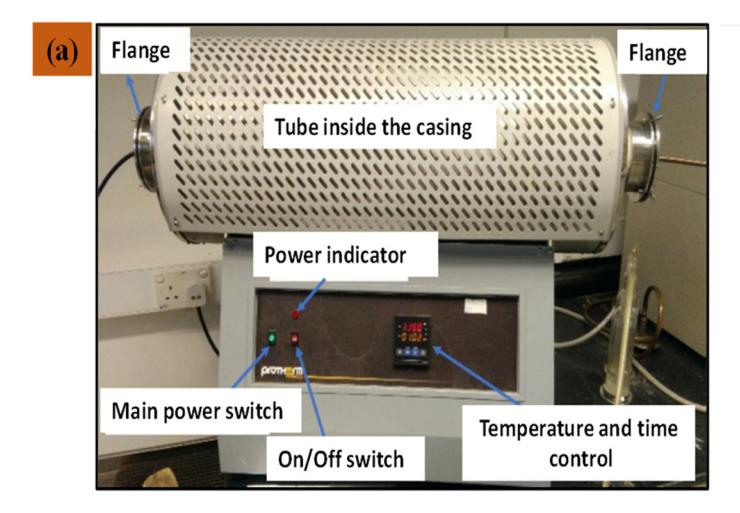
nitrogen. Air separation is the primary method of producing nitrogen.

2.1.1.4 Sintering zones

Three separate zones can be seen in a typical sintering furnace: the burn-off or pre-heating zone, the entrance zone, and the high-temperature sintering zone. The green compacts are intended to be heated gradually to a moderate temperature of around 450°C in the burn-off zone of the furnace. The volatilization and removal of the admixed lubricant are the primary purposes of this burn-off zone. Figure 17(a) and (b) illustrates the tube furnace and sintering zones for aluminum alloy-based powder.

To prevent high pressures inside the compact and potential expansion and fracture, a modest heating rate is required. Before the compacts enter the high-temperature zone, this zone must be long enough to allow for the complete removal of the lubricant. The lubricating vapors must be expelled, and this depends on the atmosphere's flow. To do this, there must be enough atmosphere gas available, and the flow must be positioned so that the vapors are evacuated toward the furnace entrance rather than into the high-heat zone.

The actual sintering of the compacts occurs at the hightemperature sintering zone. It must be adequately heated in order to obtain the desired temperature and heated for a long enough period to develop the required final qualities in the sintered pieces. The burn-off and high-temperature zones typically have similar lengths. A gastight muffle is used because a reducing environment must be present during the sintering process. In order to prevent thermal shock in the compacts and the furnace, the cooling zone



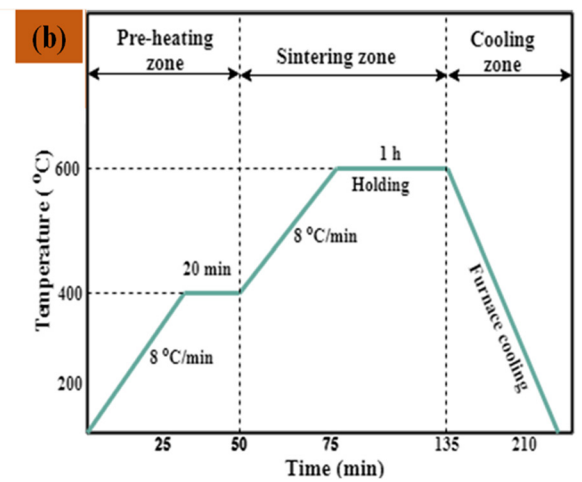


Figure 17: (a) Tube furnace for sintering of the green compacts. (b) Schematic illustrations of the sintering cycle in a controlled nitrogen atmosphere of the tube furnace.

gradually lowers the components' temperature from a high sintering temperature to a lower one. It also maintains a low temperature to stop the material from oxidizing when exposed to the air.

2.1.2 Use friction stir processing

Friction stir welding was adapted to allow for the formation of fine-grained microstructures close to the surface of metallic materials via dynamic recrystallization, and this resulted in the development of FSP. A revolving tool pin is placed into the substrate during the procedure, which causes the workpiece to become heated and pliable due to friction and plastic deformation caused by the tool. The tool pin thus encourages material mixing in the immediate area. For joining the metals, FSP uses the theory of extreme plastic deformation. This technique, which falls under the domain of solid-state joining processes [158,159], is derived from friction stir welding (invented at the TWI, UK). The procedure's potential benefit is that it does not alter the basic matrix characteristics and aids in creating AMCs with superior surface qualities. As shown in Figure 18, the FSP operating principle is displayed. During the procedure, a non-consumable tool that rotates at a rapid rate is used. Large amounts of heat are generated by friction when this revolving tool comes into contact with aluminum. The reinforced material is combined in this high heat that transforms the intended contact metal part into a plastic zone. In recent years, several research articles reported the synthesis of AMCs through FSP.

To provide the product with the appropriate shape, extrusion was used on Al-graphene MMCs. The structure of graphene was seen to stay intact following extrusion, albeit with some bending and wrinkling [160]. A fascinating finding was that the extrusion technique improved the interfacial adhesion between GNFs and the Al matrix, which was essential for enhancing the mechanical characteristics

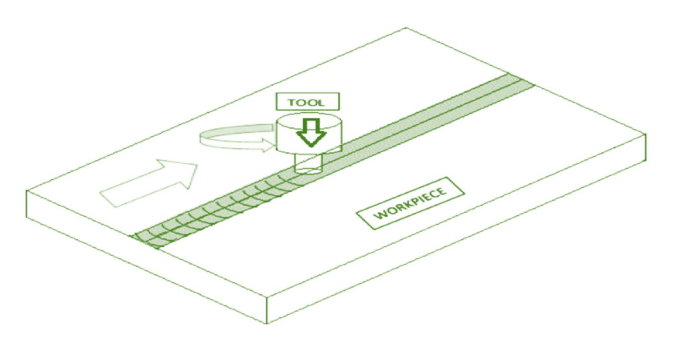


Figure 18: Schematic representation of the FSP process.

of MMCs. To enhance the GNP particle distribution, the FSP has also been investigated [161]. Multi-pass friction stirring was shown to further improve GNP dispersion and bonding in the Al matrix (Figure 19).

2.2 Liquid-state processing

In liquid-state techniques, molten metal is used to perform the dispersion of reinforcement. The Al-MMCs are produced *via* a variety of liquid-state methods, such as *in situ* processing, spray deposition, stir-casting, and compocasting [162–165].

2.2.1 Stir-casting method

In the stir-casting process, the liquid matrix melt receives reinforcement, and the MMCs subsequently solidify. After the matrix has melted, it is vigorously stirred for a while to create a vortex in the melt; next, reinforcement particles are added to the vortex's side, as shown in Figure 20. It is easy to use, affordable, and suitable for mass manufacturing. Wettability, poor interfacial bonding, and uneven reinforcement distribution have all been reported [8].

2.2.2 Squeeze-casting method

MMCs are established by pressing the molten metal onto a particulate pre-form. The matrix material is melted in a crucible along with the necessary additives, and the reinforcing element is preheated separately [166]. Finally, as shown in Figure 21, pressure is applied through a ram while the molten metal is poured on top of the reinforcement. The key advantages of this approach are low shrinkage, the capacity to create complicated shapes, and the least interfacial reactivity of the matrix with reinforcement [167].

Based on the previous discussions, Table 7 provides a comparison study outlining the advantages and drawbacks of the manufacturing techniques discussed.

3 Mechanical characteristics of AMCs

The mechanical characteristics of aluminum MMCs vary due to non-uniform distribution of reinforcing particles,

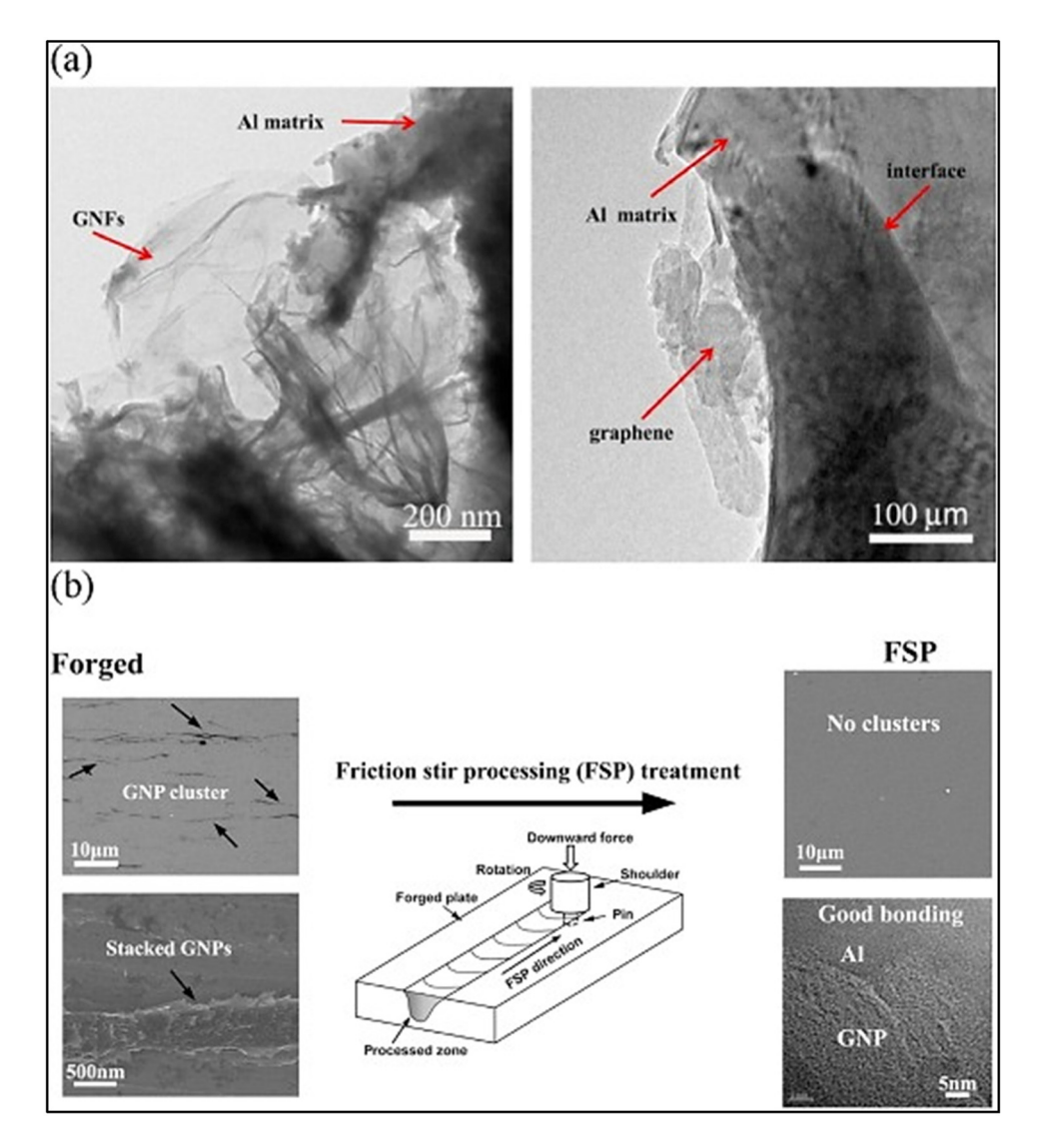


Figure 19: Effect of the processing technique on Al–graphene composites, (a) Al–GNPs (0.15 wt%) morphology [160]. (b) GNP distribution in Al–graphene composites [161].

the behavior of the reinforced element, porosity between the reinforced element and metal matrix, *etc*. The investigations that are made on the mechanical properties of the aluminum AMCs are given as follows.

3.1 Hardness behavior of AMCs

The bulk hardness of the material is increased by adding tough ceramic particles to an aluminum-based matrix. Depending on the manufacturing processes utilized, a variety of factors, including grain size, dislocation density, micron- or nano-sized reinforcing particles, heat input, porosity, and others, affect an aluminum-based composite's microhardness [168,169]. The relationship between the particle size and hardness is inverse. Smaller grain

size enhances hardness while larger grain size decreases it. Lower proportions of porosity increase the composite's hardness, whereas higher proportions of porosity reduce it. Due to improved reinforcing particle distribution and base matrix grain refinement, hardness increases [170].

Incorporating the reinforcement SiC particles affects the hardness of the Al–SiC composite. As SiC is harder than Al, thus with the addition of SiC, we can anticipate an increase in the hardness of the Al matrix. In reality, the SiC nanoparticles prevent the dislocation from moving, which lowers matrix deformation, and increases hardness. Another important factor for the increase in hardness is grain refining brought on by the inclusion of SiC. Many studies support the theoretical hypothesis [171–175]. They observed that as the weight % of SiC increased, the hardness of the Al–SiC composite also increased. Figure 22

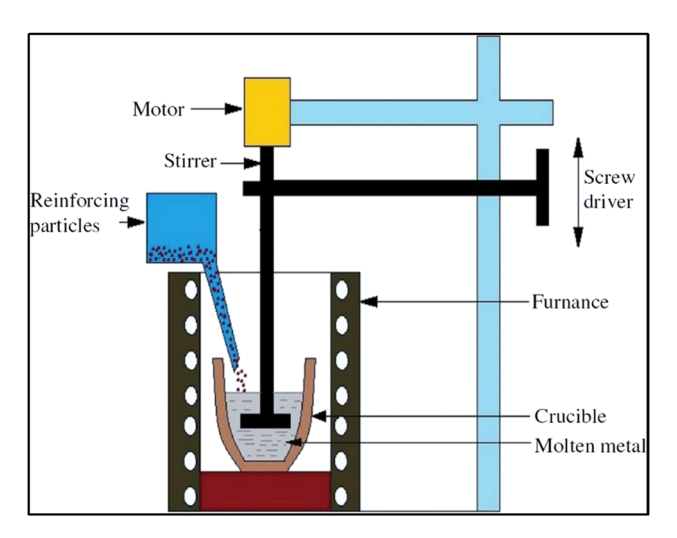


Figure 20: Schematic representation of the casting process.

illustrates how the hardness (HV) of the Al-SiC composite varies with respect to the weight percentage of SiC in earlier studies. The hardness of the Al-SiC composite is observed to decrease over a specific proportion of SiC addition [176,177]. It results from the SiC particles in the Al matrix aggregating over the optimum value. Each work has a separate SiC optimal value. It primarily depends on the kind of processing and particle sizes of Al and SiC. The hardness of the composite is also influenced by the reinforcement's particle size. The composite becomes harder when the particle size ratio of the Al-SiC matrix hits unity [178], which is due to enhanced interfacial bonding between Al and SiC and microstructural densification [172]. Similar results were also noted by Sun et al. [179]. Hall-Petch strengthening due to grain refinement is the cause for the improvement in hardness. Using heat-treated SiC particles as reinforcement improves the hardness of the Al-SiC composite

[180], which is due to the production of the third phase Si_3N_4 and SiO_2 during heat treatment of SiC [181].

Bajpai et al. [187] synthesized and investigated the hardness behavior of Al/nTiC. Figure 23(a) shows that, in comparison to the pure Al powder sample, the micro-hardness has increased by 33.3%. Additionally, the Vickers micro-hardness of the Al-6.0 wt% nano-TiCp composites is lower than the Al-4.0 wt% nano-TiCp composites. At 6.0 wt%, the nano-TiCp particles are more tightly packed together, resulting in a reduced concentration of useful nanoparticles, which causes the micro-hardness to decrease. In another study by Reddy et al. [188], the effect of TiC percentage (5, 10, and 15) on microhardness was investigated for stir-casted Al 6063/TiC composites. The increase in TiC particle weight percentage is associated with a noticeable increase in the composite hardness as depicted in Figure 23(b). The increase is due to a larger percentage of TiC particles in the base material Al 6063.

MA was used to fabricate the nanostructured Al 6061–x wt% TiC composites (x = 0.5, 1.0, 1.5, and 2.0 wt%) by Jeyasimman *et al.* [18] with a 30 h milling period. The ground-up powders were cold-uniaxially compacted and then sinter-heated at different temperatures (723, 798, and 873 K). The sintering temperature and weight percent of TiC were significantly and positively correlated with the hardness (Figure 23(c)). Al 6061–2 wt% TiC nanocomposite sintered at 873 K achieved a maximum hardness of 118 HV, which was four times greater than that of the Al 6061 micro-composite. The Al 6061 matrix's fine-grained structure and the effective dispersion of TiC nanoparticles both contributed to the material's maximum hardness.

In terms of the microhardness of the synthesized composites, the impact of mixing time on microhardness was examined by Alam *et al.* [152]. Figure 23(d) shows that all mixed composites have microhardness values that are

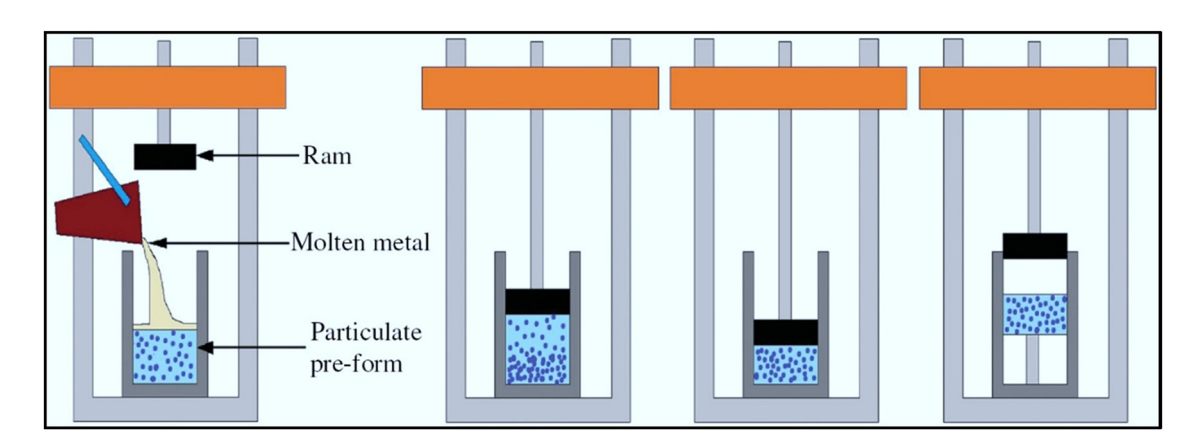


Figure 21: Schematic representation of squeeze casting.

 Table 7: Comparative analysis of AMC fabrication techniques [154]

Fabrication process Route Advantages	Route	Advantages	Limitations	Applications
	:			
PM	Solid	Solid Near net shape components	Raw material (powdered form) is costly	Cutting tools and micro drills
SPS	Solid	Sintering is uniform and it is also combined with the	combined with the Favorable for simple symmetrical shape, and expensive process	Arsenal, nozzle, and transmission
		compaction stage		conductor
FSP	Solid	Composites with superior mechanical and	Requires high setup cost	Aerospace and railways application
		tribological behavior can be produced		
Stir casting	Liquid	Simple, economical, and complicated shapes can be	Agglomerations/clustering of reinforcement in Al matrix. The	Pump housings and cylinder heads
		developed	wettability of reinforcement is of prime concern	
Squeeze casting	Liquid	Casting defects like voids, porosity, etc. are	Squeezing molten metal is a challenging task. Involves high die	Engine block, piston, connecting rod,
		eliminated	manufacturing cost	and pump case

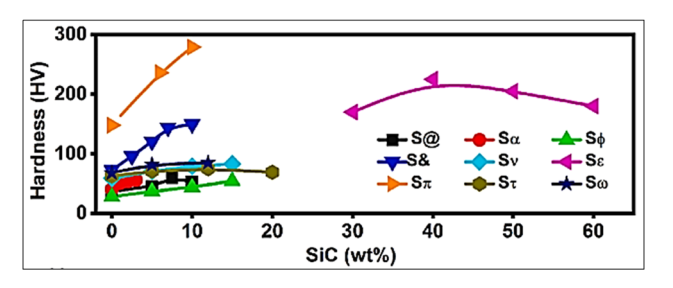


Figure 22: Variation in the hardness value by reinforcing SiC particles (vol% or wt%) [182] (S@- [5]: Sα- [183]: Sφ- [178]: S&- [184]: Sν- [172]: Sε- [176]: Sπ- [173]: Sτ- [177]: Sω- [174]: Sι- [185]: Sψ [58]: S %- [180]: Σ χ- [186]).

higher than the starting AA 7075 matrix. After 2 h of ball mixing, the microhardness increased from 56.3 HV 0.3 before the composite powder was mixed to 59.7 HV 0.3. After 6 h of mixing, the microhardness increase reached its maximum of 17.4%.

The increase in hardness is one of the main benefits of adding graphene to an Al matrix. Figure 24 shows the variation in Al–graphene composite hardness with variation in the additional weight percent of graphene/GNPs. The data from the literature are used to plot the graph. It can be attributable to the Hall–Petch strengthening brought on by the fine grains attained by the composite. Furthermore, adding GNPs causes the composite to harden under strain. At their interface, there is more tension due to the large CTE differential between GNPs and Al. These forces led to dislocation peening at the grain boundaries and an accumulation of dislocations at the interface, which in turn caused strain hardening [189].

3.2 Tensile behavior of AMCs

The tensile strength of aluminum composites reinforced by carbides and graphene has been improved significantly as compared to monolithic aluminum owing to numerous strengthening mechanisms. It is very interesting to look at the recent literature on the tensile behavior of aluminum-based composites under different particles. The tensile behavior of SiC-reinforced Al composites was studied by Mao *et al.* [190]. As illustrated in Figure 25, compared to neat Al, the engineering stress of SiCnp/AMCs and SiCµp/AMCs was increased. SiCnp/AMCs improved their UTS to 292% of pure aluminum, whereas SiCµp/AMCs exhibited an improvement to 135% of pure aluminum. In accordance with the Hall–Petch relationship, dislocation motion is hindered at smaller grains with a larger grain boundary density.

The fractography of the broken samples is depicted in Figure 26. The dimples clearly show uniformly disseminated

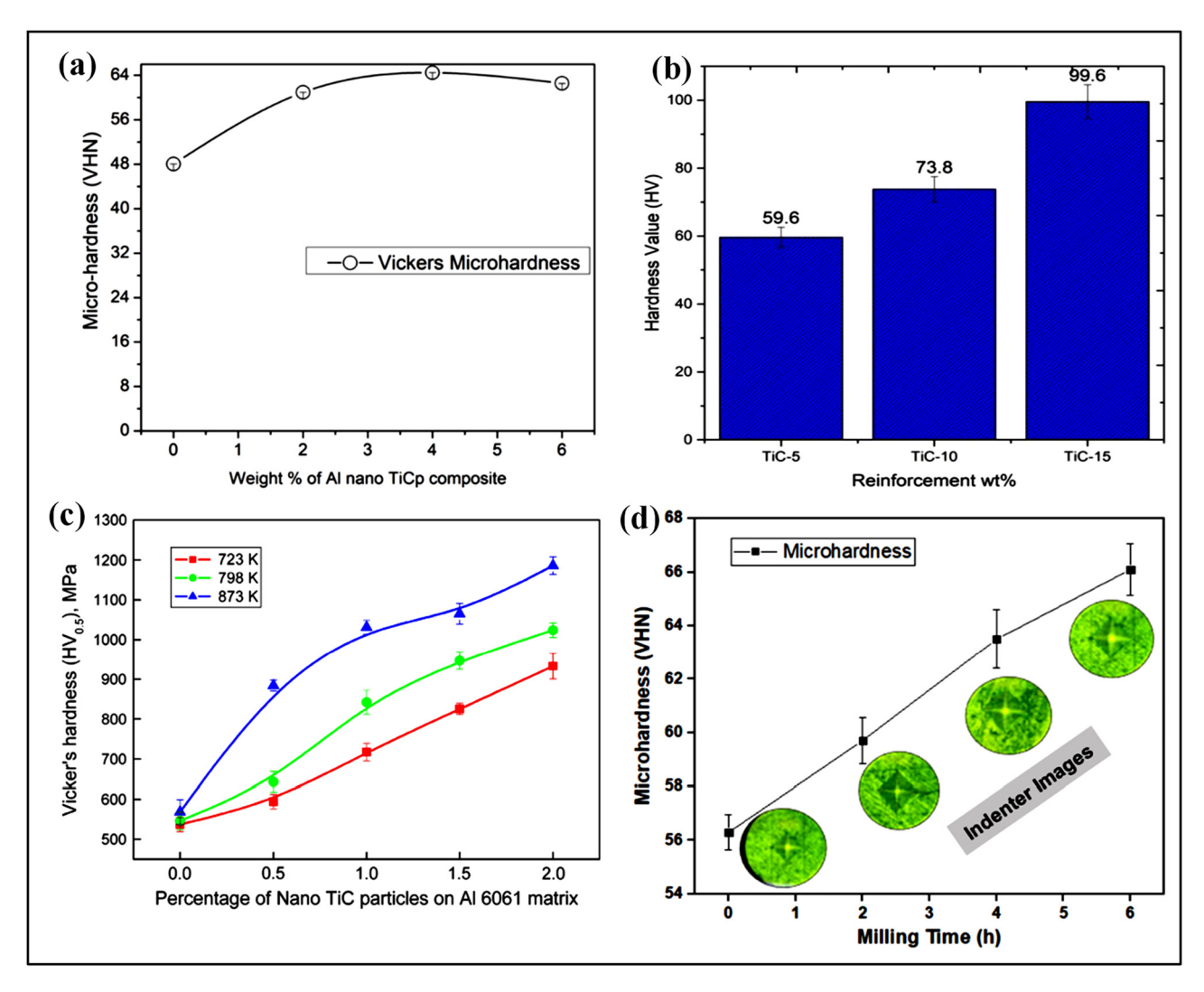


Figure 23: Improvement in the hardness by varying process parameters: (a) Microhardness of Al–nano TiC (2–6%) composites produced by PM [187]. (b) Effect of TiC wt% on microhardness of stir-casted composites [188]. (c) Variation in microhardness with sintering temperature and reinforcement content [18]. (d) Effect of milling time on microhardness [152].

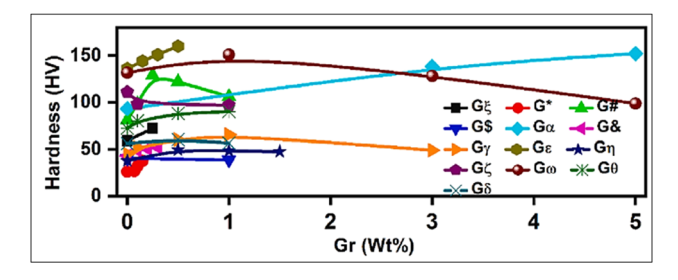


Figure 24: Effect on hardness behavior by reinforcing graphene (GNPs/r-GO wt% in aluminum-based composites [182]. Different colors and notations (G ξ - G θ -) indicate the hardness value data taken from the literature.

SiC particles (Figure 26(a) and (b)). In the magnified view (Figure 26(c)), it is clear that the nano-SiC particles in the dimples still have a strong link with the Al matrix, but in

Figure 26(d), it is clear that the micro-SiC/matrix interface has evident fissures because micro-pores are more likely to form there. Even fully detached from the matrix, some micro-SiC particles were dispersed in the dimples (Figure 26(d)). Such a weak strength of the micro-SiC/matrix interface may also contribute to the decline in mechanical characteristics.

The tensile behavior of Al–TiC (TiC content: 0, 0.5, 1.0, and 1.5 vol%) nanocomposites synthesized by PM was investigated by Reddy *et al.* [191]. The superior tensile yield strength and UTS were attained. Figure 27 displays the results of tensile tests done on Al and Al–TiC nanocomposites. The tensile stress–strain curves of Al and Al–TiC composites are exhibited in Figure 27(a). Figure 27(b) displays the differences in the yield strength, ultimate strength, and elongation of Al–TiC nanocomposites, with a 1.5 vol%

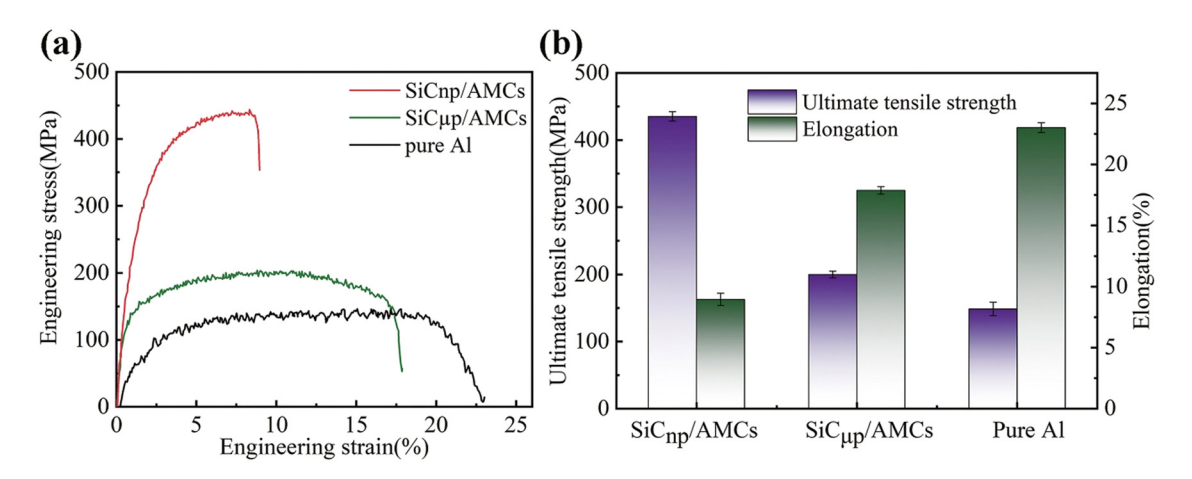


Figure 25: Mechanical characteristics of the produced composites: (a) typical engineering stress–strain curves and (b) ultimate tensile strength and elongation of SiCnp/AMCs, SiCµp/AMCs, and pure Al [190].

increase in the Al matrix. In comparison to pure Al, an increase of 56.3% in UTS and 49.5% in yield strength was noted. The strong interfacial compatibility between the hard TiC reinforcement and soft Al matrix may be accountable for this. With an increase in the TiC content, the tensile elongation shrank. When compared to monolithic Al, the presence of TiC particles and the accompanying microstructural changes cause dislocation pileups at the obstacles, which in turn cause early crack nucleation and failure. This gradual increase in resistance to dislocation

motion may be the cause of the composite's reduced elongation result.

Fractured surfaces of the Al–TiC nanocomposite samples were examined using SEM to determine the cause of the failure during the tensile test (Figure 28(a)–(d)). As shown in Figure 28(a), dimples were visible in every example, indicating ductile failure. The fracture characteristics of the pure and composite samples did not significantly differ at the studied magnifications, which may be attributed to the low content of TiC.

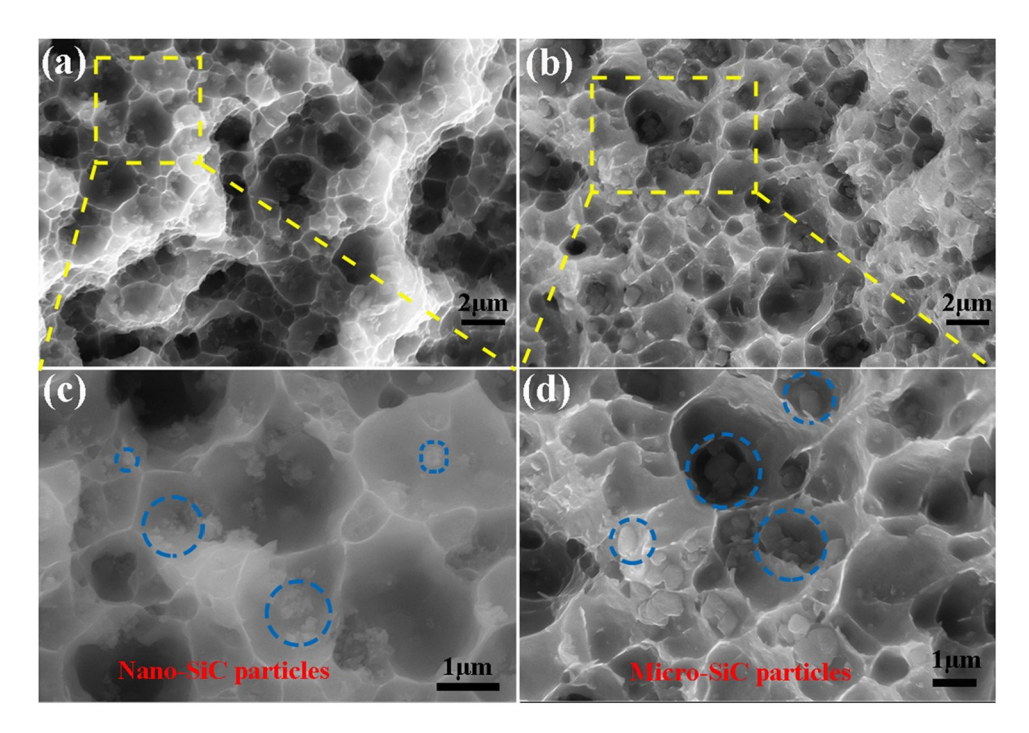


Figure 26: Distinctive fractography surfaces of (a/c) SiC_{np}/AMCs and (b/d) SiC_{up}/AMCs [190].

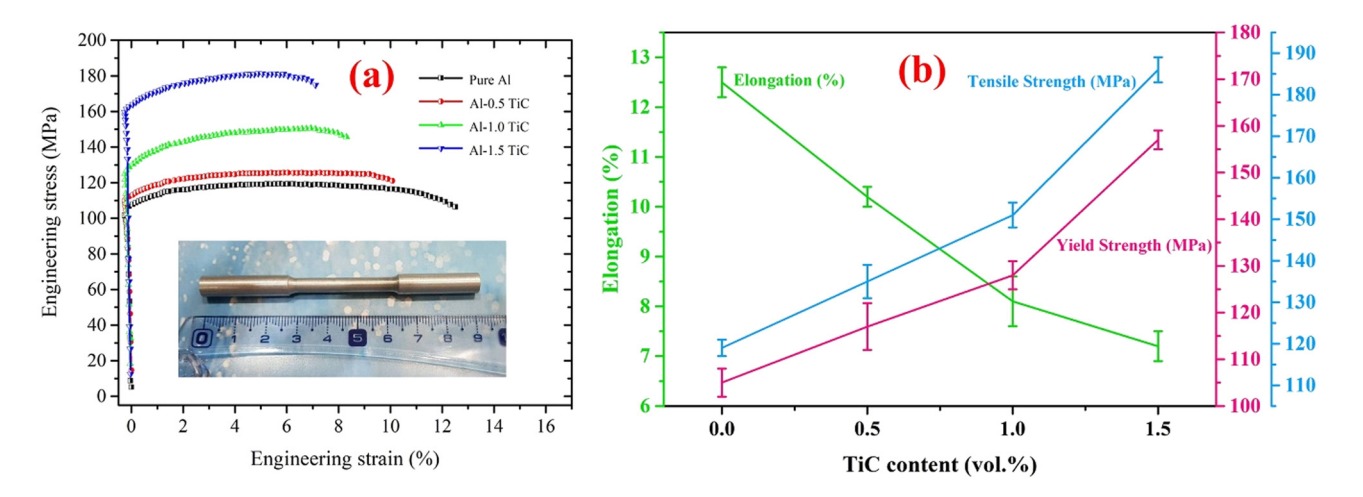


Figure 27: (a) Al-TiC nanocomposites typical tensile stress-strain curves, and (b) variations in the composites elongation, yield strength, and UTS with varying TiC particles [191].

Researchers have examined how GNP reinforcement affects the tensile behavior of AMCs made using various fabrication methods [143,146,192]. The stress and strain curves for stir-cast samples are shown in Figure 29(a). All composites purportedly have greater UTS as compared to the root matrix. The UTS recorded an increase in GNP content from 0.1 to 0. wt%, reaching its maximum level at 0.3 wt% GNP composite. The composite with the highest UTS and a 36.9% improvement over the basic matrix as-

cast UTS was one with 0.3 wt% of GNPs. The increase in strength is ascribed to the dispersion of GNPs with sufficient bonding between the aluminum matrix and reinforcement. The enhanced microstructure and improved grain dispersion caused by the ultrasonic aid led to an increase in tensile strength. Impressive interfacial strength has made it possible to transmit the load from aluminum to graphene, which has high strength. Another explanation for this increase in composites' strength is the Hall–Petch

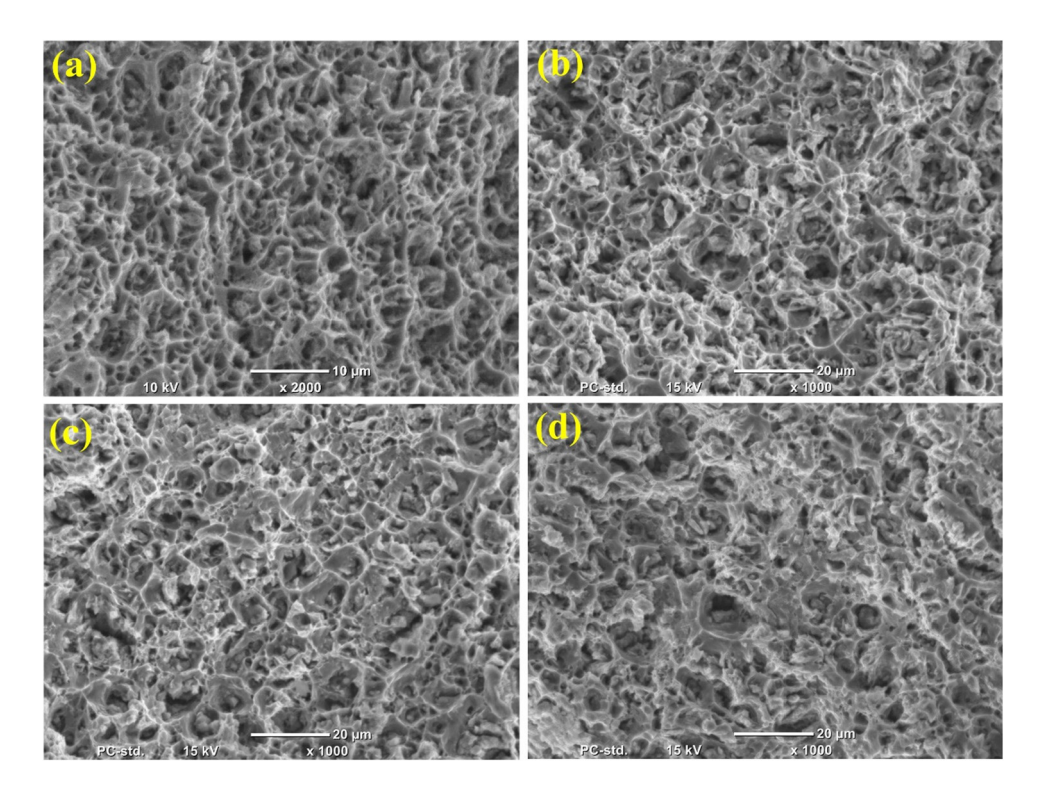


Figure 28: (a-d) Surfaces of Al-TiC nanocomposites that have undergone tensile fracture [191].

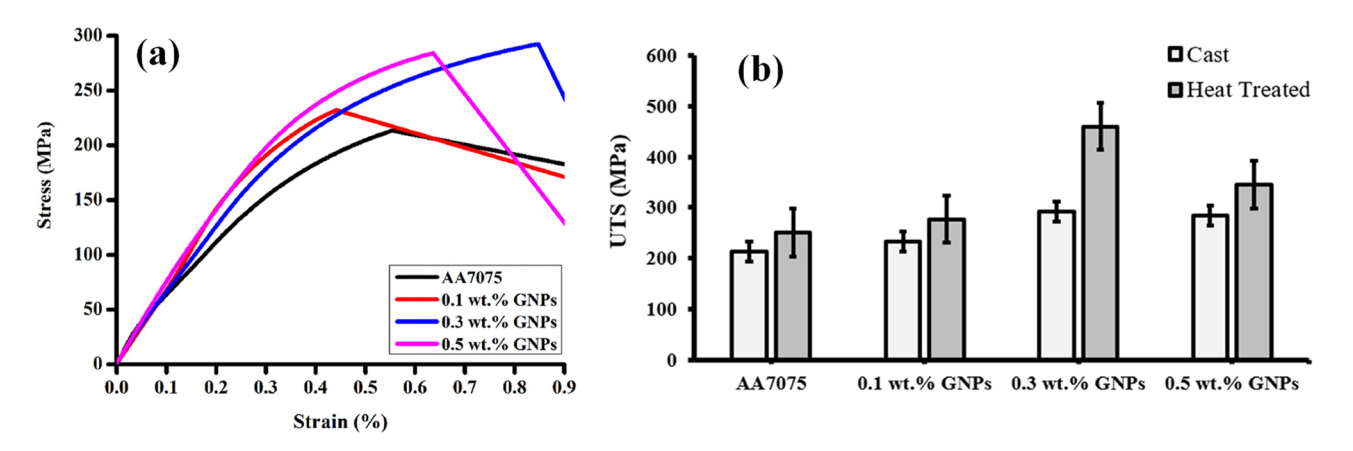


Figure 29: (a) Stress-strain curves of cast specimens. (b) Comparison of UTS for cast- and heat-treated samples [107].

effect. Similar results were obtained in the study by Fadavi Boostani *et al.* [193]. The reduction (Figure 29(a)) in UTS at higher weight percentages of GNPs (0.5 wt%) is the result of the filler and base matrix not being distributed evenly. In comparison to other composites, early failure of the composite (0.5 wt%) is caused by the aggregation or clustering of GNPs in the tensile samples. The influence of T6 heat treatment on tensile strength was evaluated. Figure 29(b) shows a comparison plot between the UTS of cast and heat-

treated specimens. All heat-treated samples indicate an improvement in UTS as compared to cast specimens. Due to the presence of intermetallic compounds like MgZn₂, heat treatment helped to reduce micro-segregation and avoid dislocation movement. The cumulative effect of these phenomena increased the tensile strength.

Figure 30 shows images of scanning electron microscopy (SEM) of specimens with fractures. The dendritic structure resembles clusters of grapes, and there are

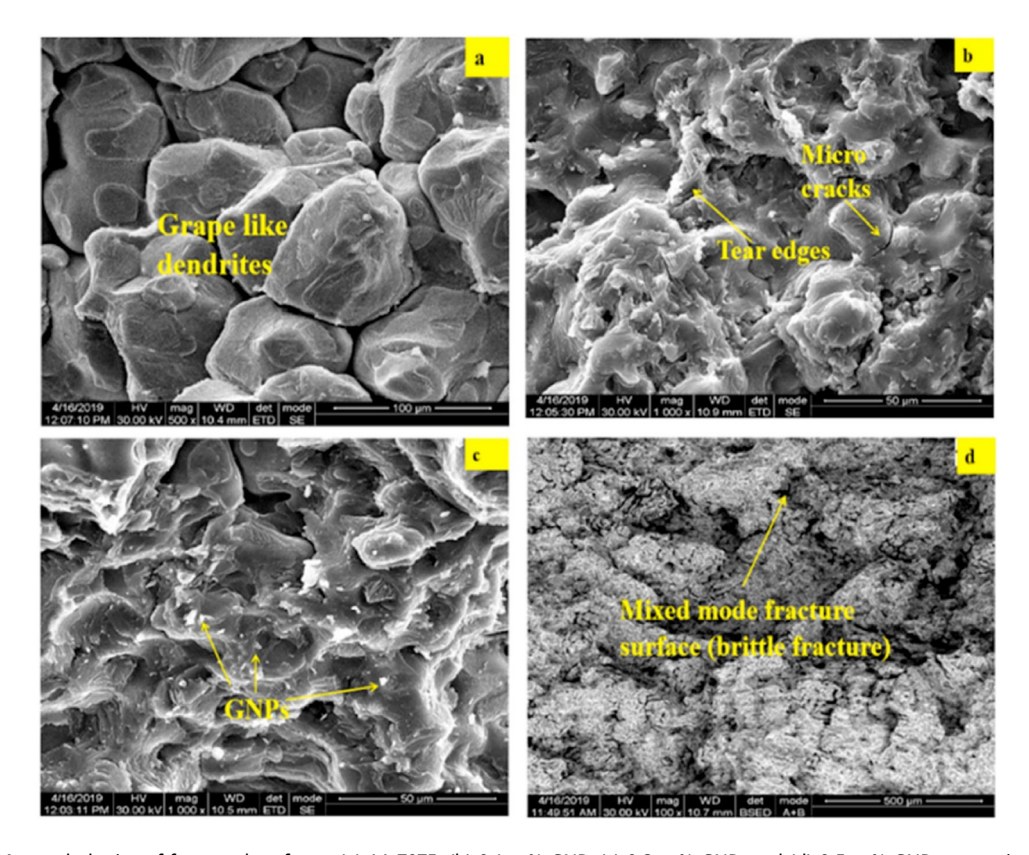


Figure 30: SEM morphologies of fractured surfaces: (a) AA 7075, (b) 0.1 wt% GNP, (c) 0.3 wt% GNP, and (d) 0.5 wt% GNP composite [107].

micro-porosities in the interdendritic zone (Figure 30(a)). Micro-porosities are detected at some spots. However, the addition of GNPs decreased the ductile dimples. The composites have changed from ductile to brittle as a result of the addition of GNPs (Figure 30(b)-(d)). The ductility of composites has been decreased as a result of the addition of GNPs in the base matrix. When compared to an aluminum matrix, the fracture morphologies of composite materials show the shift from ductile to brittle fracture. Figure 30(d) shows that the behavior of fracture progresses toward brittleness as the fraction of graphene increases. The presence of minute dimples, tear ridges, and cleavage facets suggests a mixed-mode fracture. Comparing 0.5 wt% GNP composite with 0.1 and 0.3 wt% GNP nanocomposites, the presence of cleavage facets is more prominent. Cleavage facets and a lower population of dimples indicate that the behavior of nanocomposites containing 0.5 wt% GNPs is primarily brittle.

4 Wear behavior of AMCs

Wear is the gradual loss or destruction of material from one or both surfaces when they are subjected to relative motion (sliding, rolling, or impact action). In most cases, the wear phenomenon is brought on by surface contacts at asperities. The researcher considers the surface's physiomechanical properties and physical state when developing various wear hypotheses. Holm created a wear theory based on atomic mechanics in 1938 and computed the volume wear loss of the substrate during a unit sliding route. The adhesion theory of wear was developed by Burwell and Strang (1952), Archard (1953), and Archard and Hirst (1956), who also offered a theoretical equation that was structurally identical to Holm's equation. Sliding involves repeatedly moving a fixed amount of material, which weakens it and eventually causes it to break. Numerous tribological applications, such as brake rotors, brake drums, and discs, among others, utilize aluminum composites. Al MMCs should be used in such applications, but the tribological-behavior-affecting parameters need to be thoroughly studied. The wear behavior of composites is one of the important tribological properties to sustain in harsh engineering applications such as aerospace and automation sectors and is studied by several researchers. Even though many researchers have extensively studied the tribological properties of various aluminum alloys in both dry and wet conditions, resistance to wear of the material is one of the factors to be taken into consideration before using the material in any engineering applications.

The distribution, size, shape, and number of fibers or hard/soft particles incorporated in the matrix all affect how well the composites function in terms of wear and friction. Another crucial element that influences the mechanical and tribological properties of MMCs is the interfacial bonding between the reinforcements and matrices. In general, it is a tenable opinion that the addition of hard particles as matrix reinforcements boost MMCs' strength and wear resistance while reducing their ductility. Conversely, soft particles typically serve as a solid lubricant and reduce the friction coefficient of MMCs [194]. Numerous investigations of the wear characteristics of MMCs based on aluminum and reinforced with various types of materials have been conducted during the past 20 years. Their findings demonstrate that the volume fraction of reinforcement and particle size has a substantial impact on the wear behavior of particulate-reinforced aluminum composite [195,196]. The four fundamental categories of wear mechanisms are surface-fatigue wear, abrasive wear, adhesive wear, and adhesive wear. The load, the size of the abrasive elements, the amount of abrasive particles, the toughness and hardness of the reinforcing particles are only a few of the numerous adjustable aspects that affect how easily composite samples are worn down by abrasion [80,197,198]. The wear properties of composites with TiC reinforcement based on aluminum have been studied by Tyagi [199]. The author showed that as the amount of TiC particles in the composite sample increased, the wear conduct decreased. Kostornov et al. [200] studied tribological factors to increase the wear resistance of composites made of titanium. They revealed that the chosen material can be employed as an antifriction material at faster sliding speeds. In a recent investigation of the frictional properties of composites reinforced with TiC and MoS₂, Selvakumar and Narayanasamy [201] concluded that the TiC content and sliding time affect the response (weight loss) of the composites.

For easier comparison, Table 8 lists composites with SiC, TiC, and carbon-based reinforcement where the basis alloys are primarily aluminum alloys. As can be seen, the manufacturing paths are used to sort the data provided in this table. The wear resistance of the SiC-reinforced MMCs is at its highest when PM is used, achieving a >55% improvement in wear resistance behavior compared to the neat monolithic alloy, as shown in Table 8. This further demonstrates that PM is the best manufacturing method. The average improvement in wear resistance produced by stir casting and PM methods is approximately 62 and 76%, respectively. The difference between the aforementioned improvements is likely due to better dispersion efficiency of reinforcing particles as well as more controllability of the PM-based manufacturing processes. In light of Table 8,

it is possible to speculate that solid-state techniques like PM (HDC), PM, FSP, and ARB may offer an abrasion resistance value of 96% that is superior given that poor wetting is not significant, and a greater number of additives can be incorporated. Carbon allotropes can significantly enhance the wear resistance behavior of AMCs.

Reddy et al. [188] investigated the microhardness and wear behavior of TiC-reinforced (5, 10, and 15 wt%) Al 6063based composites and concluded that the mechanical properties of Al 6063-based MMCs improved with enhancement in TiC weight percent. The effect of graphite on the wear behavior of an Al 7075/Al₂O₃/5 wt% graphite hybrid composite made using liquid metallurgy was studied by Baradeswaran and Elaya Perumal [222]. To reduce wear resistance and coefficient of friction, ceramic particles and solid lubricants were introduced into an aluminum alloy matrix. A hybrid composite of Al 7075, Al₂O₃, and graphite was created by adding 5 wt% of graphite particles and 2, 4, 6, and 8 wt% of Al₂O₃. It was found that adding more ceramic phases to the hybrid composites made of Al 7075, Al₂O₃, and graphite increases their hardness, tensile strength, flexural strength, and compression strength. The hybrid composites with graphite showed superior wear-resistance qualities in terms of their wear properties. Numerous studies have already examined the tribological properties of bare AA 7075 alloy under various load, speed, and temperature conditions [223,224]. Kumar et al. [225] investigated the impact of SiC on AA 7075 and noticed an enhancement in tensile strength, hardness, and density with the SiC addition. A related study carried out by Lakshmipathy and Kulendran [226] recorded a significant increase in wear behavior with the accumulation of SiC fragments in AA 7075.

4.1 Mechanism for wear

The primary wear mechanisms involved in the tribology of AMCs are briefly introduced in this section. When a composite material is subjected to wear loading conditions, abrasion, adhesion, delamination, oxidation, and fretting wear are frequently observed [227]. The tribological response can greatly vary depending on factors such as the amount or degree of sliding speed or distance, reinforcement type, loading conditions, interfacial bonding, weight/volume ratio, dispersion quality, and microstructural defects [228]. The key characteristics of several wear mechanisms are listed in Table 9.

The type of manufacturing method, matrix alloy, wear condition, and reinforcement size, type, and weight fraction can all affect how severe the aforementioned wear mechanisms are. This means that different wear mechanisms may manifest in different situations. Figure 31 illustrates the schematic of the usual wear mechanism as the

Table 8: Wear behavior of Al-based composites reinforced with SiC, TiC, and carbon-based reinforcements

Matrix	Reinforcements	Wt%	Fabrication route	Load (N)	Sliding speed (m/s)	Value of increment %	Ref.
Al 7075	SiC	4	SC	40	3	57	[202]
Al 7075	SiC	11.3	PM	10	0.08	82	[203]
AA 6061	SiC	10	FSP	20	0.05	73	[204]
AA 6061	SiC	33	FSP	25	0.02	91	[205]
AA 6061	SiC	2	UASC	10	1.5	58	[206]
Al 6061	SiC	1.2	UASC	40	0.5	68	[207]
AA 5052	SiC	_	FSP	40	0.08	90	[208]
AA 5252	SiC	5	PM	45	0.5	65	[209]
Al 5083	SiC	10	PM	49	1	98	[210]
Al	SiC	5	PM	20	_	84	[211]
AA 2219	SiC	1.5	SC	20,000	0.004	21	[212]
Al 1050	SiC	2.3	ARB	50	25.4	54	[213]
A 356	SiC	5	SC	10	0.5	48	[164]
A 356	SiC	5	SC	30	2.5	88	[214]
Al 5083	TiC	_	FSP	100	1	47	[215]
Al 6061	TiC	9	SC	20	1.5	30	[216]
Al 1050	TiC	1.8	SC	1	0.17	56	[217]
Al-Cu	TiC	5	PM	10	1	64	[218]
AA 6061	CNT	_	FSP	20	0.004	40	[219]
A 360	GNPs	0.25	UASC	2	_	35	[220]
AlSi10Mg	GNPs		SLM	10	0.9	53	[221]

Table 9: Key characteristics of several wear mechanisms

Wear mechanism	Key features
Fretting wear	Oxide debris, loos fragments, and minor scratches
Delamination	Big debris and flake types, porosity and deep grooves, and craters
Oxidation	Oxide debris and layers
Abrasion	Relatively small debris, longitudinal or parallel grooves, and smooth surface
Adhesion	Pits and prows, material flow, plastic deformation, and deformed debris

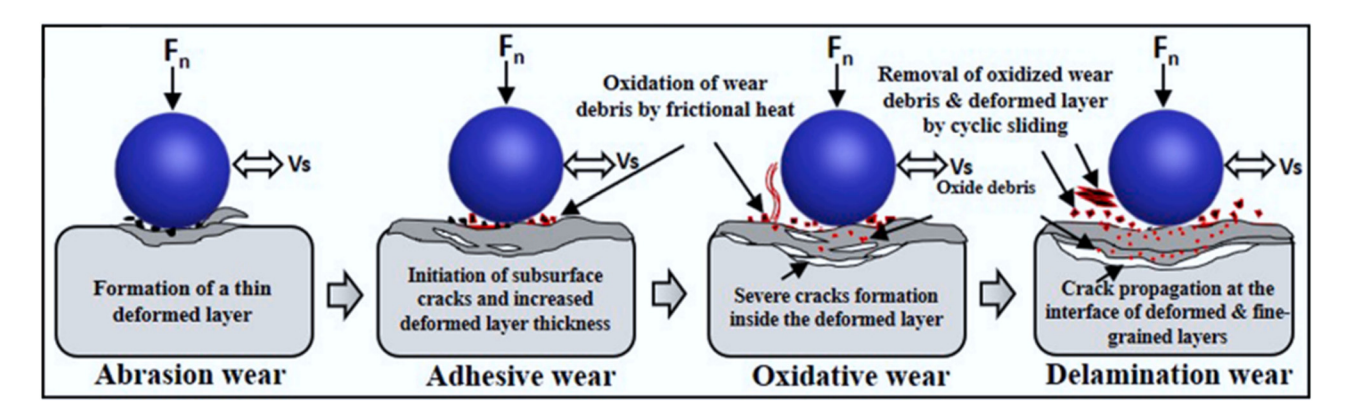


Figure 31: Schematic of the usual wear mechanism as the sliding time increases under dry sliding conditions [229].

sliding time increases. Initiated by abrasion and adhesion at the start of the sliding time, worn surface plastic deformation led to the production of a thin deformed layer with accumulated wear debris. The wear debris on the worn surface is then oxidized as a result of the frictional heat. In a recent study by Lin *et al.* [230], Al matrix hybrid composites reinforced with TiC and GNPs (Al–10.0 vol% TiC and GNPs) were fabricated *via* PM. The effect of the TiC/GNP ratio on the tribological characteristics of composites was investigated. Figure 30 demonstrates the samples'

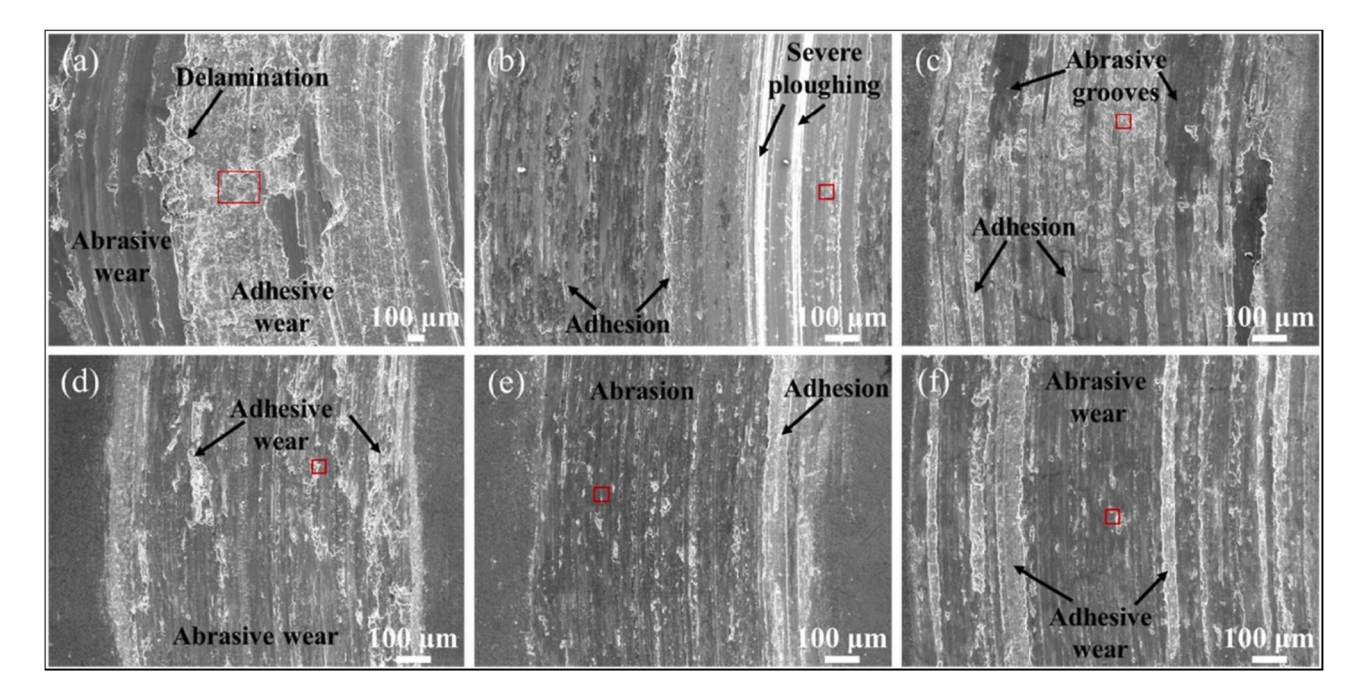


Figure 32: Worn surfaces of developed composites after wear test for varying reinforcements. (a) Al, (b) Al-10 T, (c) Al-9.5 T-0.5 G, (d) Al-9 T-1 G, (e) Al-8.5 T-1.5 G and (f) Al-8 T-2 G.

worn surfaces following the wear tests. It has been noted that Al wears significantly more severely, as demonstrated in Figure 32(a). It is possible to see grooves on the worn surfaces, which are mostly brought on by the hard microasperities of the counterpart material during sliding and signify abrasive wear. Additionally, as indicated by the arrow, somewhat rough places where delamination can be seen exhibit adhesive wear. The adhesive force holding the counterpart and sample together gradually develops as a result of the frictional heat produced during repeated sliding. Al can rapidly delaminate or fragment due to its softness and ductility under sliding wear. Evidently, the predominant mode of wear for as-sintered aluminum is adhesive wear. The larger flake wear debris of Al, as shown in Figure 33(a), further supports that the Al has considerable adhesive wear. The composite sample Al-10 T wear is lessened as compared to Al; however, some deep grooves can still be seen on the worn surfaces, suggesting severe ploughing, as illustrated in Figure 32(b). This may be attributed to the composite's presence of TiC agglomerates following the addition of a significant amount of TiC particles. The three-body abrasion is caused by the pulled-out big TiC agglomerates while wearing.

From the gathered wear debris of sample Al–10 T demonstrated in Figure 33(b), the wear debris, which resembles that of Al, is made up of big flake debris, corrugated debris, and equiaxed debris. Although the size of the debris is smaller than it was with Al, the adhesive delamination still accounts for the majority of the Al–10T wear. The

morphologies of worn surfaces for the hybrid composite Al-9.5 T-0.5 G after adding TiC and GNPs are very different from those for Al-10 T, where significant ploughing from TiC particles is not found, as illustrated in Figure 32(c). The wear fragments of Al-9.5 T-0.5 G observed in Figure 33(c) show that wear debris size falls even further from that of Al-10 T, and its morphologies are still primarily flake-shaped. Specifically, Figure 32(d) demonstrates that the adhesion in the wear of Al-9 T-1 G is clearly reduced when the fraction of GNPs surpasses 0.5 vol%. Additionally, the wear debris of Al-9 T-1 G shown in Figure 33(d) comprises finely equiaxed particles and flake debris. It implies that the wear mechanism switches to an abrasive-dominated phase with time. Figure 32(e) demonstrates that Al-8.5 T-1.5 G further reduces adhesion wear, and the abrasion areas are liable to smooth out. Figure 33(e) demonstrates that a significant amount of fineequiaxed debris is present in the wear debris of Al-8.5 T-1.5 G, which is often associated with the outstanding wear resistance of the composite. However, as demonstrated in Figure 32(f), the adhesive wear becomes more obvious and is significantly more serious than the Al-9 T-1 G sample. The monitored wear debris in Figure 33(f) is more evidence of the enhanced adhesive delamination with the use of Al-8 T-2 G. This may be connected to the agglomeration of GNPs. Even while GNPs have a lubricating influence during wear, the considerable porosity exacerbates delamination and significantly lowers wear resistance.

The wear processes on the contributions of the reinforcements to the wear of the composites are depicted

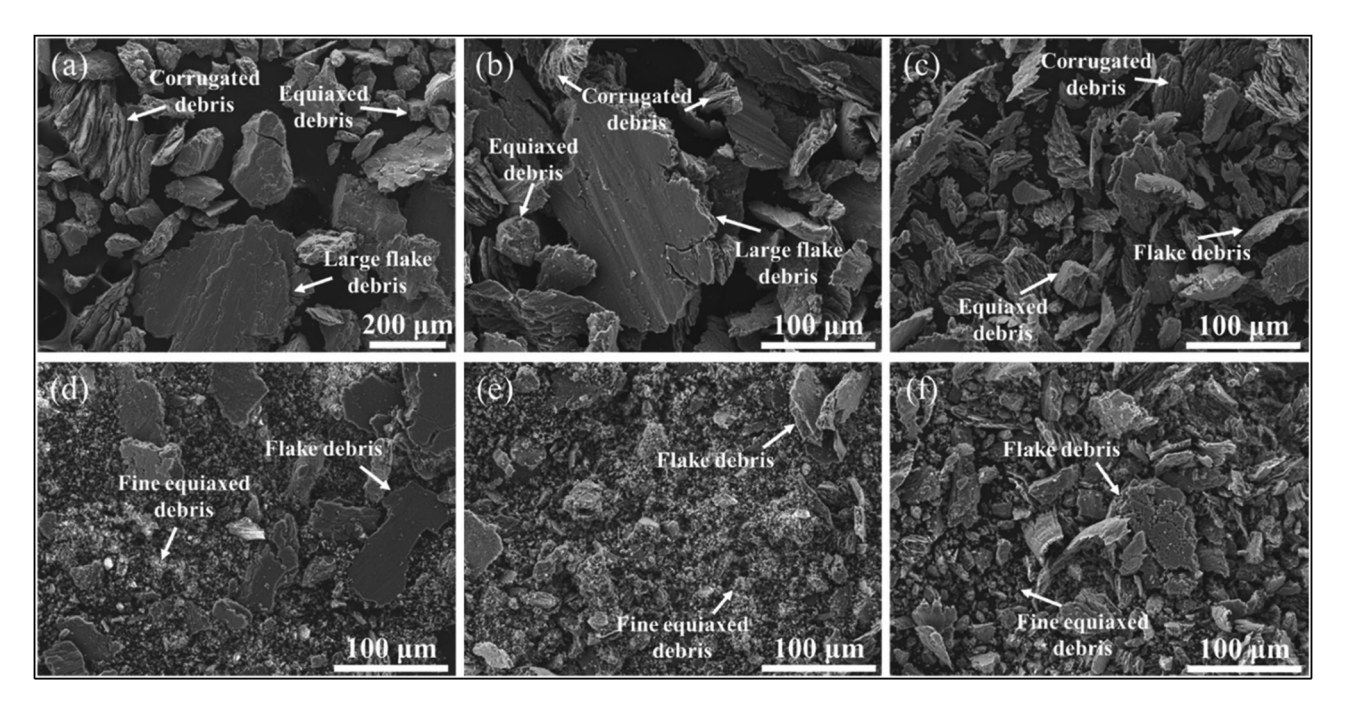


Figure 33: Microstructures of wear debris after the wear test of developed composites. (a) Al, (b) Al-10 T, (c) Al-9.5 T-0.5 G, (d) Al-9 T-1 G, (e) Al-8.5 T-1.5 G and (f) Al-8 T-2 G.

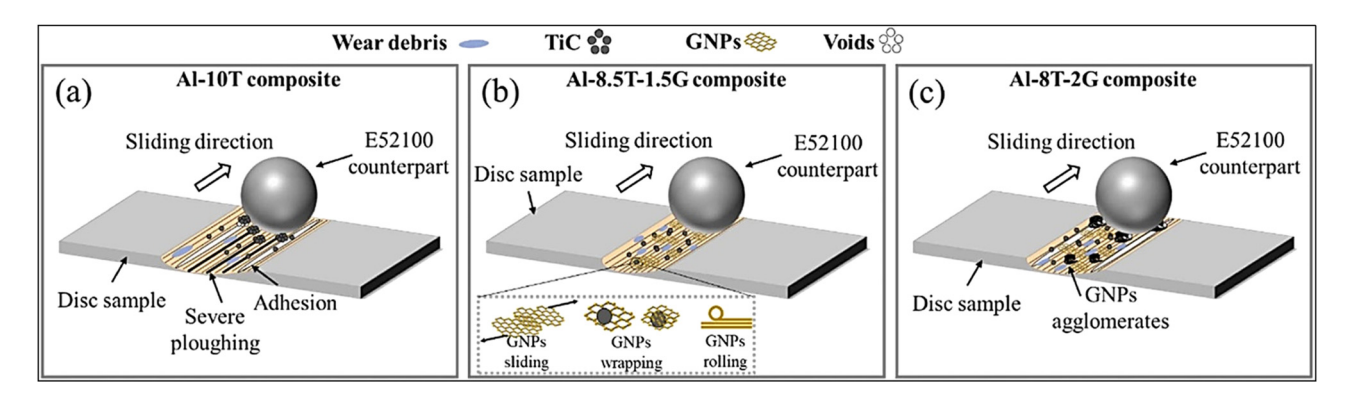


Figure 34: Schematic representation of the wear mechanisms that occur in the composites during wear. (a) Al-10T, (b) Al-8.5T-1.5G, and (c) Al-8T-2G composites.

schematically in Figure 34. It is known that the evenly dispersed TiC particles can function as a micro-polishing medium during the sliding wear by removing the microscopic abrasions from the worn surfaces, and additionally lessen interaction between the opposite and specimen by filling the troughs.

As the proportion of GNPs increases, the wear resistance of the hybrid composite is enhanced, thanks to the synergistic actions of TiC and GNPs. The homogeneous distribution of the reinforcements, the synergistically reinforcing and lubricating effects of TiC, and the lubricating effects of GNPs endow Al–8.5 T–1.5 G the best wear resistance among all the samples, with a specific wear rate of 4.99 104 mm³/N m, which is 96.9 and 78.8% lower than that of Al and Al–10 T, respectively. The wear resistance of Al–8 T–2 G significantly decreases as the GNP fraction is increased because the agglomeration of the GNPs exacerbates the severe adhesive wear and delamination of the composite while sliding wear.

5 Strengthening mechanisms

There are several factors, each of which plays a major role in determining how the Al-mechanical and tribological behavior of MMCs will change as a result of reinforcement. The overall failure process of a material can be divided into three stages: the yield stage, the fracture stage, and the elastic stage. The following factors need to be taken into account in order to understand how additional reinforcement strengthens an aluminum MMC.

5.1 Strengthening by grain refinement (Hall-Petch relationship)

The Hall-Petch effect, which is a well-known strengthening mechanism, comes from the effect of grain size on the

strength of the material; as the grain size decreases, the strength increases. It is a mechanism which improves both the strength and ductility of a composite [231]. Several reinforcement particles work as a heterogeneous nucleation catalyst during processing, which refines the grain. The Hall-Petch relationship can be used to explain the strengthening caused by finer granularity. As illustrated in Figure 35, a coarser grain allows the dislocations to freely traverse a greater distance than a finer grain. Therefore, the movement of dislocations is constrained by the matrix's finer grains. Additionally, as illustrated in Figure 36, it causes dislocations to pile up and increases dislocation density. The letters A, B, and UFG in Figure 36(a) stand for the Al region, the SiC region, and the ultra-fine grains, respectively. The strength of the composite increases as dislocation density increases. In the case of AMMCs, Al grains are frequently pinned or wrapped in reinforcing particles, which prevents grain development during processing and results in the production of finer grains. The well-known Hall-Petch equation

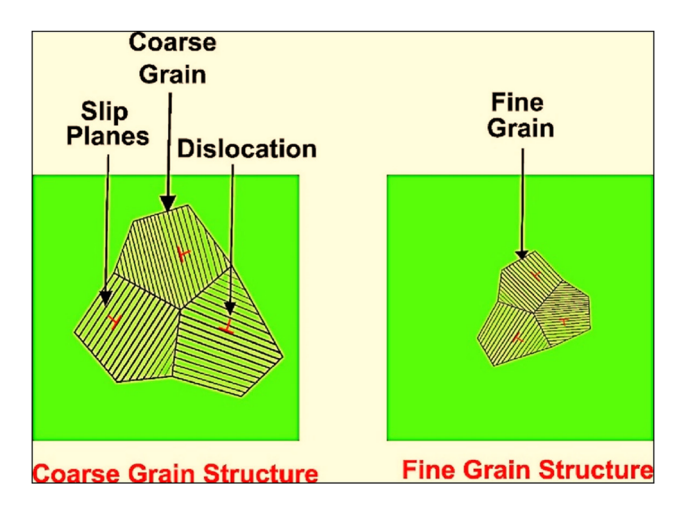


Figure 35: Schematic representation of strengthening *via* grain refinement [182].

can be used to calculate the strengthening brought about by grain refining [193]:

$$\Delta \sigma_{\text{Hall-Petch}} = K \left(d_{\text{c}}^{-\frac{1}{2}} \right),$$
 (1)

where K is the Hall–Petch coefficient. For the Al matrix, it is 0.04 MPa m^{1/2}. The dislocations and grain boundary are depicted in Figure 36(b).

It has been observed that adding nano- and micro-size SiC particles reduces the Al matrix's average grain size [5,183]. Additionally, a drop in grain size is also observed when the SiC weight percentage in the Al matrix is increased. Numerous investigations in the literature have found similar outcomes for grain refining when the volume percent of SiC in the Al matrix is increased [178,185]. The composite's strength increases as a result of grain refining. The Al-SiC matrix grain size is influenced by SiC particle size as well. It has been found that adding SiC particles of a smaller size produces grains of a smaller size. Lesser spacing is present in smaller particles, which might impede the migration of grain boundaries. With the inclusion of GNPs/GNSs/Gr, the grain refinement in the Al-Gr composite is also observed [2,146,232]. The Al-Gr composite's strength is increased by ultrafine grains.

5.2 Orowan strengthening

Orowan strengthening refers to the interaction between dislocation and distributed reinforcement that prevents the dislocation from moving close to the particles. The degree of Orowan strengthening is improved by the larger reinforcing fraction [231,234]. The Orowan strengthening

mechanism shows how the tensile strength of the aluminum MMC is increased by nano-/micro-range reinforcement particles. When the dislocations are in front of the reinforcement particles, the dislocations bend around them to generate dislocation loops. These loops cause back stress, which prevents dislocations from moving further. As shown in Figure 37, it causes a dislocation build-up, which raises the matrix's dislocation density and enhances the AMMC yield strength as a result [235,236]. Additionally, nano-sized fine precipitate can prevent dislocation from moving, resulting in the formation of dislocation loops. The T6 heat-treatment method in AMMCs results in fine precipitates [237]. Through Orowan strengthening, these precipitates can also increase the strength of the composite.

Increasing the volume fraction of micro-SiC reduces the spacing between particles in AMMCs [183]. It causes an increase in the Orowan strengthening in AMMCs [238]. When comparing it to other strengthening processes, it is invariably shown to increase the composite's strength. Strengthening due to CTE mismatch between the base matrix and the reinforcement is another significant strengthening process that contributes to increasing the strength of the composite. This has been covered in the following section.

5.3 Strengthening by dislocation due to CTE mismatch

When cooling occurs during the sintering process, dislocations arise at the reinforcement/matrix interface when the stress brought on by thermal mismatch is greater than the

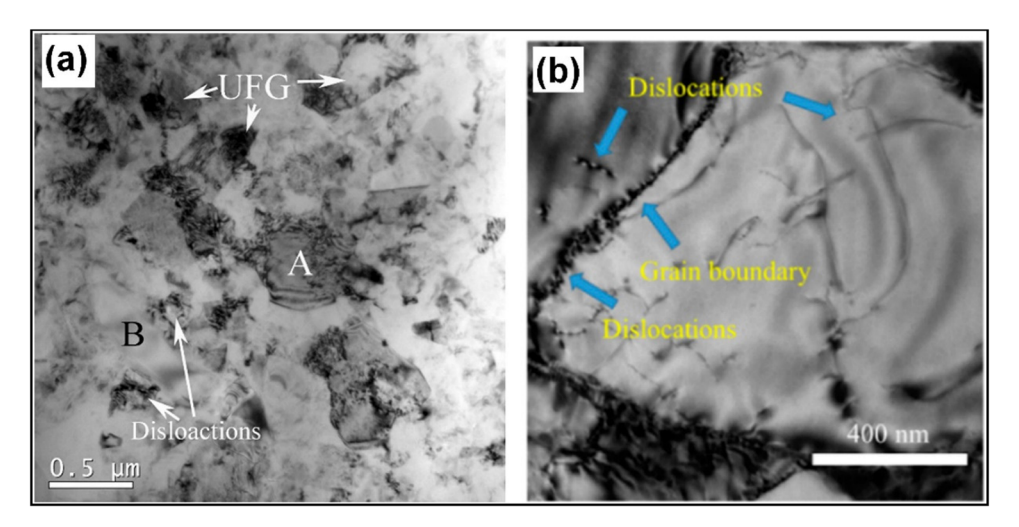


Figure 36: Dislocation piles up at the grain boundaries of the (a) Al-SiC composite [186] and (b) Al-GNP composite [233].

yield stress of the composite matrix [236]. The reinforcement particles and Al have different CTEs, which causes prismatic punching of the dislocation at the interface and increases the strength of the composite matrix. The mechanical properties of the alloy alter at high temperatures due to the rapid diffusion rate, but when reinforcement particles are introduced to the matrix, the distance between the particles reduces. The dislocations encounter more obstructions as a result, which causes them to pile up and improve the strength of the composite. Because of the mismatch in the CTE, the change in the yield strength can be described by the following equation [239,240]:

$$\Delta \sigma_{\rm CTE} = 4.33 {\rm Gm} \times b \sqrt{\frac{\Delta T \times \Delta {\rm CTE} \times v_{\rm R}}{b \times d(1 - v)}},$$
 (2)

where $\Delta\sigma_{\rm CTE}$ is the change in the yield strength due to a mismatch in the CTE, Gm is the shear modulus of Al (2.6 × 104 MPa), b is the Burgers vector of Al (0.286 nm [116]), ΔT = is the difference between the fabrication temperature and room temperature (25°C), Δ CTE is the difference of CTE, d is the mean equivalent diameter of reinforcement, and v is the volume fraction of the reinforcement in composites.

Al-SiC composite was fabricated by Maderia et al. [241] using the PM technique, and the results demonstrate an increase in strength above the monolithic Al matrix. They claimed that the primary factor increasing the composite's strength is the strengthening by dislocation caused by a CTE mismatch between Al and SiC. Additionally, the CTE mismatch enhances the damping capability of the Al-SiC composite [242]. However, the SiC particle size has a unique impact on the CTE mismatch-based strengthening of the composite. According to Ma et al. [237], SiC particles of lower sizes make CTE strengthening by mismatch easier. The CTE gap between Al and graphene in the case of Al-Gr composite is likewise wide. Contrary to other reinforcements, Gr has a fairly big lateral size. As a result, CTE mismatch strengthening has a relatively small impact on the overall strength of the Al-Gr composite [146].

5.4 Strengthening due to load transfer

Due to their exceptional mechanical properties, the reinforcing particles are challenging to deform when a composite is stressed. As a result, there are many dislocations where the aluminum matrix and the reinforcing particles meet. Due to this, a significant amount of dislocation manifests at the interface between the reinforcing particles and the aluminum matrix. The field of stress created by the dislocation stacks prevents the dislocation from moving, increasing the strength of the composite [243]. This kind of action occurs when an external load is applied, as in the case of hot pressing, hot rolling, and other thermomechanical operations.

According to the shear lag concept, the interfacial strength between the Al matrix and reinforcement plays a major role in strengthening through load transfer from matrix to reinforcement [236]. Theoretically, it is calculated using the following equation:

$$\sigma_{\rm LT} = \frac{1}{2} \nu_{\rm R} \tau_m s - \nu_{\rm R} \sigma_m, \tag{3}$$

where v_R is the volume fraction of reinforcement, σ_m is the yield strength of the reinforcement, τ_m is the yield strength of the matrix, and s is the aspect ratio of the reinforcement.

The fundamental reason for the increased strength of Al–SiC composite, according to several research studies [237,244], is the load transfer from matrix to reinforcement. It has been discovered that composite materials with strong interfacial bonds are capable of efficiently transferring loads from soft base matrix particles to hard reinforcement particles [245]. Therefore, for load transfer strengthening, high wettability between Al and reinforcement particles is crucial. Heat treatment of Al–SiC composite can increase the wettability of Al and reinforcing particles (SiC/Gr) [181]. Additionally, it can also be accomplished by adding third-phase particles, such as magnesium (Mg), to AMMCs [246,247].

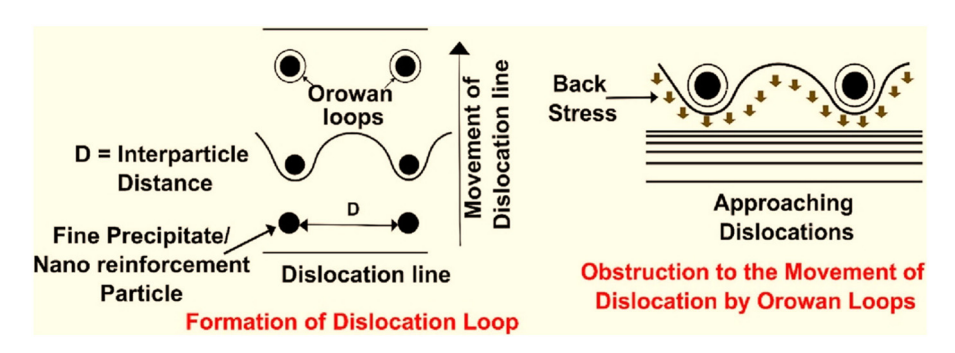


Figure 37: Schematic of the Orowanian strengthening mechanism.

The primary impediment to attaining load transfer strengthening in an Al-Gr composite is the aggregation of graphene particles brought by a weak van der Waal's force of attraction. It has been found that a large weight fraction of graphene in an aluminum composite causes agglomeration, which weakens the link between the particles of aluminum and graphene. Thus, it reduces the strength of the composite by affecting the load transmission to the graphene particles across the Al-graphene interface during deformation [145,192]. In an Al-GNP composite consisting of 1.5 wt% of GNPs, Vignesh Kumar et al. [232] demonstrated the uniform distribution of GNPs and strong interfacial connection between GNPs and Al. As a result, the composite becomes stronger through strengthened load transfer. Load transfer strengthening of the Al-Gr composite is hampered by structural degradation to the graphene layer [145,248]. For maximum strength in the composite, it is therefore essential to retain the structural integrity of graphene layers during production.

6 Conclusions

This study reviews the recent advancements in aluminumbased MMCs reinforced by carbides (SiC, TiC) and carbonbased allotropes (graphene). The mechanical and wear properties have been assessed in detail. The processing technique for producing aluminum-based hybrid composites has been discussed in detail. The recent research investigations on graphene-reinforced AMC processing are summarized to analyze various results related to enhancement in mechanical and tribological properties recorded in the last few years. It has been well understood that improvement in the AMC properties is associated with the successful incorporation of graphene in the metallic matrices. The fabrication technique for aluminum composites has been reviewed, and the PM methodology is elaborated in detail. When compared to other fabrication techniques, PM is proven to be more successful in overcoming obstacles. Additionally, the SPS process in PM is effective in comparison to the other two techniques. It offers faster densification and lowers the likelihood that undesirable phases would emerge in the matrix of the composite Al-SiC/TiC/ Al-graphene. However, compared to hot- and cold-press sintering, it is more expensive and difficult. Additionally, flaws have not yet been completely eliminated. In the end, the strengthening mechanism has been discussed in detail for aluminum composites. The Hall-Petch strengthening, Orowan strengthening, strengthening resulting from CTE mismatch, and strengthening resulting from load transfer are the principal strengthening mechanisms involved in enhancing the strength of the Al-graphene and Al-SiC composites. In the case of Al-GNP composite, Orowan and load transfer strengthening predominate over others. However, in the case of Al-SiC composites, the Orowan strengthening predominates at larger SiC fractions, whereas the fine grain strengthening predominates at lower SiC fractions. When reinforcements (SiC/graphene) are added, the composite's grain is refined, which causes Hall-Petch strengthening.

7 Future perspectives

A lot of work needs to be done in industrializing AMNCs in various applications like the automotive and aircraft sectors in order to broaden the current field. Even though AMCs have seen substantial research advancements over the past two decades, a special focus should be placed on creating commercial, and affordable composite materials with improved mechanical and tribological performance. It is anticipated that the wear studies of AMNCs can further study those natural reinforcements, such as fly ash or agrowastes. It is anticipated that significant research efforts are still needed to close the gaps in the field. For instance, despite the abundance of experimental reports, computational and numerical investigations have not been carried out to the same extent, likely due to a lack of understanding of the precise underlying mechanisms in some cases. This section outlines some of the major concerns and potential directions that will benefit both academic and commercial initiatives to support the creation of high-performance AMCs.

- Numerous research teams have worked to increase the distribution of GNPs by altering the surface of Al and functionalizing GNPs, but their efforts have not always been successful. New dispersion techniques should be investigated in future studies to account for the uniform dispersion of GNPs in Al.
- Another fascinating area for future investigation is the additive manufacturing (AM) of AMCs. There are very few studies on GNPs that have undergone SLM processing, but the findings are encouraging. Some of the existing processing issues can be resolved and the applications of GNPs can be expanded by the direct manufacturing of complex parts from powders and the quick processing times in AM.
- There are currently no investigations on the impact of GNP addition on the precipitation and creep behavior of Al alloys in the accessible literature. The authors of this review contend that the presence of GNPs significantly

affects the size, shape, and rate of coarsening of precipitates in aluminum alloys, which in turn affects the creep properties of the alloys. The majority of the aluminum alloys used in automotive and aerospace applications are precipitation hardenable, thus this is another crucial subject that needs to be studied. Commercial aluminum alloys from the 2XXX and 7XXX series as well as third-generation Al–Cu–Li alloys reinforced with GNPs should be researched under various heat treatment settings to see how GNPs affect their physical and mechanical properties.

Funding information: This study was supported and funded by Ministry of Higher Education (MOHE), Malaysia, through the Fundamental Research Grant Scheme FRGS/1/2019/TK08/UTP/02/1, and Universiti Teknologi PETRONAS, Malaysia, by Yayasan Universiti Teknologi PETRONAS grant (YUTP-FRG 1/2021), with grant number (015LCO-339).

Author contributions: All authors have accepted responsibility for the entire content of this manuscript and approved its submission.

Conflict of interest: The authors state no conflict of interest.

References

- Zhang W, Xu J. Advanced lightweight materials for automobiles: A review. Mater Des. 2022;221:110994.
- [2] Alam MA, Ya HH, Yusuf M, Sivraj R, Mamat OB, Sapuan SM, et al. Modeling, optimization and performance evaluation of TiC/graphite reinforced Al 7075 hybrid composites using response surface methodology. Materials. 2021;14(16):4703. doi: 10.3390/ ma14164703.
- [3] Lava Kumar P, Lombardi A, Byczynski G, Narayana Murty SVS, Murty BS, Bichler L. Recent advances in aluminium matrix composites reinforced with graphene-based nanomaterial: A critical review. Prog Mater Sci. Jul 2022;128:100948. doi: 10.1016/J. PMATSCI.2022.100948.
- [4] Miller WS, Zhuang L, Bottema J, Wittebrood AJ, De Smet P, Haszler A, et al. Recent development in aluminium alloys for the automotive industry. Mater Sci Eng A. 2000;280(1):37–49.
- [5] Alam MA, Ya HH, Azeem M, Hussain PB, bin Salit MS, Khan R, et al. Modelling and optimisation of hardness behaviour of sintered Al/ SiC composites using RSM and ANN: A comparative study. J Mater Res Technol. Nov 2020;9(6):14036–50. doi: 10.1016/j.jmrt.2020. 09.087.
- [6] Alam MA, Ya HH, Azeem M, Yusuf M, Soomro IA, Masood F, et al. Artificial neural network modeling to predict the effect of milling time and TiC content on the crystallite size and lattice strain of Al7075-TiC Composites fabricated by powder metallurgy. Crystals. 2022;12(3):372. doi: 10.3390/cryst12030372.

- [7] Sharma S, Patyal V, Sudhakara P, Singh J, Petru M, Ilyas RA. Mechanical, morphological, and fracture-deformation behavior of MWCNTs-reinforced (Al-Cu-Mg-T351) alloy cast nanocomposites fabricated by optimized mechanical milling and powder metallurgy techniques. Nanotechnol Rev. 2021;11(1):65–85. doi: 10.1515/ ntrev-2022-0005.
- [8] Mistry JM, Gohil PP. Research review of diversified reinforcement on aluminum metal matrix composites: Fabrication processes and mechanical characterization. Sci Eng Compos Mat. 2018;25(4):633–47. doi: 10.1515/secm-2016-0278.
- [9] Bhaskar S, Kumar M, Patnaik A. Mechanical and tribological overview of ceramic particulates reinforced aluminium alloy composites. Rev Adv Mater Sci. 2019;58(1):280–94. doi: 10.1515/ rams-2019-0033.
- [10] Song Y, Wang A, Ma D, Xie J, Wang W. Dynamic recrystallization behavior and nucleation mechanism of dual-scale SiCp/A356 composites processed by P/M method. Nanotechnol Rev. 2023;12(1):20220506. doi: 10.1515/ntrev-2022-0506.
- [11] Ikram R, Mohamed Jan B, Nagy PB, Szabo T. Recycling waste sources into nanocomposites of graphene materials: Overview from an energy-focused perspective. Nanotechnol Rev. 2023;12(1):20220512. doi: 10.1515/ntrev-2022-0512.
- [12] Md Ali A, Omar MZ, Hashim H, Salleh MS, Mohamed IF. Recent development in graphene-reinforced aluminium matrix composite: A review. Rev Adv Mater Sci. 2021;60(1):801–17. doi: 10.1515/ rams-2021-0062.
- [13] Yunus M, Alamro T. Evaluation of wear and corrosion properties of FSWed aluminum alloy plates of AA2020-T4 with heat treatment under different aging periods. Rev Adv Mater Sci. 2022;61(1):687–97. doi: 10.1515/rams-2022-0261.
- [14] Gao Y, Vini MH, Daneshmand S. Effect of nano Al2O3 particles on the mechanical and wear properties of Al/Al2O3 composites manufactured via ARB. Rev Adv Mater Sci. 2022;61(1):734–43. doi: 10.1515/rams-2022-0268.
- [15] Khatkar SK. Hybrid magnesium matrix composites: A review of reinforcement philosophies, mechanical and tribological characteristics. Rev Adv Mater Sci. 2023;62(1):20220294. doi: 10.1515/ rams-2022-0294.
- [16] Lou S, Li X, Guo G, Ran L, Liu Y, Zhang P, et al. Hot deformation behavior and microstructure of a 0.5 wt% graphene nanoplatelet reinforced aluminum composite. Sci Eng Compos Mater. 2022;29(1):97–112. doi: 10.1515/secm-2022-0009.
- [17] Zhang WW, Hu Y, Wang Z, Yang C, Zhang GQ, Prashanth KG, et al. A novel high-strength Al-based nanocomposite reinforced with Ti-based metallic glass nanoparticles produced by powder metallurgy. Mater Sci Eng A. 2018;734(February):34–41. doi: 10.1016/j. msea.2018.07.082.
- [18] Jeyasimman D, Sivasankaran S, Sivaprasad K, Narayanasamy R, Kambali RS. An investigation of the synthesis, consolidation and mechanical behaviour of Al 6061 nanocomposites reinforced by TiC via mechanical alloying. Mater Des. 2014;57:394–404. doi: 10. 1016/j.matdes.2013.12.067.
- [19] Scudino S, Liu G, Prashanth KG, Bartusch B, Surreddi KB, Murty BS, et al. Mechanical properties of Al-based metal matrix composites reinforced with Zr-based glassy particles produced by powder metallurgy. Acta Mater. 2009;57(6):2029–39. doi: 10.1016/ j.actamat.2009.01.010.
- [20] Ravi Kumar K, Kiran K, Sreebalaji VS. Micro structural characteristics and mechanical behaviour of aluminium matrix composites

- reinforced with titanium carbide. J Alloys Compd. Nov 2017;723:795-801. doi: 10.1016/j.jallcom.2017.06.309.
- [21] Ashkenazi D. How aluminum changed the world: A metallurgical revolution through technological and cultural perspectives. Technol Forecast Soc Change. Jun 2019;143:101-13. doi: 10.1016/J. TECHFORE.2019.03.011.
- [22] Arif S, Jamil B, Naim Shaikh MB, Aziz T, Ansari AH, Khan M. Characterization of surface morphology, wear performance and modelling of graphite reinforced aluminium hybrid composites. Eng Sci Technol an Int J. 2020;23(3):674-90. doi: 10.1016/j.jestch. 2019.07.001.
- [23] Rahimi B, Khosravi H, Haddad-Sabzevar M. Microstructural characteristics and mechanical properties of Al-2024 alloy processed via a rheocasting route. Int I Miner Metall Mater. 2015;22(1):59-67. doi: 10.1007/s12613-015-1044-8.
- [24] Kumar KA, Natarajan S, Duraiselvam M, Ramachandra S. Synthesis, characterization and mechanical behavior of Al 3003 -TiO 2 surface composites through friction stir processing. Mater Manuf Process. 2019;34(2):183-91. doi: 10.1080/10426914.2018. 1544711.
- Ahmadi E, Ranjkesh M, Mansoori E, Fattahi M, Mojallal RY, [25] Amirkhanlou S. Microstructure and mechanical properties of Al/ ZrC/TiC hybrid nanocomposite filler metals of tungsten inert gas welding fabricated by accumulative roll bonding. J Manuf Process. 2017;26:173-7. doi: 10.1016/j.jmapro.2017.02.012.
- Bauri R, Yadav D, Shyam Kumar CN, Balaji B. Tungsten particle [26] reinforced Al 5083 composite with high strength and ductility. Mater Sci Eng A. 2015;620:67-75. doi: 10.1016/j.msea.2014.09.108.
- [27] Natrayan L, Senthil Kumar M. An integrated artificial neural network and Taguchi approach to optimize the squeeze cast process parameters of AA6061/Al2O3/SiC/Gr hybrid composites prepared by novel encapsulation feeding technique. Mater Today Commun. 2020;25(June):101586. doi: 10.1016/j.mtcomm.2020.
- [28] Manohar G, Pandey KM, Maity SR. Effect of microwave sintering on the microstructure and mechanical properties of AA7075/B4C/ ZrC hybrid nano composite fabricated by powder metallurgy techniques. Ceram Int. Aug 2021;47:32610-8. doi: 10.1016/J. CERAMINT.2021.08.156.
- Hu Q, Zhao H, Li F. Effects of manufacturing processes on microstructure and properties of Al/A356-B4C composites. Mater Manuf Process. 2016;31(10):1292-300. doi: 10.1080/10426914. 2016.1151049.
- Rao RN, Das S. Effect of SiC content and sliding speed on the wear behaviour of aluminium matrix composites. Mater Des. 2011;32(2):1066-71.
- [31] Natarajan N, Vijayarangan S, Rajendran I. Wear behaviour of A356/25SiCp aluminium matrix composites sliding against automobile friction material. Wear. 2006;261(7-8):812-22.
- [32] Shafiei-Zarghani A, Kashani-Bozorg SF, Zarei-Hanzaki A. Microstructures and mechanical properties of Al/Al2O3 surface nano-composite layer produced by friction stir processing. Mater Sci Eng A. 2009;500(1-2):84-91.
- Bandil K, Vashisth H, Kumar S, Verma L, Jamwal A, Kumar D. [33] Microstructural, mechanical and corrosion behaviour of Al - Si alloy reinforced with SiC metal matrix composite. J Compos Mat. 2019;53:4215-23. doi: 10.1177/0021998319856679.
- Jamwal A, Vates UK, Gupta P, Aggarwal A, Sharma BP. Fabrication and characterization of Al₂O₃ - TiC-reinforced aluminum matrix composites. Singapore: Springer; 2019.

- [35] Mustansar C, Gupta P, Engineering M, Prakash A, Shimla G, Pradesh H. Advance research progresses in aluminium matrix composites: Manufacturing & applications. Integr Med Res. 2019;8(5):4924-39. doi: 10.1016/j.jmrt.2019.06.028.
- [36] Garg P, Gupta P, Kumar D, Parkash O. Structural and mechanical properties of graphene reinforced aluminum matrix composites. J Mater Environ Sci. 2016;7(5):1461-73.
- [37] Ahamad N. Mohammad A. Wear, optimization and surface metal matrix composites. Proc Inst Mech Eng J. 2020;235:93-102. doi: 10.1177/1350650120970432.
- [38] Ahamad N, Mohammad A. Phase, microstructure and tensile strength of Al - Al 2 O 3 - C hybrid metal matrix composites. Proc Inst Mech Eng C. 2020;234(13):1-13. doi: 10.1177/ 0954406220909846.
- [39] Ahamad N, Mohammad A. Structural and mechanical characterization of stir cast Al - Al 2 O 3 - TiO 2 hybrid metal matrix composites. J Compos Mat. 2020;54:2985-97. doi: 10.1177/ 0021998320906207.
- [40] Jamwal A, Mittal P, Agrawal R, Gupta S, Kumar D, Sadasivuni KK. Towards sustainable copper matrix composites: Manufacturing routes with structural, mechanical, electrical and corrosion behaviour. J Compos Mat. 2020;54:2635-49. doi: 10.1177/ 0021998319900655.
- [41] Rahaman MN. Ceramic processing and sintering. Boca Raton: CRC Press; 2017.
- Jang BZ, Zhamu A. Processing of nanographene platelets (NGPs) [42] and NGP nanocomposites: A review. J Mater Sci. 2008;43(15):5092-101.
- [43] Carter CB, Norton MG. Ceramic materials: Science and engineering. Springer New York: Springer Science & Business Media; 2007.
- [44] Sujith SV, Mahapatra MM, Mulik RS. Microstructural characterization and experimental investigations into two body abrasive wear behavior of Al-7079/TiC in-situ metal matrix composites. Proc Inst Mech Eng Part | | Eng Tribol. 2020;234(4):588-607. doi: 10.1177/1350650119883559.
- [45] Mohapatra S, Chaubey AK, Mishra DK, Singh SK. Fabrication of Al - TiC composites by hot consolidation technique: Its microstructure and mechanical properties. Integr Med Res. 2015;5(2):117-22. doi: 10.1016/j.jmrt.2015.07.001.
- Moorthy CVKNSN, Kumar GN, Srinivas V, Kumar MA, Reddy K, [46] Vasundhara DN, et al. Metallography, microstructure, and wear analysis of AA 6063/TiC composites for augmented dry sliding property at room. Temp Metallogr Microstruct Anal. 2020;9(2):140-51. doi: 10.1007/s13632-020-00625-6.
- [47] Prasad SV, Asthana R. Aluminum metal-matrix composites for automotive applications: Tribological considerations. Tribol Lett. 2004;17(3):445-53. doi: 10.1023/B:TRIL.0000044492.91991.f3.
- [48] Kamrani S, Riedel R, Seyed Reihani SM, Kleebe HJ. Effect of reinforcement volume fraction on the mechanical properties of Alg -SiC nanocomposites produced by mechanical alloying and consolidation. J Compos Mater. 2010;44(3):313-26. doi: 10.1177/ 0021998309347570.
- [49] Prashantha Kumar HG, Anthony Xavior M. Effect of graphene addition and tribological performance of Al 6061/graphene flake composite. Tribol - Mater Surfaces Interfaces. 2017;11(2):88-97. doi: 10.1080/17515831.2017.1329920.
- [50] Dhand V, Rhee KY, Ju Kim H, Ho Jung D. A comprehensive review of graphene nanocomposites: Research status and trends. J Nanomater. 2013;2013:1-14. doi: 10.1155/2013/763953.

- [51] Tabandeh-Khorshid M, Omrani E, Menezes PL, Rohatgi PK. Tribological performance of self-lubricating aluminum matrix nanocomposites: Role of graphene nanoplatelets. Eng Sci Technol an Int J. 2016;19(1):463–9. doi: 10.1016/j.jestch.2015. 09.005.
- [52] Thomas S, Umasankar V. Review of recent progress in the development and properties of aluminum metal matrix composites reinforced with multiwalled carbon nanotube by powder metallurgy route. Mater Perform Charact. 2019;8(3):20180140. doi: 10.1520/mpc20180140.
- [53] Pan S, Saso T, Yu N, Sokoluk M, Yao G, Umehara N, et al. New study on tribological performance of AA7075-TiB2 nanocomposites. Tribol Int. May 2020;152:106565. doi: 10.1016/j.triboint.2020. 106565.
- [54] Khorashadizade F, Abazari S, Rajabi M, Bakhsheshi-Rad HR, Ismail AF, Sharif S, et al. Overview of magnesium-ceramic composites: Mechanical, corrosion and biological properties. J Mater Res Technol. 2021;15:6034–66. doi: 10.1016/j.jmrt.2021. 10.141
- [55] Hu Q, Zhao H, Li F. Microstructures and properties of SiC particles reinforced aluminum-matrix composites fabricated by vacuumassisted high pressure die casting. Mater Sci Eng A. 2017;680:270–7.
- [56] Arif S, Alam T, Ansari AH, Siddiqui MA, Mohsin M. Study of mechanical and tribological behaviour of Al/SiC/ZrO 2 hybrid composites fabricated through powder metallurgy technique. Mater Res Express 4:076511.
- [57] Almotairy SM, Alharthi NH, Alharbi HF, Abdo HS. Superior mechanical performance of inductively sintered Al/SiC nanocomposites processed by novel milling route. Sci Rep. 2020;10(1):1–13. doi: 10.1038/s41598-020-67198-w.
- [58] Pu B, Lin X, Li B, Chen X, He C, Zhao N. Effect of SiC nanoparticles on the precipitation behavior and mechanical properties of 7075Al alloy. J Mater Sci. 2020;55(14):6145–60. doi: 10.1007/ s10853-020-04381-4.
- [59] Khajelakzay M, Bakhshi SR. Optimization of spark plasma sintering parameters of Si3N4-SiC composite using response surface methodology (RSM). Ceram Int. 2017;43(9):6815–21. doi: 10.1016/j. ceramint.2017.02.099.
- [60] Kutzhanov MK, Matveev AT, Kvashnin DG, Corthay S, Kvashnin AG, Konopatsky AS, et al. Al/SiC nanocomposites with enhanced thermomechanical properties obtained from microwave plasmatreated nanopowders. Mater Sci Eng A. Sep 2021;824:141817. doi: 10.1016/J.MSEA.2021.141817.
- [61] Pakseresht AH, Baghbaderani HA, Yazdani-Rad R. Role of different fractions of nano-size SiC and milling time on the microstructure and mechanical properties of Al–SiC nanocomposites. Trans Indian Inst Met. 2016;69(5):1007–14.
- [62] Walczak M, Pieniak D, Zwierzchowski M. The tribological characteristics of SiC particle reinforced aluminium composites. Arch Civ Mech Eng. 2015;15(1):116–23.
- [63] Dhanashekar M, Loganathan P, Ayyanar S, Mohan SR, Sathish T. Mechanical and wear behaviour of AA6061/SiC composites fabricated by powder metallurgy method. Mater Today Proc. 2020;21:1008–12. doi: 10.1016/j.matpr.2019.10.052.
- [64] Shaikh MBN, Arif S, Aziz T, Waseem A, Shaikh MAN, Ali M. Microstructural, mechanical and tribological behaviour of powder metallurgy processed SiC and RHA reinforced Al-based composites. Surf Interfaces. 2019;15(May 2018):166–79. doi: 10.1016/j. surfin.2019.03.002.

- [65] Surya MS, Prasanthi G. Manufacturing, microstructural and mechanical characterization of powder metallurgy processed Al7075/SiC metal matrix composite. Mater Today Proc. 2020;39:1175–9. doi: 10.1016/j.matpr.2020.03.315.
- [66] Mousavian RT, Khosroshahi RA, Yazdani S, Brabazon D, Boostani AF. Fabrication of aluminum matrix composites reinforced with nano-to micrometer-sized SiC particles. Mater Des. 2016:89:58–70.
- [67] Reddy MP, Shakoor RA, Parande G, Manakari V, Ubaid F, Mohamed A, et al. Enhanced performance of nano-sized SiC reinforced Al metal matrix nanocomposites synthesized through microwave sintering and hot extrusion techniques. Prog Nat Sci Mater Int. 2017;27(5):606–14.
- [68] Manohar G, Maity SR, Pandey KM. Microstructural and mechanical properties of microwave sintered AA7075/graphite/SiC hybrid composite fabricated by powder metallurgy techniques. Silicon. 2021;14:5179–89. doi: 10.1007/s12633-021-01299-7.
- [69] Tan A, Teng J, Zeng X, Fu D, Zhang H. Fabrication of aluminium matrix hybrid composites reinforced with SiC microparticles and TiB2 nanoparticles by powder metallurgy. Powder Metall. 2017;60(1):66–72. doi: 10.1080/00325899.2016.1274816.
- [70] Roy P, Singh S, Pal K. Enhancement of mechanical and tribological properties of SiC-and CB-reinforced aluminium 7075 hybrid composites through friction stir processing. Adv Compos Mater. 2019;28(sup1):1–18.
- [71] Bathula S, Anandani RC, Dhar A, Srivastava AK. Synthesis and characterization of Al-alloy/SiC p nanocomposites employing high energy ball milling and spark plasma sintering. Adv Mater Res. 2012;410:224–7. doi: 10.4028/www.scientific.net/AMR. 410.224.
- [72] Li XP, Liu CY, Ma MZ, Liu RP. Microstructures and mechanical properties of AA6061-SiC composites prepared through spark plasma sintering and hot rolling. Mater Sci Eng A. 2016;650:139–44. doi: 10.1016/j.msea.2015.10.015.
- [73] Leszczyńska-madej B, Garbiec D, Madej M. Effect of sintering temperature on microstructure and selected properties of spark plasma sintered Al-SiC composites. Vacuum. 2020;164(March 2019):250–5. doi: 10.1016/j.vacuum.2019.03.033.
- [74] Surya MS. Effect of SiC weight percentage and sintering duration on microstructural and mechanical behaviour of Al6061/SiC composites produced by powder metallurgy technique. Silicon. 2021;14:2731–9. doi: 10.1007/s12633-021-01053-z.
- [75] Reddy MP, Shakoor RA, Parande G, Manakari V, Ubaid F, Mohamed A, et al. Progress in natural science: Materials international enhanced performance of nano-sized SiC reinforced Al metal matrix nanocomposites synthesized through microwave sintering and hot extrusion techniques. Prog Nat Sci Mater Int. 2017;27(5):606–14. doi: 10.1016/j.pnsc.2017.08.015.
- [76] Rahman MH, Al Rashed HMM. Characterization of silicon carbide reinforced aluminum matrix composites. Procedia Eng. 2014;90:103–9. doi: 10.1016/j.proeng.2014.11.821.
- [77] Devaganesh S, Kumar PKD, Venkatesh N, Balaji R. Study on the mechanical and tribological performances of hybrid SiC-Al7075 metal matrix composites. J Mater Res Technol. 2020;9(3):3759–66. doi: 10.1016/j.jmrt.2020.02.002.
- [78] Ramkumar KR, Sivasankaran S, Al-mufadi FA, If TD, Siddharth S. ScienceDirect Investigations on microstructure, mechanical, and tribological behaviour of AA 7075 x wt.% TiC composites for aerospace applications. Arch Civ Mech Eng. 2019;19(2):428–38. doi: 10.1016/j.acme.2018.12.003.

- [79] Saravanan C, Subramanian K, Anandakrishnan V, Sathish S. Tribological behavior of AA7075-TiC composites by powder metallurgy. Ind Lubr Tribol. 2018;70:1066–71.
- [80] Baskaran S, Anandakrishnan V, Duraiselvam M. Investigations on dry sliding wear behavior of in situ casted AA7075 – TiC metal matrix composites by using Taguchi technique. J Mater. 2014;60:184–92. doi: 10.1016/j.matdes.2014.03.074.
- [81] Nemati N, Khosroshahi R, Emamy M, Zolriasatein A. Investigation of microstructure, hardness and wear properties of Al-4.5wt.% Cu-TiC nanocomposites produced by mechanical milling. Mater Des. 2011;32(7):3718–29. doi: 10.1016/j.matdes.2011.03.056.
- [82] Ghasali E, Fazili A, Alizadeh M, Shirvanimoghaddam K. Evaluation of microstructure and mechanical properties of Al-TiC metal matrix composite prepared by conventional, microwave and spark. Materials (Basel, Switzerland). 2017;10:1255. doi: 10.3390/ ma10111255.
- [83] Azimi A, Shokuhfar A, Nejadseyfi O. Mechanically alloyed Al7075 TiC nanocomposite: Powder processing, consolidation and mechanical strength. Mater Des. 2015;66:137–41. doi: 10.1016/j. matdes.2014.10.046.
- [84] Salur E, Acarer M, Şavkliyildiz İ. Improving mechanical properties of nano-sized TiC particle reinforced AA7075 Al alloy composites produced by ball milling and hot pressing. Mater Today Commun. Jun 2021;27:102202. doi: 10.1016/j.mtcomm.2021.102202.
- [85] Kar C, Surekha B. Effect of red mud and TiC on friction and wear characteristics of Al 7075 metal matrix composites. Aust J Mech Eng. 2019;20:1–10.
- [86] Rao VR, Ramanaiah N, Sarcar MMM. Tribological properties of aluminium metal matrix composites (AA7075 reinforced with titanium carbide (TiC) particles). Int J Adv Sci Technol. 2016;88:13–26.
- [87] Devaneyan SP, Ganesh R, Senthilvelan T. On the Mechanical properties of hybrid aluminium 7075 Matrix composite material reinforced with SiC and TiC produced by powder metallurgy method. Indian J Mat Sci. 2017;2017:3067257.
- [88] Cabeza M, Feijoo I, Merino P, Pena G, Pérez MC, Cruz S, et al. Effect of high energy ball milling on the morphology, microstructure and properties of nano-sized TiC particle-reinforced 6005A aluminium alloy matrix composite. Powder Technol. 2017;321:31–43. doi: 10.1016/j.powtec.2017.07.089.
- [89] Gopalakrishnan S, Murugan N. Production and wear characterisation of AA 6061 matrix titanium carbide particulate reinforced composite by enhanced stir casting method. Compos Part B Eng. Mar 2012;43(2):302–8. doi: 10.1016/j.compositesb.2011.08.049.
- [90] Zhang W, Zhou S, Ren W, Yang Y, Shi L, Zhou Q, et al. Uniformly dispersing GNPs for fabricating graphene-reinforced pure Ti matrix composites with enhanced strength and ductility. J Alloys Compd. 2021;888:161527. doi: 10.1016/j.jallcom.2021.161527.
- [91] Yang Y, Liu M, Zhou S, Ren W, Zhou Q, Shi L. Breaking through the strength-ductility trade-off in graphene reinforced Ti6Al4V composites. J Alloys Compd. 2021;871:159535. doi: 10.1016/j.jallcom. 2021.159535.
- [92] Bartolucci SF, Paras J, Rafiee MA, Rafiee J, Lee S, Kapoor D, et al. Graphene-aluminum nanocomposites. Mater Sci Eng A. 2011;528(27):7933–7. doi: 10.1016/j.msea.2011.07.043.
- [93] Geim AK, Novoselov KS. The rise of graphene. In: Rodgers P, editor. Nanoscience and technology: A collection of reviews from nature journals. Toh Tuck Link Singapore: World Scientific; 2010. p. 11–9.

- [94] Yihong W, Zexiang S, Ting Y. Two-dimensional carbon: Fundamental properties, synthesis, characterization, and applications. New York: CRC Press; 2014.
- [95] Singh V, Joung D, Zhai L, Das S, Khondaker SI, Seal S. Graphene based materials: Past, present and future. Prog Mater Sci. 2011;56(8):1178–271. doi: 10.1016/j.pmatsci.2011.03.003.
- [96] Lee C, Wei X, Kysar JW, Hone J. Measurement of the elastic properties and intrinsic strength of monolayer graphene. Science (80). 2008;321(5887):385–8.
- [97] Ruoff RS, Lorents DC. Mechanical and thermal properties of carbon nanotubes. Carbon N Y. 1995;33(7):925–30.
- [98] Chae SH, Lee YH. Carbon nanotubes and graphene towards soft electronics. Nano Converg. 2014;1(1):1–26.
- [99] Mayorov AS, Gorbachev RV, Morozov SV, Britnell L, Jalil R, Ponomarenko LA, et al. Micrometer-scale ballistic transport in encapsulated graphene at room temperature. Nano Lett. 2011;11(6):2396–9.
- [100] Balandin AA, Ghosh S, Bao W, Calizo I, Teweldebrhan D, Miao F, et al. Superior thermal conductivity of single-layer graphene. Nano Lett. 2008;8(3):902–7.
- [101] Naseer A, Ahmad F, Aslam M, Guan BH, Harun W, Muhamad N, et al. A review of processing techniques for graphene-reinforced metal matrix composites. Mater Manuf Process. 2019;34(9):957–85. doi: 10.1080/10426914.2019.1615080.
- [102] Ghazanlou SI, Eghbali B, Petrov R. Microstructural evolution and strengthening mechanisms in Al7075/graphene nano-plates/ carbon nano-tubes composite processed through accumulative roll bonding. Mater Sci Eng A. 2021;807(February):140877. doi: 10. 1016/j.msea.2021.140877.
- [103] Şenel MC, Gürbüz M, Koç E. Mechanical and tribological behaviours of aluminium matrix composites reinforced by graphene nanoplatelets. Mater Sci Technol. Nov 2018;34(16):1980–9. doi: 10.1080/02670836.2018.1501839.
- [104] Khoshghadam-Pireyousefan M, Rahmanifard R, Orovcik L, Švec P, Klemm V. Application of a novel method for fabrication of graphene reinforced aluminum matrix nanocomposites: Synthesis, microstructure, and mechanical properties. Mater Sci Eng A. 2020;772(September 2019):138820. doi: 10.1016/j.msea.2019. 138820
- [105] Seyed Pourmand N, Asgharzadeh H. Aluminum matrix composites reinforced with graphene: A review on production, microstructure, and properties. Crit Rev Solid State Mater Sci. 2020;45(4):289–337. doi: 10.1080/10408436.2019.1632792.
- [106] Papageorgiou DG, Kinloch IA, Young RJ. Mechanical properties of graphene and graphene-based nanocomposites. Progress in Materials Science. Oct 1, 2017;90:75–127. Elsevier Ltd. doi: 10.1016/ j.pmatsci.2017.07.004.
- [107] Chak V, Chattopadhyay H. Fabrication and heat treatment of graphene nanoplatelets reinforced aluminium nanocomposites. Mater Sci Eng A. 2020;791(January):139657. doi: 10.1016/j.msea. 2020.139657.
- [108] Papageorgiou DG, Kinloch IA, Young RJ. Mechanical properties of graphene and graphene-based nanocomposites. Prog Mater Sci. 2017;90:75–127. doi: 10.1016/j.pmatsci.2017.07.004.
- [109] Shin SE, Bae DH. Deformation behavior of aluminum alloy matrix composites reinforced with few-layer graphene. Compos Part A Appl Sci Manuf. 2015;78:42–7. doi: 10.1016/j.compositesa.2015. 08.001.

- [110] Yan SJ, Dai SL, Zhang XY, Yang C, Hong QH, Chen JZ, et al. Investigating aluminum alloy reinforced by graphene nanoflakes. Mater Sci Eng A. 2014;612:440–4.
- [111] Pérez-Bustamante R, Bolaños-Morales D, Bonilla-Martínez J, Estrada-Guel I, Martínez-Sánchez R. Microstructural and hardness behavior of graphene-nanoplatelets/aluminum composites synthesized by mechanical alloying. J Alloys Compd. 2015;615(S1):S578–82. doi: 10.1016/j.jallcom.2014.01.225.
- [112] Wang J, Li Z, Fan G, Pan H, Chen Z, Zhang D. Reinforcement with graphene nanosheets in aluminum matrix composites. Scr Mater. 2012;66(8):594–7. doi: 10.1016/j.scriptamat.2012.01.012.
- [113] Rashad M, Pan F, Tang A, Asif M. Effect of graphene nanoplatelets addition on mechanical properties of pure aluminum using a semi-powder method. Prog Nat Sci Mater Int. Apr 2014;24(2):101–8. doi: 10.1016/j.pnsc.2014.03.012.
- [114] Bastwros M, Kim GY, Zhu C, Zhang K, Wang S, Tang X, et al. Effect of ball milling on graphene reinforced Al6061 composite fabricated by semi-solid sintering. Compos Part B Eng. 2014;60:111–8. doi: 10.1016/j.compositesb.2013.12.043.
- [115] Gürbüz M, Can Şenel M, Koç E. The effect of sintering time, temperature, and graphene addition on the hardness and microstructure of aluminum composites. J Compos Mater. 2018;52(4):553–63. doi: 10.1177/0021998317740200.
- [116] Abazari S, Shamsipur A, Bakhsheshi-rad HR, Ramakrishna S. Graphene family nanomaterial reinforced magnesium-based matrix composites for biomedical application: A comprehensive review. Digit J Ophthalmol. 2015;21:1–41.
- [117] Shukla AK, Nayan N, Murty S, Sharma SC, Chandran P, Bakshi SR, et al. Processing of copper–carbon nanotube composites by vacuum hot pressing technique. Mater Sci Eng A. 2013;560:365–71.
- [118] Jiang LY, Huang Y, Jiang H, Ravichandran G, Gao H, Hwang KC, et al. A cohesive law for carbon nanotube/polymer interfaces based on the van der Waals force. J Mech Phys Solids. 2006;54(11):2436–52.
- [119] So KP, Lee IH, Duong DL, Kim TH, Lim SC, An KH, et al. Improving the wettability of aluminum on carbon nanotubes. Acta Mater. 2011;59(9):3313–20.
- [120] Saboori A, Pavese M, Badini C, Fino P. Microstructure and thermal conductivity of Al–graphene composites fabricated by powder metallurgy and hot rolling techniques. Acta Metall Sin (English Lett). 2017;30(7):675–87.
- [121] Zhou W, Fan Y, Feng X, Kikuchi K, Nomura N, Kawasaki A. Creation of individual few-layer graphene incorporated in an aluminum matrix. Compos Part A Appl Sci Manuf. 2018;112:168–77.
- [122] Dasari BL, Morshed M, Nouri JM, Brabazon D, Naher S. Mechanical properties of graphene oxide reinforced aluminium matrix composites. Compos Part B Eng. 2018;145:136–44.
- [123] Zhang L, Hou G, Zhai W, Ai Q, Feng J, Zhang L, et al. Aluminum/ graphene composites with enhanced heat-dissipation properties by in-situ reduction of graphene oxide on aluminum particles. J Alloys Compd. 2018;748:854–60.
- [124] Noguchi T, Magario A, Fukazawa S, Shimizu S, Beppu J, Seki M. Carbon nanotube/aluminium composites with uniform dispersion. Mater Trans. 2004;45(2):602–4.
- [125] Choi H, Shin J, Min B, Park J, Bae D. Reinforcing effects of carbon nanotubes in structural aluminum matrix nanocomposites. J Mater Res. 2009;24(8):2610–6.
- [126] He CN, Zhao NQ, Shi CS, Song SZ. Mechanical properties and microstructures of carbon nanotube-reinforced Al matrix

- composite fabricated by in situ chemical vapor deposition. J Alloys Compd. 2009;487(1–2):258–62.
- [127] Sridhar I, Narayanan KR. Processing and characterization of MWCNT reinforced aluminum matrix composites. J Mater Sci. 2009;44(7):1750-6.
- [128] Hu Z, Tong G, Lin D, Chen C, Guo H, Xu J, et al. Graphene-reinforced metal matrix nanocomposites A review. Mater Sci Technol (United Kingdom). 2016;32(9):930–53. doi: 10.1080/02670836.2015.1104018.
- [129] Li N, Zhang L, Xu M, Xia T, Ruan X, Song S, et al. Preparation and mechanical property of electrodeposited Al-graphene composite coating. Mater Des. 2016;111:522–7.
- [130] Ju J-M, Wang G, Sim K-H. Facile synthesis of graphene reinforced Al matrix composites with improved dispersion of graphene and enhanced mechanical properties. J Alloys Compd. 2017;704:585–92.
- [131] Murray JW, Rance GA, Xu F, Hussain T. Alumina-graphene nanocomposite coatings fabricated by suspension high velocity oxyfuel thermal spraying for ultra-low-wear. J Eur Ceram Soc. 2018;38(4):1819–28.
- [132] Zhang H, Zhang B, Gao Q, Song J, Han G. A review on microstructures and properties of graphene-reinforced aluminum matrix composites fabricated by friction stir processing. J Manuf Process. 2021;68:126–35.
- [133] Suryanarayana C. Mechanical alloying: A novel technique to synthesize advanced materials. Research. 2019;2019:1–17. doi: 10. 34133/2019/4219812.
- [134] Li JL, Xiong YC, Wang XD, Yan SJ, Yang C, He WW, et al.

 Microstructure and tensile properties of bulk nanostructured aluminum/graphene composites prepared *via* cryomilling. Mater Sci Eng A. 2015;626:400–5. doi: 10.1016/j.msea.2014.12.102.
- [135] Shin SE, Choi HJ, Shin JH, Bae DH. Strengthening behavior of fewlayered graphene/aluminum composites. Carbon N Y. 2015;82(C):143–51. doi: 10.1016/j.carbon.2014.10.044.
- [136] Zhan K, Wu Y, Li J, Zhao B, Yan Y, Xie L, et al. Investigation on surface layer characteristics of shot peened graphene reinforced Al composite by X-ray diffraction method. Appl Surf Sci. 2018;435:1257–64. doi: 10.1016/j.apsusc.2017.11.242.
- [137] Choi W, Lahiri I, Seelaboyina R, Kang YS. Synthesis of graphene and its applications: A review. Crit Rev Solid State Mater Sci. 2010;35(1):52–71.
- [138] Li Z, Fan G, Tan Z, Guo Q, Xiong D, Su Y, et al. Uniform dispersion of graphene oxide in aluminum powder by direct electrostatic adsorption for fabrication of graphene/aluminum composites. Nanotechnology. 2014;25(32):325601.
- [139] Li Z, Guo Q, Li Z, Fan G, Xiong DB, Su Y, et al. Enhanced mechanical properties of graphene (reduced graphene oxide)/aluminum composites with a bioinspired nanolaminated structure. Nano Lett. 2015;15(12):8077–83.
- [140] Gao X, Yue H, Guo E, Zhang H, Lin X, Yao L, et al. Preparation and tensile properties of homogeneously dispersed graphene reinforced aluminum matrix composites. Mater Des. 2016;94:54–60.
- [141] Liu J, Khan U, Coleman J, Fernandez B, Rodriguez P, Naher S, et al. Graphene oxide and graphene nanosheet reinforced aluminium matrix composites: Powder synthesis and prepared composite characteristics. Mater Des. 2016;94:87–94.
- [142] Saboori A, Pavese M, Badini C, Fino P. Development of Al-and Cubased nanocomposites reinforced by graphene nanoplatelets: Fabrication and characterization. Front Mater Sci. 2017;11(2):171–81.

- [143] Bisht A, Srivastava M, Kumar RM, Lahiri I, Lahiri D. Strengthening mechanism in graphene nanoplatelets reinforced aluminum composite fabricated through spark plasma sintering. Mater Sci Eng A. 2017;695:20–8.
- [144] Asgharzadeh H, Sedigh M. Synthesis and mechanical properties of Al matrix composites reinforced with few-layer graphene and graphene oxide. | Alloys Compd. 2017;728:47–62.
- [145] Baig Z, Mamat O, Mustapha M, Mumtaz A, Sarfraz M, Haider S. An efficient approach to address issues of graphene nanoplatelets (GNPs) incorporation in aluminium powders and their compaction behaviour. Metals (Basel). 2018;8(2):1–16. doi: 10.3390/ met8020090.
- [146] Yu H, Zhang SQ, Xia JH, Su Q, Ma BC, Wu JH, et al. Microstructural evolution, mechanical and physical properties of graphene reinforced aluminum composites fabricated via powder metallurgy. Mater Sci Eng A. 2021;802:140669. doi: 10.1016/j.msea.2020. 140669
- [147] Zhou W, Mikulova P, Fan Y, Kikuchi K, Nomura N, Kawasaki A. Interfacial reaction induced efficient load transfer in few-layer graphene reinforced Al matrix composites for high-performance conductor. Compos Part B Eng. 2019;167:93–9. doi: 10.1016/j. compositesb.2018.12.018.
- [148] Bartolucci SF, Paras J, Rafiee MA, Rafiee J, Lee S, Kapoor D, et al. Graphene–aluminum nanocomposites. Mater Sci Eng A. 2011;528(27):7933–7.
- [149] Etter T, Schulz P, Weber M, Metz J, Wimmler M, Löffler JF, et al. Aluminium carbide formation in interpenetrating graphite/aluminium composites. Mater Sci Eng A. 2007;448(1):1–6. doi: 10. 1016/j.msea.2006.11.088.
- [150] Groover MP. Fundamentals of modern manufacturing: Materials, processes, and systems. Hoboken New Jersy USA: John Wiley & Sons: 2020
- [151] Marigo M, Cairns DL, Davies M, Ingram A, Stitt EH. Developing mechanistic understanding of granular behaviour in complex moving geometry using the discrete element method: Part B: Investigation of flow and mixing in the Turbula® mixer. Powder Technol. 2011;212(1):17–24.
- [152] Alam MA, Ya HH, Azeem M, Yusuf M, Sapuan SM. Investigating the effect of mixing time on the crystallite size and lattice strain of the AA7075/TiC composites. Materwiss Werksttech. 2021;52:1112–20. doi: 10.1002/mawe.202000324.
- [153] Obadele BA, Masuku ZH, Olubambi PA. Turbula mixing characteristics of carbide powders and its influence on laser processing of stainless steel composite coatings. Powder Technol. 2012;230:169–82. doi: 10.1016/j.powtec.2012.07.025.
- [154] Samal P, Vundavilli PR, Meher A, Mahapatra MM. Recent progress in aluminum metal matrix composites: A review on processing, mechanical and wear properties. J Manuf Process. 2020;59(November 2019):131–52. doi: 10.1016/j.jmapro.2020.09.010.
- [155] Upadhyaya GS. Powder metallurgy technology. Cambridge, England: Cambridge Int Science Publishing; 1997.
- [156] German RM. Powder metallurgy science. Vol. 279. 105 Coll. Rd. E, Princeton, NJ, 08540, USA: Met. Powder Ind. Fed.; 1984.
- [157] Pease LF, West WG. Fundamentals of powder metallurgy. Princeton, USA: Metal Powder Industries Federation; 2008.
- [158] Gibson BT, Lammlein DH, Prater TJ, Longhurst WR, Cox CD, Ballun MC, et al. Friction stir welding: Process, automation, and control. J Manuf Process. 2014;16(1):56–73. doi: 10.1016/j.jmapro. 2013.04.002.

- [159] Chak V, Chattopadhyay H, Dora TL. A review on fabrication methods, reinforcements and mechanical properties of aluminum matrix composites. J Manuf Process. 2020;56:1059–74. doi: 10.1016/j.jmapro.2020.05.042.
- [160] Khanna V, Kumar V, Bansal SA. Mechanical properties of aluminium-graphene/carbon nanotubes (CNTs) metal matrix composites: Advancement, opportunities and perspective. Mater Res Bull. 2021:138:111224.
- [161] Zhang ZW, Liu ZY, Xiao BL, Ni DR, Ma ZY. High efficiency dispersal and strengthening of graphene reinforced aluminum alloy composites fabricated by powder metallurgy combined with friction stir processing. Carbon N Y. 2018;135:215–23.
- [162] Popov VA, Burghammer M, Rosenthal M, Kotov A. In situ synthesis of TiC nano-reinforcements in aluminum matrix composites during mechanical alloying. Compos Part B. 2018;145(February):57–61. doi: 10.1016/j.compositesb.2018. 02.023.
- [163] Shao C, Lo C, Bhagavathula K, McDonald A, Hogan J. High strength particulate aluminum matrix composite design: Synergistic strengthening strategy. Compos Commun. Jun 2021;25:100697. doi: 10.1016/j.coco.2021.100697.
- [164] Alam MT, Arif S, Ansari AH, Alam MN. Optimization of wear behaviour using Taguchi and ANN of fabricated aluminium matrix nanocomposites by two-step stir casting. Mater Res Express. 2019;6(6):65002.
- [165] Salarieh S, Nourouzi S, Jamshidi Aval H. An Investigation on the microstructure and mechanical properties of Al-Zn-Mg-Cu/Ti composite produced by compocasting. Int J Met. 2022;16(3):1397–1414. doi: 10.1007/s40962-021-00698-1.
- [166] Kannan C, Ramanujam R. Comparative study on the mechanical and microstructural characterisation of AA 7075 nano and hybrid nanocomposites produced by stir and squeeze casting. J Adv Res. 2017;8(4):309–19. doi: 10.1016/j.jare.2017.02.005.
- [167] Natrayan L, Senthil Kumar M. An integrated artificial neural network and Taguchi approach to optimize the squeeze cast process parameters of AA6061/Al2O3/SiC/Gr hybrid composites prepared by novel encapsulation feeding technique. Mater Today Commun. Dec 2020;25:101586. doi: 10.1016/j.mtcomm.2020.
- [168] Al-Qutub AM, Allam IM, Qureshi TW. Effect of sub-micron Al2O3 concentration on dry wear properties of 6061 aluminum based composite. J Mater Process Technol. Mar 2006;172(3):327–31. doi: JMATPROTEC.2005.10.022">10.1016/J.JMATPROTEC.2005.10.022.
- [169] Joshua KJ, Vijay SJ, Selvaraj DP. Effect of nano TiO2 particles on microhardness and microstructural behavior of AA7068 metal matrix composites. Ceram Int. Dec 2018;44(17):20774–81. doi: CERAMINT.2018.08.077">10.1016/J.CERAMINT.2018.08.077.
- [170] Kumar CAV, Rajadurai JS. Influence of rutile (TiO2) content on wear and microhardness characteristics of aluminium-based hybrid composites synthesized by powder metallurgy. Trans Nonferrous Met Soc China. Jan 2016;26(1):63–73. doi: 10.1016/ S1003-6326(16)64089-X.
- [171] Shaikh MBN, Aziz T, Arif S, Ansari AH, Karagiannidis PG, Uddin M. Effect of sintering techniques on microstructural, mechanical and tribological properties of Al-SiC composites. Surf Interfaces. 2020;20(July):100598. doi: 10.1016/j.surfin.2020.100598.
- [172] Jafari F, Sharifi H, Saeri MR, Tayebi M. Effect of reinforcement volume fraction on the wear behavior of Al-SiC p composites prepared by spark plasma sintering. Silicon. 2018;10:2473–81.

- [173] Bathula S, Anandani RC, Dhar A, Srivastava AK. Microstructural features and mechanical properties of Al 5083/SiCp metal matrix nanocomposites produced by high energy ball milling and spark plasma sintering. Mater Sci Eng A. 2012;545:97–102.
- [174] Abdullahi K, Al-Aqeeli N. Mechanical alloying and spark plasma sintering of nano-SiC reinforced Al–12Si–0.3 Mg alloy. Arab J Sci Eng. 2014;39:3161–8.
- [175] Rezaei MR, Albooyeh A, Shayestefar M, Shiraghaei H. Microstructural and mechanical properties of a novel Al-based hybrid composite reinforced with metallic glass and ceramic particles. Mater Sci Eng A. 2020;786:139440. doi: 10.1016/j.msea. 2020.139440.
- [176] Erdemir F, Canakci A, Varol T. Microstructural characterization and mechanical properties of functionally graded Al2024/SiC composites prepared by powder metallurgy techniques. Trans Nonferrous Met Soc China. 2015;25(11):3569–77.
- [177] Al-Aqeeli N, Abdullahi K, Hakeem AS, Suryanarayana C, Laoui T, Nouari S. Synthesis, characterisation and mechanical properties of SiC reinforced Al based nanocomposites processed by MA and SPS. Powder Metall. 2013;56(2):149–57.
- [178] Fathy A, Sadoun A, Abdelhameed M. Effect of matrix/reinforcement particle size ratio (PSR) on the mechanical properties of extruded Al–SiC composites. Int J Adv Manuf Technol. 2014;73:1049–56.
- [179] Sun C, Song M, Wang Z, He Y. Effect of particle size on the microstructures and mechanical properties of SiC-reinforced pure aluminum composites. J Mater Eng Perform. 2011;20:1606–12.
- [180] Rajavel Muthaiah VM, Meka SR, Venkata Manoj Kumar B. Processing of heat-treated silicon carbide-reinforced aluminum alloy composites. Mater Manuf Process. 2019;34(3):312–20.
- [181] Van Trinh P, Lee J, Minh PN, Phuong DD, Hong SH. Effect of oxidation of SiC particles on mechanical properties and wear behavior of SiCp/Al6061 composites. J Alloys Compd. 2018;769:282–92. doi: 10.1016/j.jallcom.2018.07.355.
- [182] Sadhu KK, Mandal N, Sahoo RR. SiC/graphene reinforced aluminum metal matrix composites prepared by powder metallurgy: A review. J Manuf Process. 2023;91(November 2022):10–43. doi: 10.1016/j.jmapro.2023.02.026.
- [183] Zeng X, Liu W, Xu B, Shu G, Li Q. Microstructure and mechanical properties of Al–SiC nanocomposites synthesized by surfacemodified aluminium powder. Metals (Basel). 2018;8(4):253.
- [184] Vijaya Kumar P, Jebakani D, Velmurugan C, Senthilkumar V. Effect of SiC on mechanical and microstructural characteristics of Al based functionally graded material. Silicon. 2022;14:1–6.
- [185] Kollo L, Bradbury CR, Veinthal R, Jäggi C, Carreño-Morelli E, Leparoux M. Nano-silicon carbide reinforced aluminium produced by high-energy milling and hot consolidation. Mater Sci Eng A. 2011;528(21):6606–15.
- [186] Li XP, Liu CY, Ma MZ, Liu RP. Microstructures and mechanical properties of AA6061–SiC composites prepared through spark plasma sintering and hot rolling. Mater Sci Eng A. 2016;650:139–44.
- [187] Bajpai G, Tiwari A, Purohit R, Panchore V, Dwivedi R, Satyanarayana K. Development, testing and characterization of al nanoticp composites through powder metallurgy techniques.

 J Compos Sci. 2021;5(8):1–9. doi: 10.3390/jcs5080224.
- [188] Reddy PV, Prasad PR, Krishnudu DM, Goud EV. An investigation on mechanical and wear characteristics of Al 6063/TiC metal matrix composites using RSM. J Bio- Tribo-Corrosion. 2019;5(4):1–10. doi: 10.1007/s40735-019-0282-0.

- [189] Khan M, Din RU, Wadood A, Syed WH, Akhtar S, Aune RE. Effect of graphene nanoplatelets on the physical and mechanical properties of Al6061 in fabricated and T6 thermal conditions. J Alloys Compd. 2019;790:1076–91.
- [190] Mao D, Meng X, Xie Y, Yang Y, Xu Y, Qin Z, et al. Strength-ductility balance strategy in SiC reinforced aluminum matrix composites via deformation-driven metallurgy. J Alloys Compd. 2022;891:162078. doi: 10.1016/j.jallcom.2021.162078.
- [191] Reddy MP, Himyan MA, Ubaid F, Shakoor RA, Vyasaraj M, Gururaj P, et al. Enhancing thermal and mechanical response of aluminum using nanolength scale TiC ceramic reinforcement. Ceram Int. Jun 2018;44(8):9247–54. doi: 10.1016/J.CERAMINT.2018. 02 135
- [192] Baig Z, Mamat O, Mustapha M. Recent progress on the dispersion and the strengthening effect of carbon nanotubes and graphenereinforced metal nanocomposites: A review. Crit Rev Solid State Mater Sci. 2018;43(1):1–46. doi: 10.1080/10408436.2016.1243089.
- [193] Fadavi Boostani A, Yazdani S, Taherzadeh Mousavian R, Tahamtan S, Azari Khosroshahi R, Wei D, et al. Strengthening mechanisms of graphene sheets in aluminium matrix nanocomposites. Mater Des. 2015;88:983–9.
- [194] Bhushan B. Introduction to tribology. UK: John Wiley & Sons: 2013.
- [195] Prasad SV, Rohatgi PK. Tribological properties of Al alloy particle composites. JOM. 1987;39(11):22–6.
- [196] Shrivastava AK, Singh KK, Dixit AR. Tribological properties of Al 7075 alloy and Al 7075 metal matrix composite reinforced with SiC, sliding under dry, oil lubricated, and inert gas environments. Proc Inst Mech Eng Part J J Eng Tribol. 2018;232(6):693–8. doi: 10. 1177/1350650117726631.
- [197] Abd El-Aziz K, Saber D, Sallam HE-DM. Wear and corrosion behavior of Al–Si matrix composite reinforced with alumina. J Bioand Tribo-Corrosion. 2015;1(1):5.
- [198] Basavarajappa S, Chandramohan G, Mukund K, Ashwin M, Prabu M. Dry sliding wear behavior of Al 2219/SiCp-Gr hybrid metal matrix composites. J Mater Eng Perform. 2006;15(6):668–74.
- [199] Tyagi R. Synthesis and tribological characterization of in situ cast Al–TiC composites. Wear. 2005;259(1–6):569–76.
- [200] Kostornov AG, Fushchich OI, Chevychelova TM, Varchenko VT, Kostenko AD. Prospects of improving the tribotechnical characteristics of titanium composites. Powder Metall Met Ceram. 2013;51(11–12):687–96.
- [201] Selvakumar N, Narayanasamy P. Optimization and effect of weight fraction of MoS2 on the tribological behavior of Mg-TiC-MoS2 hybrid composites. Tribol Trans. 2016;59(4):733–47. doi: 10. 1080/10402004.2015.1110866.
- [202] Suresh S, Harinath Gowd G, Deva Kumar MLS. Wear behaviour of Al 7075/SiC/Mg metal matrix nano composite by liquid state process. Adv Compos Hybrid Mater. 2018;1(4):819–25. doi: 10. 1007/s42114-018-0054-1.
- [203] Majzoobi GH, Atrian A, Enayati MH. Tribological properties of Al7075-SiC nanocomposite prepared by hot dynamic compaction. Compos Interfaces. Sep 2015;22(7):579–93. doi: 10.1080/ 09276440.2015.1055955.
- [204] Saadatmand M, Aghazadeh Mohandesi J. Optimization of mechanical and wear properties of functionally graded Al6061/ SiC nanocomposites produced by friction stir processing (FSP). Acta Metall Sin (English Lett). 2015;28(5):584–90. doi: 10.1007/ s40195-015-0235-7.

- [205] Qu J, Xu H, Feng Z, Frederick DA, An L, Heinrich H. Improving the tribological characteristics of aluminum 6061 alloy by surface compositing with sub-micro-size ceramic particles *via* friction stir processing. Wear. 2011;271(9):1940–5. doi: 10.1016/j.wear.2010. 11.046.
- [206] Reddy AP, Krishna PV, Rao RN. Dry sliding wear behaviour of ultrasonically-processed AA6061/SiCp nanocomposites. Int J Automot Mech Eng. 2017;14(4):4568–747.
- [207] Manivannan I, Ranganathan S, Gopalakannan S, Suresh S, Nagakarthigan K, Jubendradass R. Tribological and surface behavior of silicon carbide reinforced aluminum matrix nanocomposite. Surf Interfaces. 2017;8:127–36. doi: 10.1016/j.surfin. 2017.05.007.
- [208] Dolatkhah A, Golbabaei P, Besharati Givi MK, Molaiekiya F. Investigating effects of process parameters on microstructural and mechanical properties of Al5052/SiC metal matrix composite fabricated via friction stir processing. Mater Des. May 2012;37:458–64. doi: 10.1016/J.MATDES.2011.09.035.
- [209] Moazami-Goudarzi M, Akhlaghi F. Wear behavior of Al 5252 alloy reinforced with micrometric and nanometric SiC particles. Tribol Int. 2016;102:28–37. doi: 10.1016/j.triboint.2016.05.013.
- [210] Bathula S, Saravanan M, Dhar A. Nanoindentation and wear characteristics of Al 5083/SiCp Nanocomposites synthesized by high energy ball milling and spark plasma sintering. J Mater Sci Technol. 2012;28(11):969–75. doi: 10.1016/S1005-0302(12)60160-1.
- [211] Arif S, Alam MT, Aziz T, Ansari AH. Morphological and wear behaviour of new Al-SiCmicro-SiCnano hybrid nanocomposites fabricated through powder metallurgy. Mater Res Express. 2018;5(4):46534.
- [212] Faisal N, Kumar K. Mechanical and tribological behaviour of nano scaled silicon carbide reinforced aluminium composites. J Exp Nanosci. Feb 2018;13(sup1):S1–S13. doi: 10.1080/17458080.2018. 1431846.
- [213] Darmiani E, Danaee I, Golozar MA, Toroghinejad MR, Ashrafi A, Ahmadi A. Reciprocating wear resistance of Al–SiC nano-composite fabricated by accumulative roll bonding process. Mater Des. 2013;50:497–502. doi: 10.1016/j.matdes.2013.03.047.
- [214] Alam MT, Arif S, Ansari AH. Wear behaviour and morphology of stir cast aluminium/SiC nanocomposites. Mater Res Express. 2018;5(4):45008.
- [215] Yuvaraj N, Aravindan S, Vipin. Wear characteristics of Al5083 surface hybrid nano-composites by friction stir processing. Trans Indian Inst Met. 2017;70(4):1111–29. doi: 10.1007/s12666-016-0905-9.
- [216] George SM, Priya R, Vijayakumar GNS, Pradeep JA. Study on mechanical characteristics of the nano-TiC reinforced Al6061 metal matrix composites. Mater Today Proc. 2022;62:2224–9. doi: 10.1016/j.matpr.2022.03.457.
- [217] Lekatou A, Karantzalis AE, Evangelou A, Gousia V, Kaptay G, Gácsi Z, et al. Aluminium reinforced by WC and TiC nanoparticles (ex-situ) and aluminide particles (in-situ): Microstructure, wear and corrosion behaviour. Mater Des. 2015;65:1121–35.
- [218] Nemati N, Khosroshahi R, Emamy M, Zolriasatein A. Investigation of microstructure, hardness and wear properties of Al–4.5wt.% Cu–TiC nanocomposites produced by mechanical milling. Mater Des. 2011;32(7):3718–29. doi: 10.1016/j.matdes.2011.03.056.
- [219] Sharma A, Fujii H, Paul J. Influence of reinforcement incorporation approach on mechanical and tribological properties of AA6061-CNT nanocomposite fabricated *via* FSP. J Manuf Process. 2020;59:604–20. doi: 10.1016/j.jmapro.2020.10.016.

- [220] Martin S, Kandemir S, Antonov M. Investigation of the high temperature dry sliding wear behavior of graphene nanoplatelets reinforced aluminum matrix composites. J Compos Mater. Dec. 2020;55(13):1769–82. doi: 10.1177/0021998320979037.
- [221] Wu L, Zhao Z, Bai P, Zhao W, Li Y, Liang M, et al. Wear resistance of graphene nano-platelets (GNPs) reinforced AlSi10Mg matrix composite prepared by SLM. Appl Surf Sci. 2020;503:144156.
- [222] Baradeswaran A, Elaya Perumal A. Study on mechanical and wear properties of Al 7075/Al2O 3/graphite hybrid composites. Compos Part B Eng. 2014;56:464–71. doi: 10.1016/j.compositesb.2013. 08.013
- [223] Yang ZR, Sun Y, Li XX, Wang SQ, Mao TJ. Dry sliding wear performance of 7075 Al alloy under different temperatures and load conditions. Rare Met. 2015;41:2–7. doi: 10.1007/s12598-015-0504-7.
- [224] Irfan M, Haq U. Friction and wear behavior of AA 7075- Si 3 N 4 composites under dry conditions: Effect of sliding speed. Silicon. 2018;11:1047–53.
- [225] Kumar GBV, Rao CSP, Selvaraj N. Mechanical and dry sliding wear behavior of Al7075 alloy-reinforced with SiC particles. J Compos Mater. 2012;46(10):1201–9. doi: 10.1177/0021998311414948.
- [226] Lakshmipathy J, Kulendran B. Reciprocating wear behaviour of 7075Al/SiC and 6061Al/Al₂O₃ composites: A study of effect of reinforcement, stroke and load. Tribol Ind. 2014;36(2.
- [227] Idusuyi N, Olayinka JI. Dry sliding wear characteristics of aluminium metal matrix composites: A brief overview. J Mater Res Technol. 2019;8(3):3338–46.
- [228] Pan S, Jin K, Wang T, Zhang Z, Zheng L, Umehara N. Metal matrix nanocomposites in tribology: Manufacturing, performance, and mechanisms. Friction. 2022;10:1–39.
- [229] Nagarjuna C, You HJ, Ahn S, Song JW, Jeong KY, Madavali B, et al. Worn surface and subsurface layer structure formation behavior on wear mechanism of CoCrFeMnNi high entropy alloy in different sliding conditions. Appl Surf Sci. 2021;549:149202. doi: 10. 1016/j.apsusc.2021.149202.
- [230] Lin F, Ren M, Wu H, Jia F, Lu Y, Huo M, et al. Investigation of microstructure and tribological performances of high-fraction TiC/graphene reinforced self-lubricating Al matrix composites. Tribol Int. 2023;177(August 2022):108018. doi: 10.1016/j.triboint. 2022.108018.
- [231] Tang XC, Meng LY, Zhan JM, Jian WR, Li WH, Yao XH, et al. Strengthening effects of encapsulating graphene in SiC particlereinforced Al-matrix composites. Comput Mater Sci. 2018;153:275–81.
- [232] Vignesh Kumar R, Harichandran R, Vignesh U, Thangavel M, Chandrasekhar SB. Influence of hot extrusion on strain hardening behaviour of graphene platelets dispersed aluminium composites. J Alloys Compd. 2021;855:157448. doi: 10.1016/j.jallcom. 2020.157448.
- [233] Azar M, Sadri, Nemati, Angizi, Shaeri, Minárik, et al. Investigating the microstructure and mechanical properties of aluminummatrix reinforced-graphene nanosheet composites fabricated by mechanical milling and equal-channel angular pressing. Nanomaterials. 2019;9(8):1070.
- [234] Zhang Z, Chen DL. Contribution of Orowan strengthening effect in particulate-reinforced metal matrix nanocomposites. Mater Sci Eng A. 2008;483:148–52.
- 235] Chen B, Shen J, Ye X, Jia L, Li S, Umeda J, et al. Length effect of carbon nanotubes on the strengthening mechanisms in metal matrix composites. Acta Mater. 2017;140:317–25.

- [236] Bhadauria A, Singh LK, Laha T. Combined strengthening effect of nanocrystalline matrix and graphene nanoplatelet reinforcement on the mechanical properties of spark plasma sintered aluminum based nanocomposites. Mater Sci Eng A. 2019;749:14–26.
- [237] Ma G, Wang D, Xiao B, Ma Z. Effect of particle size on mechanical properties and fracture behaviors of age-hardening SiC/ Al-Zn-Mg-Cu. Compos Acta Metall Sin (English Lett). 2021:34:1447-59.
- [238] Salem MA, El-Batanony IG, Ghanem M, ElAal Abd MI. Effect of the matrix and reinforcement sizes on the microstructure, the physical and mechanical properties of Al-SiC composites. J Eng Mater Technol. 2017;139(1):011007.
- [239] AbuShanab WS, Moustafa EB, Ghandourah E, Taha MA. Effect of graphene nanoparticles on the physical and mechanical properties of the Al2024-graphene nanocomposites fabricated by powder metallurgy. Results Phys. 2020;19(June):103343. doi: 10. 1016/j.rinp.2020.103343.
- [240] Rashad M, Pan F, Tang A, Asif M. Effect of graphene nanoplatelets addition on mechanical properties of pure aluminum using a semi-powder method. Prog Nat Sci Mater Int. 2014;24(2):101–8. doi: 10.1016/j.pnsc.2014.03.012.
- [241] Madeira S, Miranda G, Carneiro VH, Soares D, Silva FS, Carvalho O. The effect of SiCp size on high temperature damping capacity and dynamic Young's modulus of hot-pressed AlSi–SiCp MMCs. Mater Des. 2016;93:409–17. doi: 10.1016/j.matdes.2015. 12.147
- [242] Madeira S, Miranda G, Soares D, Silva FS, Carvalho O. Study on damping capacity and dynamic Young's modulus of aluminium

- matrix composite reinforced with SiC particles. Ciência Tecnol dos Mater. 2017;29(1):e92–6. doi: 10.1016/j.ctmat.2016.08.003.
- [243] Rong Y, He HP, Zhang L, Li N, Zhu YC. Molecular dynamics studies on the strengthening mechanism of Al matrix composites reinforced by grapnene nanoplatelets. Comput Mater Sci. 2018;153:48–56. doi: 10.1016/j.commatsci.2018.06.023.
- [244] Zheng KL, Wei XS, Yan B, Yan PF. Ceramic waste SiC particlereinforced Al matrix composite brake materials with a high friction coefficient. Wear. 2020;458–459:203424. doi: 10.1016/j.wear. 2020.203424.
- [245] Zhang H, Zhao Y, Yan Y, Fan J, Wang L, Dong H, et al.
 Microstructure evolution and mechanical properties of Mg matrix
 composites reinforced with Al and nano SiC particles using spark
 plasma sintering followed by hot extrusion. J Alloys Compd.
 2017;725:652–64. doi: 10.1016/j.jallcom.2017.07.159.
- [246] Abazari S, Shamsipur A, Bakhsheshi-Rad HR, Ismail AF, Sharif S, Razzaghi M, et al. Carbon nanotubes (CNTs)-reinforced magnesium-based matrix composites: A comprehensive review. Materials. 2020;13(19):4421. doi: 10.3390/ma13194421.
- [247] Venkatesh VSS, Deoghare AB. Modelling and optimisation of wear parameters for spark plasma sintered Al– SiC–kaoline hybrid composite. Adv Mater Process Technol. Oct 2022;8(sup3):1286–1304. doi: 10.1080/2374068X.2021.1939561.
- [248] Baig Z, Mamat O, Mustapha M, Sarfraz M. Influence of surfactant type on the dispersion state and properties of graphene nanoplatelets reinforced aluminium matrix nanocomposites.

 Fullerenes Nanotubes Carbon Nanostruct. 2017;25(9):545–57. doi: 10.1080/1536383X.2017.1362396.